Capacity and Earthquake Response Analysis of RC-Shear Walls

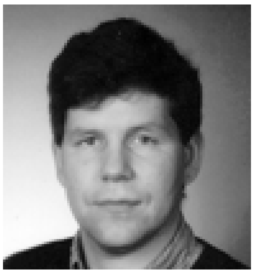

Bjarni Bessason
Ph.D., Associate Professor
Earthquake Engineering Research Centre, University of Iceland
Austurvegur 2a, 800 Selfoss, Iceland
E-mail: bb@hi.is

Thórdur Sigfússon
M.Sc., Civil Engineer
Faculty of Engineering, University of Iceland
Austurvegur 2a, 800 Selfoss, Iceland
E-mail: thordur@vgs.is

ABSTRACT

The South Iceland Lowland is an active seismic zone. Approximately, 60% of all residential houses in the region are one or two stories reinforced-concrete buildings. In June 2000, two major earthquakes of magnitude 6½ struck the South Iceland. The earthquakes caused considerable damage, especially to older structures. No building collapsed, and no people suffered serious injuries. In this paper, a non-linear, finite-element model is calibrated by experimental data, and then used to evaluate the load-deformation curves of reinforced-concrete shear wall with different reinforcement configurations. The shear wall geometry is typical for Icelandic residential buildings. The evaluated load-deformation curves are then used in earthquake response analysis, using recorded strong motion data from the South Iceland earthquakes of June 2000.

Key words: Reinforced-concrete shear walls, non-linear pushover analysis, capacity curves, earthquake response.

1. INTRODUTION

1.1 Background

The seismicity in Iceland is related to the Mid-Atlantic plate boundary crossing the island. Within Iceland, the boundary shifts eastward through two complex fracture zones. One is located in the South Iceland Lowland, called the South Iceland Seismic Zone (SISZ), while the other, lying mostly off the northern coast of Iceland, is called the Tjörnes Fracture Zone. The largest earthquakes in Iceland have occurred within these zones. The SISZ crosses the biggest agricultural region in Iceland. In this region, there are villages, schools, medical centres, industrial plants, hydro-electric power plants, and some major bridges. The population is around 16,000 inhabitants, and the number of residential houses is approximately 5,300. Most of the houses are low-rise buildings of one or two stories. Based on the official real property database, approximately 30% of all houses are wooden houses, 10% are masonry houses made of hollow pumice blocks, and 60% are in-situ-cast concrete houses. The majority of the houses are built after 1940. In June 2000, two major earthquakes of moment magnitude M_w=6.6 and M_w=6.5 occurred in SISZ. No houses collapsed, but numbers of houses were damaged, and at least 35 houses were estimated as unrepairable and were renewed. Most of the damage was found in older shear-wall concrete and masonry buildings with poor reinforcement. In older houses reinforcement was usually just placed around window and door openings, and even only above the openings, see [1]. Figure 1 shows as an example of damage to two older houses during the South Iceland earthquakes of June 2000. It should be noted that the cracks are few but severe.

1.2 Objective

In this study, a finite element program is calibrated and verified against experimental data. Then the program is used to evaluate the capacity, represented by non-linear load-deformation curves, of reinforced-concrete shear wall with the same geometry but different reinforcement. The shear wall geometry is typical for Icelandic low-rise concrete residential houses. The capacity curves are then used as bases for non-linear earthquake response analysis of an idealised single-story residential building, which is excited by recorded acceleration time histories from the South Iceland earthquakes of June 2000. The main aim is to study the effect of different amounts of reinforcement on the capacity curves and to see if observed damage in the South Iceland earthquakes of June 2000 can be back-calculated.

Figure 1 - Houses damaged during the South Iceland earthquakes of June 2000.

2. NONLINEAR ANALYSIS OF REINFORCED CONCRETE

2.1 General

Non-linear response of reinforced concrete (RC) is caused by cracking, plastic deformations in compression and crushing of the concrete and plastic deformations of the reinforcement. Other, usually less important, time-independent non-linearity arises from bond slip between steel and concrete, aggregate interlock of cracked concrete and dowel action. Time-dependent effects, such as creep, shrinkage and temperature change, also affect non-linear response but can be ignored for short-duration earthquake loads. In the following, only non-linear properties due to cracking, plastic deformations of concrete and steel, and aggregate interlock are considered. A perfect bond between the steel bars and the concrete is assumed, but according to [2], this assumption usually gives reasonably accurate results.

Many mathematical models have been proposed for non-linear finite element (FE) analysis of reinforced concrete structures. An overview of these models and how they can by modelled with the FE approximations can be found in [3] and [4].

A number of computer programs are available for non-linear analysis of reinforced concrete. The constitutive models and plasticity models used in these programs, however, are different, and it is generally not straightforward to apply these models. Some of the input parameters are fictive and have to be adjusted. In this work, the computer program ANSYS [5] is adapted and calibrated against experimental data.

2.2 Finite element model

The solid element SOLID65 in the ANSYS program is used in the analysis [5]. It can be used for three-dimensional modelling of solids with or without reinforcing bars. Eight nodes define the element, each having three translation degrees of freedom. Reinforcement can be defined in three different directions.

The solid part of the element, e.g., the concrete, is capable to describe cracking, plastic deformations and crushing. The plasticity model for concrete is based on the flow theory of plasticity, von Mises' yield criterion, isotropic hardening and associated flow rule, see [3]. Cracking is permitted in three orthogonal directions at each integration point. The cracking is modelled through an adjustment of the material properties (i.e., by changing the element stiffness matrixes) that effectively treat the cracking as “smeared” cracks. The concrete material is assumed to be initially isotropic. If the concrete at an integration point fails in uniaxial, biaxial, or triaxial compression, the concrete is assumed crushed at that point. Crushing is defined as the complete deterioration of the structural integrity of the concrete (e.g., concrete spalling).

The reinforcement is assumed smeared throughout the elements. An idealised elasto-plastic material model models the reinforcement. It cannot carry shear, i.e., transverse forces.

2.3 Input parameters

The following material parameters are necessary for the concrete model: uniaxial secant moduls of elasticity, E_c; uniaxial secant modulus of plasticity, E_{cp}; uniaxial compression strength, f_{cc}; uniaxial tension strength, f_{ct}; uniaxial yield strength, f_{cy}; ultimate strain for concrete, ε_{cu}; shear coefficient for open crack, β_t; shear coefficient for closed crack, β_c; multiplayer for tensile stress relaxation, T_c; and finally Poisson’s ratio, ν_c. Some of the parameters have a clear physical meaning, while others are more fictive. The uniaxial stress-strain curve shown in Figure 2 can be used to explain some of the parameters above. However, the simple curve in Figure 2 is not representative of the general case of multiaxial stress state. In such cases, the curve is replaced by yield surfaces (von Mises) and fracture surfaces that are functions of principal stresses or principal-stress invariants, see [3] for more details.

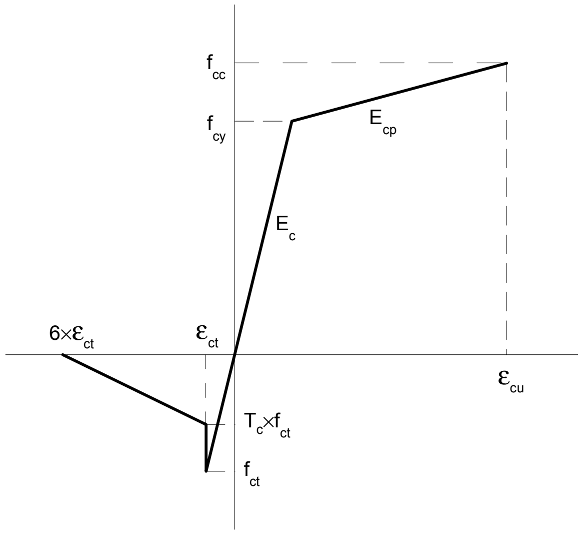

Figure 2 – Uniaxial concrete material model.

Based on studies presented by Hemmaty, see [2] and [6], it was decided to use β_c=1.0 and β_t=0.1 in all analyses. Furthermore, the default values, T_c=0.6 and f_{cy} =0.8×f_{cc}, recommended in [5] and used in [2] and [6], were also used for all runs. The steel parameters are simpler and consist of: modulus of elasticity, E_s; modulus of plasticity, E_{sp}; yield strength, f_{sy}; ultimate strain, ε_{su}; and, finally, Poisson's ratio ν_s.

2.4 Verification against experimental data

Two laboratory-tested RC-beams and two laboratory-tested RC-walls were analysed with the computer program ANSYS [5]. The experimental data for the RC-beams were obtained from Bresler & Scordelis [7]. The beams were simply supported, 3660mm long, 305mm wide, 552mm high, and loaded with vertical force in the middle. Both beams had tension steel, but only one of the beams had shear reinforcement and compression steel in addition. Due to symmetry, only one half of the beam was modelled. Solid 3D elements were used: six elements in the height, two in the width and twelve in the length (6×2×12=144). All physical input data (geometry, concrete and steel parameters) were according to the experimental data. In Figure 3, the experimental load-deflection curve for the beam with the shear reinforcement and the compression steel is compared with the FE-analysis curve. The load and the deflection shown are based on the applied force and the measured and computed deflection at the middle of the beam. As can be seen, the curves are quite similar. For more details, see [1].

The experimental data for the RC walls are obtained from Barda [8]. Laboratory tests of eight scaled, low-rise shear walls with boundary elements are described. All the shear-walls have the same geometry, but the reinforcement varies between the tests. The boundary elements were supposed to simulate the effect of cross walls and an overlying floor slab. The horizontal length of the test walls was 1910mm; the height was 610mm, and the thickness was 102mm. Only two tests were analysed with the ANSYS program. In Figure 4a the tilt-up from the laboratory tests [8] is shown, and in Figure 4b the FE-model of the test is shown. In Figure 5 the measured and computed load-deflection curves are shown for one of the shear walls. As can be seen, the FE-analysis can simulate the test results fairly well.

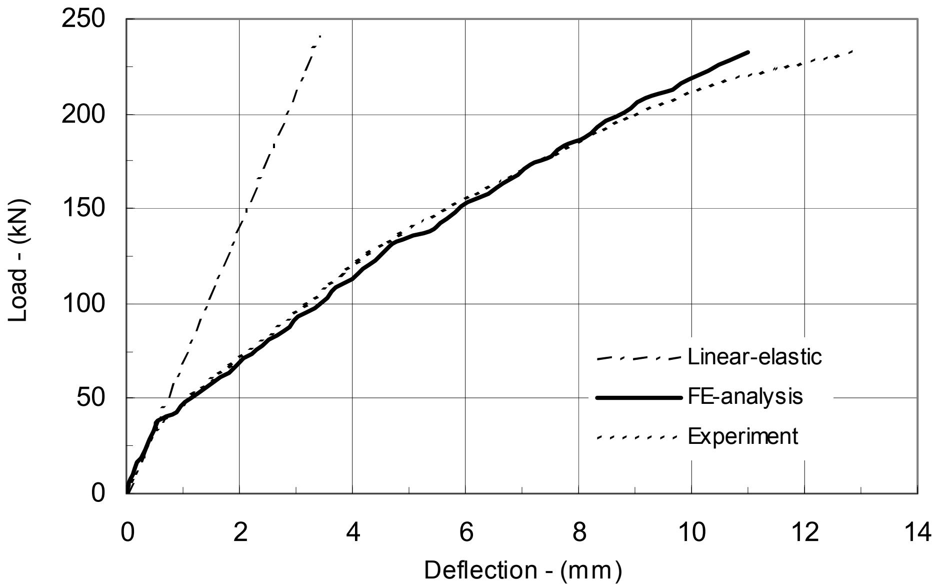

Figure 3 - Comparison of experimental [7] and FE-analysis [1] load-deflection curves for simply supported beam with shear reinforcement.

The main conclusion from the verification examples is that the FE-program can be used to simulate the whole load-deformation curve, i.e., the elastic part, the initiation of cracking, shear cracks and crushing, and the yielding of the steel bars fairly well. However, the determination of ultimate load is difficult as it is affected by the hardening rule, convergence criteria and iteration method used, [1]. It should be noted that each experiment considered was only based on one test, and no estimates for standard deviation or bonds of the results are available. It is likely that repeated tests would have resulted in some variations.

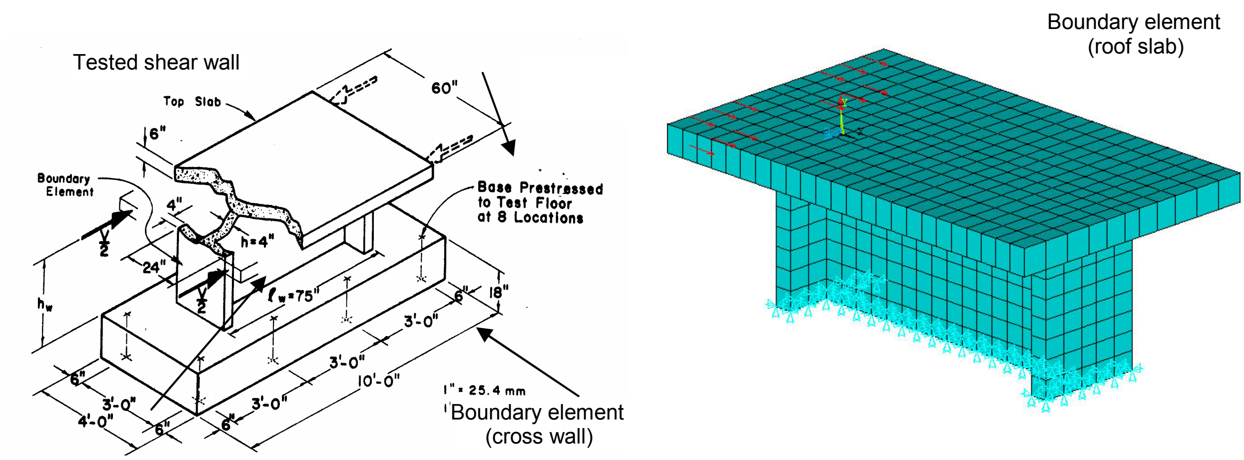

Figure 4 – a) Tilt-up of laboratory tested shear wall with boundary elements, from [8]. b) FE-model of the laboratory test from [1].

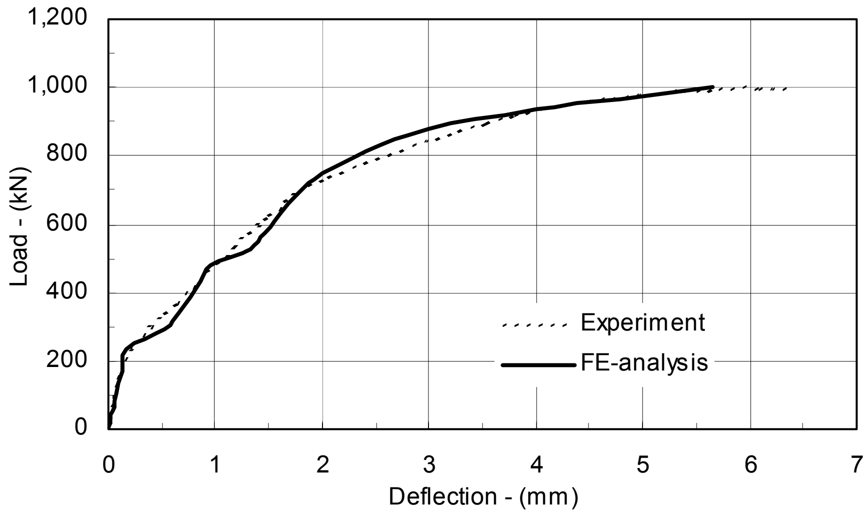

Figure 5 - Comparison of experimental [8] and FE-analysis [1] load-deflection curves for reinforced concrete shear wall with boundary elements.

3. PUSHOVER ANALYSIS OF LOW-RISE RC SHEAR WALL

3.1 Typical residential concrete house

The capacity spectrum method used in the field of earthquake engineering compares the capacity of a structure with the demands of earthquake ground motion on it, see for instance [9] and [10]. The capacity of the structure is represented by a load-displacement curve, obtained by non-linear static analysis where the load is stepwise increased. This way of evaluating the load-displacement curve is often called a pushover analysis.

Approximately 60% of all residential houses in the South Iceland Lowland (SIL) are concrete buildings. In the period 1996-1997, a field survey was carried out in the SIL as a part of an earthquake mitigation program called SEISMIS, see [11]. The surveying procedure was based upon standardised questionnaires and inspection of architectural and engineering drawings. The field survey showed that concrete residential houses are usually one- to two-story shear-wall buildings, with 110-150m^2 living area and built after 1940. They are more or less symmetric, and most, and sometimes all, of the interior walls are non-bearing. The foundations are typically made of concrete with limited reinforcement and founded on rock or gravel. The exterior shear walls are typically 180mm thick. Concrete roof slabs are common, usually 150mm thick. In houses built before 1980, the concrete strength corresponds to approximately C16 concrete (characteristic compressive cylinder strength, f_{ck}=16MPa), but in houses built after 1980, it normally corresponds to C20 concrete (f_{ck}=20MPa), for more details see [12]. Today, only ribbed steel bars are used in concrete, but prior to 1965, plain steel bars were the only alternative. Before 1965, it was common to use only one or two horizontal, 12mm steel bars over window and door openings. Between 1965 and 1980, this reinforcement was increased to one or two 12mm steel bars around all openings. After 1980 the building authorities requested one layer of reinforcement grid in the entire wall. Normally, this was made of 10mm steel bars with a centre-to-centre (c/c) distance of 250mm in both the horizontal and vertical directions. After 1990, the reinforcement has increased, and it is now common to use double steel grid reinforcement, usually 2×(10 mm c/c 250mm).

In Figure 6 a concrete shear wall is defined that can be assumed to be representative of an exterior wall in a typical single-story residential house. This wall will be used in the pushover analysis. The wall is 0.18m thick, 8m wide and 2.75m high, with two windows and one door. Openings are 27% of the area, and the height to length ratio is 0.34. The geometry will be the same throughout the analysis, while the reinforcement configuration varies. The different reinforcement configurations are shown in Table 1. The steel type assumed is S400 (f_{sy}=400MPa) in all cases, and the concrete strength corresponds to C20 concrete, see [12].

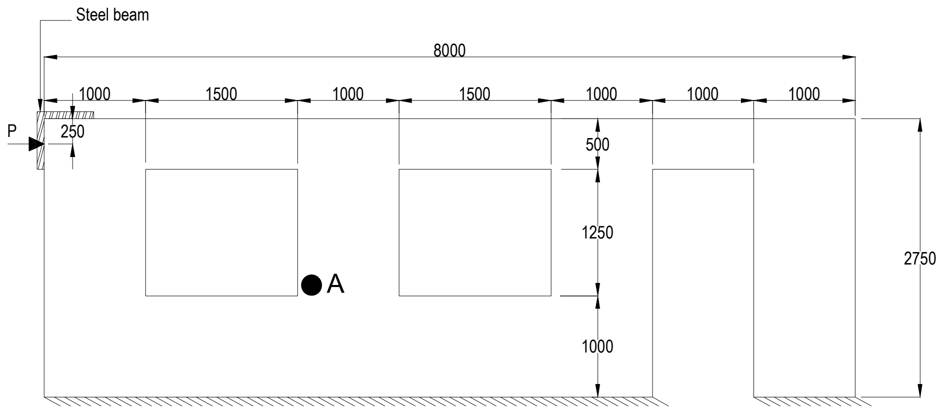

Figure 6 – Wall geometry used in pushover analysis. The reinforcement configuration is defined in Table 1. The dot to the right of the right window shows the location where the steel stresses are computed, in the diagram shown in Figure 9.

Table 1 - Reinforcement configuration used for the shear wall

Wall types	Reinforcement	A_s/A_c vertical	A_s/A_c horizontal
W1	No reinforcement	-	-
W2	1K12 around openings (1K12 - one 12 mm steel bar)	-	-
W3	2K12 around openings	-	-
W4	1K12 c/c250mm grid in the entire wall	0.25 %	0.25 %
W5	2K12 c/c250mm grid in the entire wall	0.5 %	0.5 %
W6	Minimum reinforcement according to Eurocode 2 (EC2) [12] without reinforcement around openings and boundary reinforcement.	0.4 %	0.2 %
W7	Minimum reinforcement according to EC2 with 2K16 around openings but no boundary reinforcement	0.4 %	0.2 %

3.2 FE-model

The shear wall is modelled with 256 solid elements (Solid65, see [5]). All the elements have the same size, i.e., height×wide×thickness is 250×250×180mm. A steel square, modelled by linear beam elements, is put on the top left corner, where the load is applied, in order to distribute the load at the corner. It should be noticed that the element size might affect the results slightly, see for instance [13]. The Newton-Rapson iteration technique is used with displacement convergence criteria. The material properties for the concrete as well as the steel are based on mean values (expected values) and not on design values. For the concrete, the following values are used: E_c=28.8MPa, E_{cp}=1.85MPa, f_{cc}=25MPa, f_{ct}=2.2MPa, f_{cy}=0.8×f_{cc}=20MPa, ε_{cu}=3.5‰,

β_t =0.1, β_c =1.0, T_c =0.6, ν_c=0.2. For the steel: E_s =200GPa, E_{sp}=1.04MPa, f_{sy} =400MPa, ε_{su}=15‰ and ν_s =0.3. The horizontal load, *P*, is monotonic and applied stepwise at the top of the wall. In addition, the self-weight of the structure is included in the analysis, i.e., the dead load of the wall and the dead load of an idealised roof slab and roof structure supported by the wall.

3.3 Capacity curves

In Figure 7, the capacity curves for the wall types W2 to W7 are shown. The deflection shown is defined by the horizontal deflection at the top left corner.

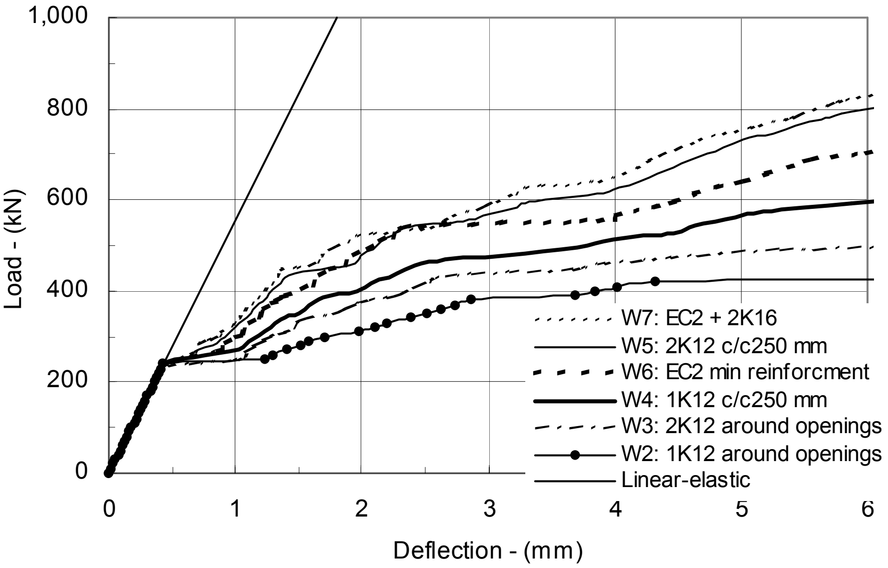

Figure 7 - Capacity curves for the shear wall with varying reinforcement.

In all the walls the initial cracking started at the load of 240kN and at a deflection of 0.44mm. Wall-W1 is not shown in the figure because it became unstable right after cracking. All curves have been cut off at deflection of 6mm although all wall types had higher ultimate displacement. This is done because at a displacement of 4mm, corresponding to a ductility of approximately μ=8, it is expected that the structural stability of the walls is insufficient with buckling, brittle failure, etc., see for instance [14]. Walls with little reinforcement, i.e., walls W2 and W3, develop a kind of shear failure near initial cracking load. This can partly be seen in Figure 8 where the crack pattern in the W2-wall and the W7-wall is shown at a load of *P*=250kN, i.e., just after initial cracking. As seen, the W2-wall is cracked through the section, while only a few elements have cracked in the W7-wall. Due to the steel bars around the openings, the capacity of the W2-wall is nevertheless not exhausted. Here, as for the simulation of the experimental data, it is difficult to compute the ultimate load.

From Figure 8, it can also be seen that increasing reinforcement increases wall resistance. For instance, the W2-wall resists a load of approximately 410kN at a 4mm deflection. For the same deflection, the resisting load is 15%, 30%, 57%, 40% and 70% higher than this, for the W3-, W4-, W5-, W6- and W7-walls, respectively. In Figure 9, the steel stresses in the element to the right of the right window shown in Figure 6 (dot A) are shown as a function of deflection. From Figure 9, it can be seen, for example, that for the W2-wall the steel stresses at the observation point yield at approximately a 1.5mm deflection. For the W7-wall, the steel yields at the same point at a deflection of 5.5mm.

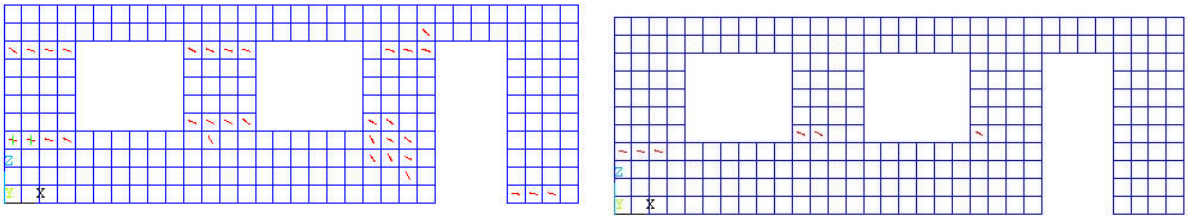

(a) W2 (b) W7

Figure 8 - Initial cracking in wall W2 and W7 at a load of 250kN.

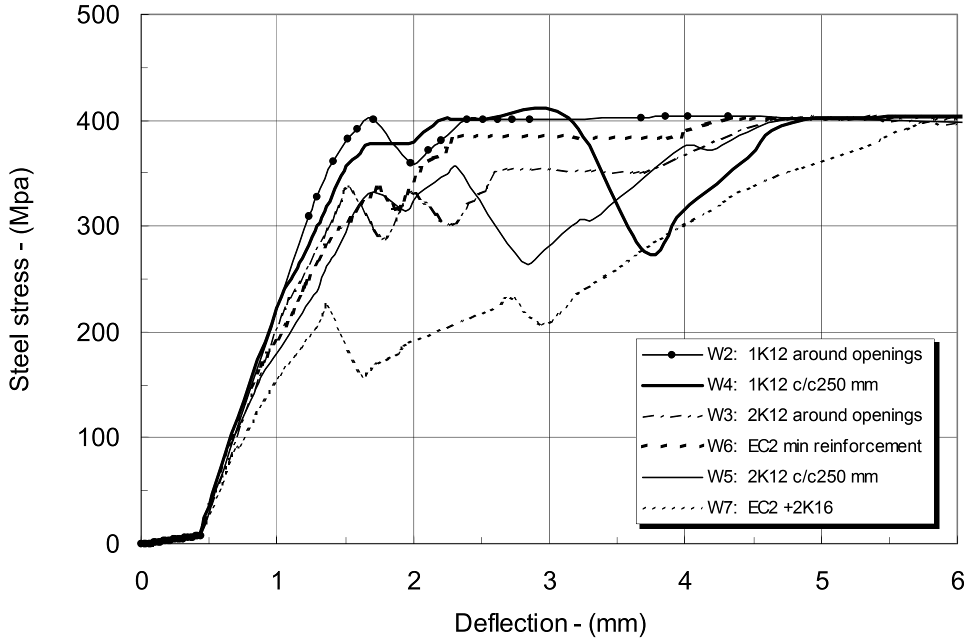

Figure 9 – Computed steel stresses at point A in Figure 6 for different reinforcement configurations as a function of deflection.

4. EARTHQUAKE RESPONSE

4.1 Tectonic

In June 2000, two major earthquakes occurred in the South Iceland Lowland (SIL). The first earthquake occurred on June 17, 2000, 15:41, (GMT). The moment magnitude has been estimated as M_w=6.6, the earthquake epicentre at 63.97°N and 20.36°W and the focal depth 6.3km, approximately. The second earthquake occurred on June 21, 2000, 00:52, (GMT). The moment magnitude has been estimated as M_w=6.5, the earthquake epicentre at 63.97°N and 20.71°W, and the focal depth as 5.3km, approximately. Observed surface fissures were found in a 20-25 km north-south elongated area i both earthquakes. Both events were right-lateral strike-slip earthquakes.

4.2 Strong motion records

The Earthquake Engineering Research Centre of the University of Iceland (EERC-UI) operates the strong motion network in Iceland. During the South Iceland earthquakes of June 2000, a number of records were recorded in the SIL. In the village Hella, with approximately 700 inhabitants, many houses were damaged in the first earthquake. The distance from the village to the closest surface fault rupture was only 2 to 3km. In this earthquake, the recorded horizontal peak ground acceleration (PGA) was 0.47g, see [15]. At the Kaldárholt Farm the residential house was damaged during the first earthquake and deemed un-repairable. The shortest distance between the farm and the surface fault rupture was 6km. The recorded PGA at the farm was 0.62g. In [15], elastic response spectra and constant-ductility response spectra for Hella and Kaldárholt are presented.

4.3 Earthquake response of residential houses

In this section the shear wall geometry used in the pushover analysis is assumed to be an exterior wall of an idealised 8×15m rectangular building with 150mm thick concrete roof slab. Furthermore, it is assumed that the lateral stiffness of the opposite exterior wall is identical, and that there are no parallel interior walls resisting lateral loads. Then the shear wall will resist 50% of the horizontal earthquake force in the longitudinal direction of the wall. It is estimated that the tributary weight of the roof slab and the roof structure, resisted by the shear wall, is 255kN, and that the half weight of the wall is 36kN, total W=291kN. Hence, most of the tributary weight is at the top of the shear wall. The wall can be assumed to resist earthquake forces as a single degree of freedom (SDOF) system, with the resisting forces defined by the capacity curves. This is shown schematically in Figure 10. For small earthquake loads, the wall would behave elastically, and for larger forces, exceeding the initial crack force, the wall would respond non-linearly. Using the initial stiffness of the system before cracking, the elastic natural period can be estimated from the capacity curve as:

$$T_E = 2\pi\sqrt{\frac{M}{F_Y / D_Y}} \tag{1}$$

where F_Y=240kN is the initial crack force; D_Y= 0.44mm is the initial crack deflection; $M=W/g$ is the tributary mass of the system, and g is the acceleration of gravity. Based on this, the elastic natural period is found to be T_E=0.046s. The so-called seismic coefficient, $S_A(\xi, T_E)$, where ξ is the damping ratio, and T_E is the elastic natural period of an SDOF-system, is a well-known parameter in the field of earthquake engineering, see for instance [16]. It is computed as a function of the two above parameters for a given acceleration time history, and presented in the form of so-called response spectra. Multiplying the mass of the SDOF-system by the seismic coefficient gives the maximum earthquake force on the system for the given acceleration time histories, i.e.:

$$F = M \cdot S_A(\xi, T_E) \tag{2}$$

For an appropriate damping ratio for the wall, the seismic coefficient has to be greater than F_Y/M=0.82g in order to initiate cracking and inelastic response of the walls. If the seismic coefficient is lower than this the wall will respond elastically and stay uncracked.

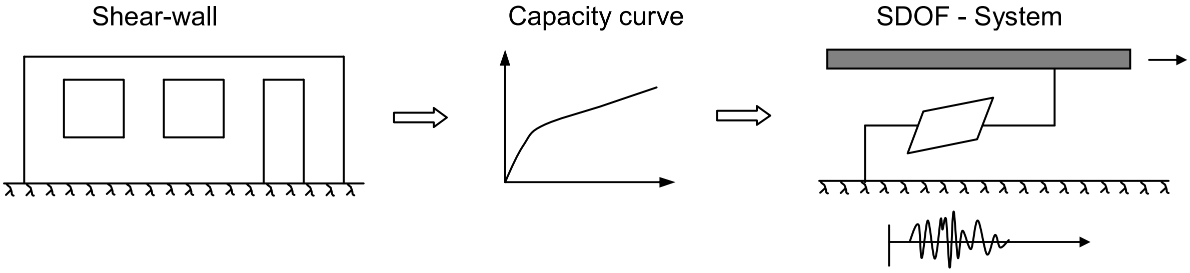

Figure 10 – Non-linear SDOF model of the shear walls, using the capacity curves to define the skeleton of the hysteresis rule.

In Figure 11, the linear elastic response spectra, for a 2% damping ratio is shown at the village Hella and at Kaldárholt Farm. The spectra are based on recorded acceleration time histories at these two sites during the South Iceland earthquake of June 17, 2000. Both components at each place are shown. The "crack point" for the shear walls (T_E= 0.046s, S_A= 0.82g) is also shown on the plot.

According to Figure 11, the shear wall would have behaved elastically at Hella during the June 17, earthquake, even if it had been unreinforced. However, it should be kept in mind, as can be seen in [1], that walls with weaker concrete, i.e., C16, which is common in older houses, are more flexible and have a lower yield point. Further, more unfavourable wall geometries, i.e., more openings, also, reduce its capacity.

If the wall would have been in Kaldárholt, see Figure 11, then the earthquake forces would have exceeded the elastic capacity of the wall, and yielding of the wall would have occurred. This would have been the case for both the horizontal components of the earthquake. The inelastic earthquake response of the walls can be estimated by using the capacity curves to define the skeleton of a hysteresis rule for the SDOF-system, and then by using time-history analysis and step-by-step integration [9]. Below, this method is applied to the W2- and W7-walls, using the N-S acceleration time histories from Kaldárholt as excitation, see Figure 12.

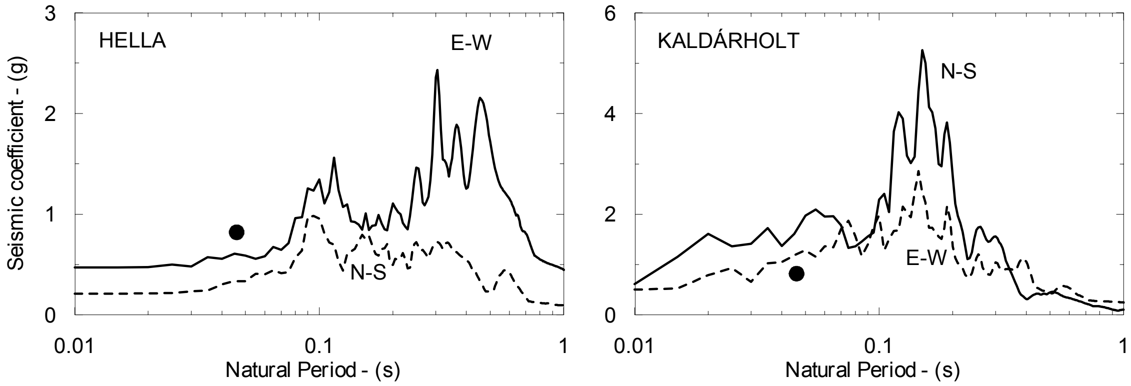

Figure 11 - Linear elastic response spectra with 2% damping ratio at Hella and Kaldárholt, based on the South Iceland earthquake of June 17, 2000. Both the horizontal components are shown. The dot shows the crack point for the shear wall in Figure 6.

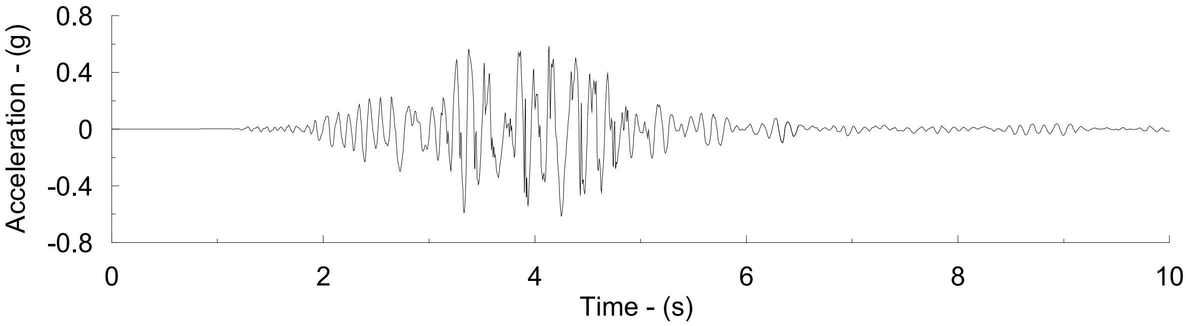

Figure 12 – The recorded N-S acceleration component in Kaldárholt during the South Iceland Earthquake of June 17, 2000.

In Figure 13, the W2 and W7 capacity curves have been fitted by bilinear curves. These curves are used to define a bilinear hysteresis rule for the system, see Figure 10. The program Ruaumoko [17] is used for the analysis. The results are given in Table 2. The calculated deflections are low and do not exceed the limits of the bilinear curve in Figure 12, meaning that the bilinear fit is acceptable. The results indicate that the wall type W7 would have resisted the severe earthquake excitation in Kaldárholt with low ductility demand, μ=1.7, and limited cracking. The pushover analysis, showed that for this ductility, the steel stresses are about 50% of the steel yield stress, see Figure 9. On the other hand, the W2-wall only has reinforcement around openings, and as soon the wall cracks, they will very probably be severe. Recalling from Figure 5 that for P=250kN, it should be noted that the cracks in the W2-wall already stretched between the openings. In the above, no attempt has been made to consider the effect of cumulative damage and strength degradation due to the cycling earthquake load.

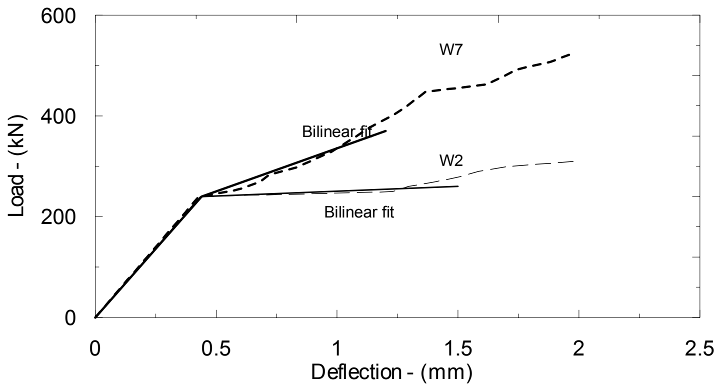

Figure 13 - Capacity curves for shear walls W2 and W7 from Figure 7 fitted with bilinear curves.

Table 2 - Earthquake response of the W2 and W7-walls, modelled by bilinear SDOF-system and excited by the recorded N-S acceleration component from Kaldárholt in the South Iceland earthquake of June 17 2000.

Wall types	Maximum deflection	Ductility demand	Shear force	Seismic coefficient
W2	0.97 mm	2.1	249 kN	0.86 g
W7	0.76 mm	1.7	296 kN	1.02 g

5. SUMMARY AND CONCLUSIONS

Nonlinear pushover analysis was carried out for low-rise, reinforced, concrete shear walls with openings. All the walls had the same type of concrete and geometry but different reinforcement configurations. The reinforcement varied from none to Eurocode 2 minimum requirements with extra reinforcements around openings. The results clearly indicate that changing the reinforcement greatly affects the capacity of the walls. The analysis indicated that all the walls crack at the same load level. Walls with little reinforcement developed shear failure just after the initial crack load. The crack widths were not evaluated, but it is likely that these cracks are open and severe as soon as they form. Such severe cracks were observed in the damaged houses with poor reinforcement in the South Iceland earthquakes of June 2000. The model showed that well reinforced shear walls distributed the cracks over a greater area than the poorly reinforced walls, and these cracks are generally more closed, especially when the steel is below the yield point. The analysis also indicated that the capacity of the shear wall is highly affected by the reinforcement around the openings.

Two of the analysed shear walls were assumed to be an exterior wall in a single story, 120-m^2 residential house with a roof slab. One of the walls had poor reinforcement, while the other was properly reinforced. The walls were supposed to resist 50% of the lateral earthquake load on the house in the longitudinal direction of the walls. From the capacity curve, the so-called crack point could be found, defined by the elastic natural period and the crack capacity of the walls. This crack point was then compared with the elastic demand spectra developed from the South Icelandic earthquakes of June 17, 2000. The response spectra were based on recorded data from the Kaldárholt Farm and the village of Hella. In both these places, severe damage was experienced during the June 17 earthquake. The comparison indicated that the crack limits for the walls was not exceeded at Hella. In Kaldárholt the crack limits were exceeded, and the walls would be subjected for inelastic response. Nonlinear dynamic analysis indicated that the poorly reinforced wall would probably be seriously damaged in the June 17 earthquake, while the more properly reinforced walls would have resisted the severe earthquake excitation with minor or no damage. When evaluating the results, it should be kept in mind, that the concrete strength in the analysis was relatively high with respect to the older buildings. Furthermore, mean values were used in the analysis, and strength distribution and/or degradation were not considered.

The study shows that nonlinear pushover analysis is a realistic and reliable method for evaluating the structural response of reinforced concrete structures in seismic zones. In further studies, shear walls with different geometries, reinforcement layout and material properties should be analysed as well as existing walls that failed in the South Iceland earthquakes of June 2000. Furthermore, the method can be used in the design of new structures and in repairing and retrofitting structures as well as in code calibration and risk assessment.

ACKNOWLEDGEMENTS

The Icelandic Concrete Association supported this work. This support is gratefully acknowledged

REFERENCES

1. Sigfússon Th., *Nonlinear analysis of reinforced concrete shear walls in low-rise Icelandic residential Buildings,* Master Thesis, University of Iceland, 2001.
2. Hemmaty, Y., De Roeck G., Vandewalle, L. & Mortelmans, F., Parametric study of RC corner joints subjected to positive bending moment by a nonlinear FE Model, *ANSYS Conference*, Pittsburgh, PA, 1992.
3. Chen, W.F. *Plasticity in reinforced concrete*, John Wiley & sons, Inc, New York, 1982.
4. ASCE Committee 447 on finite element analysis of reinforced concrete. *State-of-the-art report on finite element analysis of reinforced concrete*, American Society of Civil Engineering (ASCE), 1982.
5. ANSYS Engineering Analysis System. *User and Theoretical Manual*. ANSYS, Inc. Southpointe, Canonsburg, Pennsylvania, Version 5.6.2, 1998.
6. Hemmaty Y. Modeling of the shear force transferred between cracks in reinforced and fibre reinforced concrete structures, *ANSYS Conference*, Pittsburgh, PA, 1998.
7. Bresler, B. & Scordelis, A.C., *Shear strength of reinforced concrete beams*, Institute of Engineering research, University of California Berkeley, California, 1964.
8. Barda, F., *Shear strength of low-rise walls with boundary elements*, Ph.D. Thesis, Lehigh University, Bethlehem, Pennsylvania, 1972.
9. Fajfar. P., Capacity spectrum method based on inelastic demand spectra, *Earthquake Engineering and Structural Dynamics*, 1999; 28(9): 979-93.
10. Chopra, A.K. & Rakesh K.G, Capacity-demand-diagram methods based on inelastic design spectrum, *Earthquake Spectra*, 1999; 15(4): 637-56
11. Sigbjörnsson, R., Bessason, B., Sigfússon, Th.I., Sigfússon, Th., & Thorvaldsdóttir, S., Earthquake risk mitigation in South Iceland, *Proceedings of the Eleventh European Conference on Earthquake Engineering*, Balkema, Rotterdam, 1998.
12. CEN, *Eurocode 2 – Design of concrete Structures – Part 1: General rules and rules for buildings,* (ENV 1992-1-1), CEN, Berlin, 1991
13. Shayanfar, M.A., Element size effects in nonlinear analysis of reinforced concrete members. Computers & Structures, 1997; 62(2); 339-52.
14. Paulay, T. & Priestley M.J.N., *Seismic Design of Reinforced Concrete and Masonry Buildings,* John Wiley & Sons, Inc., New York, 1992.
15. Sigbjörnsson, R., Snaebjornsson, J., Ólafsson, S., Bessason, B., Baldvinsson, G.I. & Thórarinsson, Ó., *Earthquakes in South Iceland*, Report no. 0001, Earthquake Engineering Research Centre, University of Iceland, 2000 (written in Icelandic).
16. Chopra, A., *Dynamics of Structures: Theory and Application to Earthquake Engineering,* Prentice-Hall, 2nd ed., 2000.
17. Carr, J., *Ruaumoko – program for inelastic dynamic analysis*, University of Canterbury, 1981-2000.

CORROSION PROTECTION IN PREFABRICATED ELEMENTS OF LIGHTWEIGHT AGGREGATE CONCRETE WITH OPEN STRUCTURE

Per Goltermann,
RAMBOLL, Bredevej 2, 2830 Virum, Denmark
Tel: +45 4598 6726, Fax: +45 4598 6302, e-mail: peg@ramboll.dk.

ABSTRACT

The current Danish Code-of-Practice for lightweight structures of lightweight concrete elements DS 420 [1] and the future European product standard for precast reinforced components of lightweight aggregate concrete with open structure prEN 1520 [2] allow both verification by testing of the corrosion protection of the structural reinforcement, but differ in their test methods, corrosion classifications and acceptance criteria.

The paper describes the results of an investigation and a test program to verify the current corrosion protection systems (cover, density, coating) and to verify the new test methods.

The conclusions are that a short-term test method is suitable and corresponds well to experience in practice and that the requirements in prEN 1520 lead to realistic assessments of the corrosion protection.

Keywords: Corrosion, testing, lightweight aggregate concrete, open structure.

1. INTRODUCTION

The use of pre-cast concrete elements of lightweight aggregate concrete with open structure (LAC) dominates the construction of offices and houses in Denmark. The LAC-elements are produced by roller-compaction of no-slump concrete [3, 4, 5, 6] and this process results in a concrete with more or less open structure and a more or less efficient corrosion protection. The LAC ranges in strength from 3 to 30 MPa and in dry density (ρ) from 500 to 2000 kg/m^3 as illustrated in Figure 1.

The Danish Code-of-Practice for lightweight structures of lightweight concrete elements DS 420 [1] prescribes an initial type-testing [4], which also includes a testing of the corrosion protection of the reinforcement. The future European product standard prEN 1520 [2] requires an initial type testing, including the corrosion protection.

The required test methods, classification of corrosion degrees in the tested samples and the acceptance criteria do, however, differ between the code and the product standard. This lead the Danish Association of Full-wall Element Producers (BIH) to finance an investigation and a testing of the corrosion protection (densities, covers and coating) in order to gain experience with the new European standards and establish an overview of the current corrosion protection.

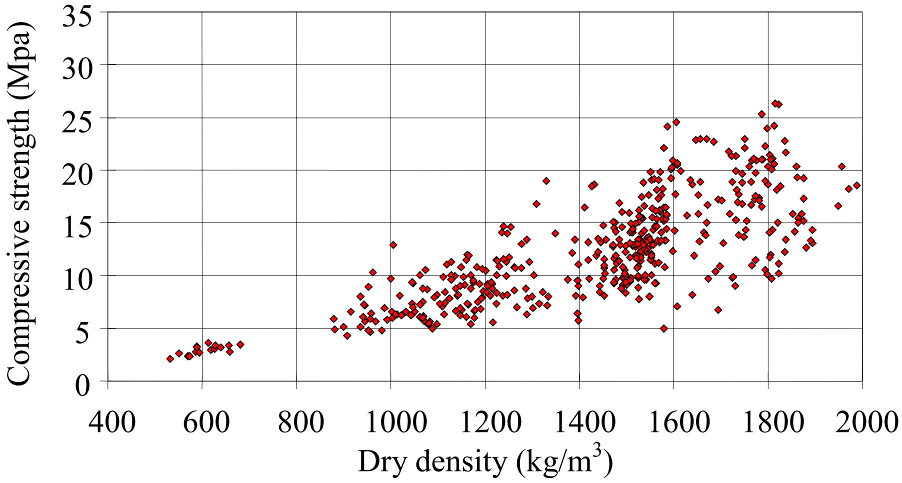

Figure 1. Dry density and compressive strength in current Danish LAC-production [3,4,5].

2. CURRENT PRACTICE

The current practice for the corrosion protection of structural reinforcement in precast lightweight aggregate concrete elements is that the reinforcement is either embedded in a fairly dense concrete with a high density (above 1200 kg/m^3 is usually found to be a realistic limit in the current Danish productions), or that the reinforcement is coated with a cement-latex coating and embedded in the LAC.

The elements are used for building structures and protected against rain and excessive amounts of water, which means that the elements are used either in passive environments or in moderate environments, where the relative humidity rarely exceeds 75 %. The elements are not subjected to salt and the risk of corrosion is therefore limited. The DS 420 [1] does, however require that one of the following procedures are followed:

- The corrosion protection of the reinforcement is tested annually,
- the reinforcement is embedded in dense concrete with a cover of 10 or 20 mm,
- the reinforcement is only used for transport purposes either in passive environments with no risk of corrosion or where any corrosion or corrosive products will not harm the elements performance.

This system seems so far to have worked well, as no observations of corrosion have been made in the moderate environment where the elements are intended to be used.

A large Norwegian investigation [9] and some Danish investigations [7,8] have looked into this by sampling reinforcement bars from roof or floor elements in slightly more aggressive environments, leading to the observations in Table 1.

The main conclusion from the Norwegian investigation was that the cement-latex coating gave a sufficient corrosion protection in the normal environments, where the relative humidity only occasionally exceeded 75 %.

Table 1. Observations in Norwegian and Danish structures. C-L denotes cement-latex coating and G galvanized surface. (Normal cover is 10 to 15 mm in this type of elements).

Id	Storage	Exposure time	ρ kg/m^3	Coating	Carbo-nated	Corrosion	Ref
	Outdoors	7 years	1400	C-L	Yes	Almost none	[7]
	Outdoors	7-10 years	1400	C-L	Yes	No	[8]
Type A	15-20^{o}C, 50%RF	24 years	1000	C-L	No	Rust on 2/3 of surface	[9]
Type C	25^{o}C, 60-90%RF	24 years	1000	G		No	[9]
Tovik 1	20-50^{o}C, 75-100%RF	15 years	1000	C-L	Yes	Surface rust	[9]
Tovik 2	20-50^{o}C, 75-100%RF	15 years	1000	C-L	Yes	Surface rust	[9]
Stjørdal 1	20-30^{o}C, 75-95%RF	15 years	1000	C-L	Yes	Surface rust	[9]
Vestnes 1	20-50^{o}C, 75-100%RF	12 years	1600	C-L	No	Rusty layer	[9]
Vestnes 2	20-50^{o}C, 75-100%RF	12 years	1600	C-L	Yes	Rusty layer	[9]
Vestnes 3	20-50^{o}C, 75-100%RF	12 years	1600	C-L	No	No	[9]

This conclusion is consistent with observations in normal concrete, where the concrete is able to protect the reinforcement in environments without chlorides, as long as the concrete is not carbonated. Reinforcement embedded in a carbonated concrete will corrode, but only slowly unless the relative humidity is above app. 80 % [10].

3. TEST PROGRAMME

3.1 Test methods

The testing of the corrosion protection can be carried out according to one of the four methods in EN 990 [11], which has been implemented in all CEN-countries since the mid-nineties. The four methods differ roughly in the following way:

- Method 1: The test specimens are exposed to 10 cycles of drying and soaking in salt water.
- Method 2: The test specimens are exposed to 30 cycles with drying in ventilated air for 21 hours at 40^{o}C, followed by wetting in tap water (2 hours at 20^{o}C), corresponding to the short-term method in DIN 4232 [12].
- Method 3: The test specimens are exposed to 4 daily temperature cycles between 25^{o}C and 55^{o}C in air with a RH > 95 % for a total of 28 days (corresponding to DS434.8 [13]).
- Method 4. The test specimens are stored for one year in humid air (RH > 95 %), corresponding to the long-term method in DIN 4232 [12].

It was decided to use methods 2 and 4 in the testing, as the method 4 was intended as the reference method in prEN 1520, while method 2 seemed to correspond best to the moderate environment, where the elements are used.

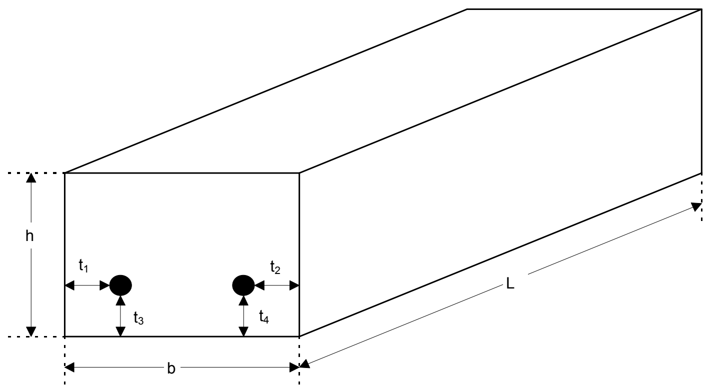

Figure 2. Geometry of the test specimens . (L = 400 mm, b = h = 100 mm, $t_1,\ldots,t_4$ = 10 or 20 mm).

3.2 Testing plan

It was decided to test the corrosion protection of the reinforcement in four representative concrete types, which are produced today in order to cover the most relevant density range (above 1000 kg/m^3). It was also decided to test the corrosion protection with and without a cement-latex coating and with two different cover depths, as shown in Table 2.

Table 2. Testing plan (the strength class denotes a lower characteristic value and the Danish producers associations density class denotes a lower density, including a certain water content).

Series	Strength class (MPa)	Density class (kg/m^3)	Intended cover (mm)	Coating
1	13	1800	10	No
2	13	1800	20	No
3	13	1800	20	C-L
4	9	1500	10	No
5	9	1500	20	No
6	9	1500	20	C-L
7	5	1200	10	No
8	5	1200	20	C-L
9	5	1200	20	No
10	5	1000	10	No
11	5	1000	20	C-L
12	5	1000	20	No

The test specimens were manufactured by three factories in the autumn 1997, by producing a number of precast elements with some of the concrete types and cement-latex coatings currently used in their productions.

All the 12 test specimens in each series were cut from the same element and each specimen contains two Ø 10 mm reinforcement bars. The 144 specimens were coated on the ends as prescribed in EN 990, using Isopunkt [14] and transported to RAMBOLL's laboratory for the testing, which was carried out in 1997 and 1998 [15,16].

4. TEST RESULTS

The moisture contents were determined by weighing at the delivery (D) to RAMBOLL's laboratory and later at the end of the short-term testing, when the 36 specimens (S) and the corresponding 36 reference samples (SR) were opened and the reinforcement bar extracted. The same procedure was used for the 36 long-term tested specimens (L) and their 36 reference samples (LR).

Table 3. Results of the short-term testing (D denotes at delivery, S and SR denotes the value at the end of the short-term test for respectively the test samples and for the reference samples).

Series	Coating	ρ (kg/m^3)	Moisture content (% by mass) D	Moisture content (% by mass) S	Moisture content (% by mass) SR	Cover (mm) Mean	Corroded area (%) S	Corroded area (%) SR 2)
1	No	1911	3.9	3.6	2.2	12.3	8.3	2.9
2	No	1949	3.9	3.7	2.4	21.5	2.6	6.8 1)
3	C-L	1938	3.7	3.9	2.4	18.1	0.0	0.2
4	No	1577	4.2	4.8	2.4	13.6	1.7	1.1
5	No	1563	4.4	4.8	2.7	18.2	2.2	1.3
6	C-L	1586	4.3	4.4	2.9	22.4	0.0	0.0
7	No	1134	16.2	10.7	6.4	12.2	21.7	6.9
8	C-L	1166	13.8	9.8	6.0	20.4	0.6	0.7
9	No	1133	14.7	9.9	6.0	19.0	7.5	6.0
10	No	1048	15.2	7.5	3.4	7.9	12.2	0.9
11	C-L	1074	9.8	8.2	3.2	17.6	0.1	0.0
12	No	1065	10.9	7.9	3.8	18.2	5.3	0.1

Note 1): The measurement of the corroded area along one of the lines of one of the bars did show an extreme degree of corrosion. Ignoring this extreme observation will lead to a decrease of the corroded area from 6.9 % to 3.9 %.
Note 2): The reinforcement bars were selected from the bars used in the normal production in the factories and had in some cases a minor amount of corrosion before the castings.

Table 4. Results of the long-term testing (D denotes at delivery, L and LR denotes the value at the end of the long-term test for respectively the test samples and for the reference samples).

Series	Coating	ρ (kg/m^3)	Moisture content (% by mass) D	Moisture content (% by mass) L	Moisture content (% by mass) LR	Cover (mm) Mean	Corroded area (%) L	Corroded area (%) LR 2)
1	No	1918	3.7	8.4	1.7	12.2	0.8	1.8
2	No	1941	3.7	8.2	1.6	21.6	1.9	1.7
3	C-L	1933	3.6	8.9	1.7	18.9	0.5	0.4
4	No	1576	4.4	5.5	2.0	11.9	1.3	1.3
5	No	1568	4.4	5.6	2.0	18.0	2.1	1.0
6	C-L	1588	4.5	5.5	2.1	23.7	0.0	0.0
7	No	1129	15.5	16.2	3.5	12.1	5.9	6.3
8	C-L	1162	14.4	15.2	3.7	20.8	1.1	1.1
9	No	1130	14.3	16.8	3.1	18.4	6.9	4.5
10	No	1063	13.5	13.5	2.0	10.3	1.4	1.7
11	C-L	1077	8.9	13.8	2.2	21.0	0.0	0.0
12	No	1069	11.2	12.3	2.1	20.8	1.1	0.1

Note 2): See note 2 to Table 3.

The weight of the remains of each specimen were then determined before and after the oven drying in order to determine the moisture contents, listed in Tables 3 and 4.

The corroded area was measured along four lines on each reinforcement bar, ignoring the 50 mm near the specimens ends and the average values from the 2*3=6 bars are listed in the Tables 3 and 4. The average of the four cover depths from Figure 2 measured on each specimen are also listed in Tables 3 and 4.

A sample was taken from one of the specimens of the four concrete types used in the long-term testing and plane-sections and thin-sections were produced in order to determine the structure of the LAC as shown in Figure 3.

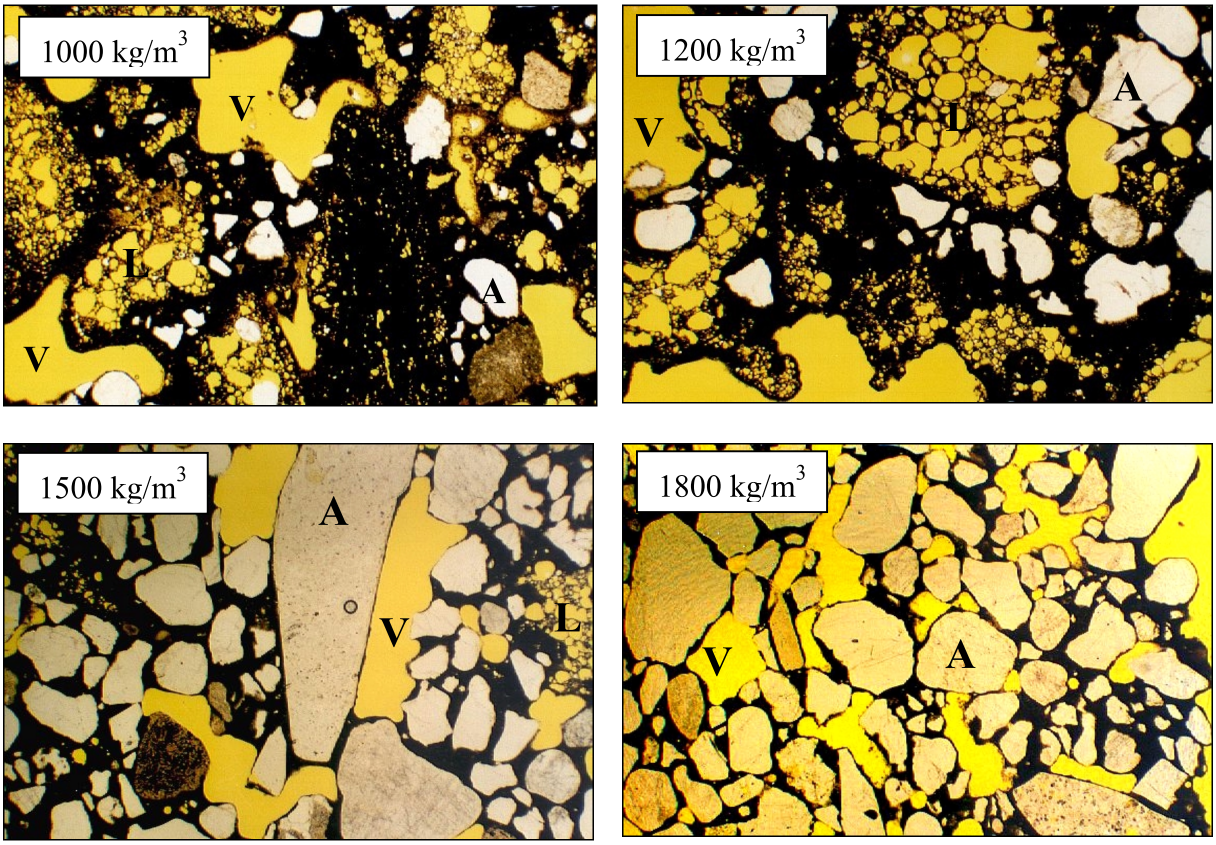

Figure 3. Thin-sections images (4 x 3 mm) of different typical types of lightweight aggregate concrete. A denotes aggregate, L lightweight aggregate and V voids.

The density classes of 1000, 1200, 1500 and 1800 kg/m^3 shown in the Figures 3 and 4 correspond to average dry densities in the series of 1066, 1142, 1576 and 1932 kg/m^3.

Figure 4 illustrates the fact that the carbonation has progressed fairly deep into the concretes, but it also shows that the carbonation depth is not a function of the density. This is probably due to the fact that a low density can be obtained by a number of different combinations of air in fairly large voids in the concrete and of lightweight aggregates, so that a decrease of the amount of lightweight aggregate and an increase of large air voids may not change the density, but may make the concrete more porous and thus increase the carbonation depth.

Figure 4 also illustrates that the carbonation front is less clear than in ordinary concrete with dense structure, where the zone between the fully carbonated concrete and the non-carbonated concrete usually has an extension of app. 1 mm. Use of thin-section showed that the concrete in the long-term reference samples after 1 year in the laboratory had carbonated areas all through the samples, but that isolated pockets of non-carbonated concrete were found, even near the surface.

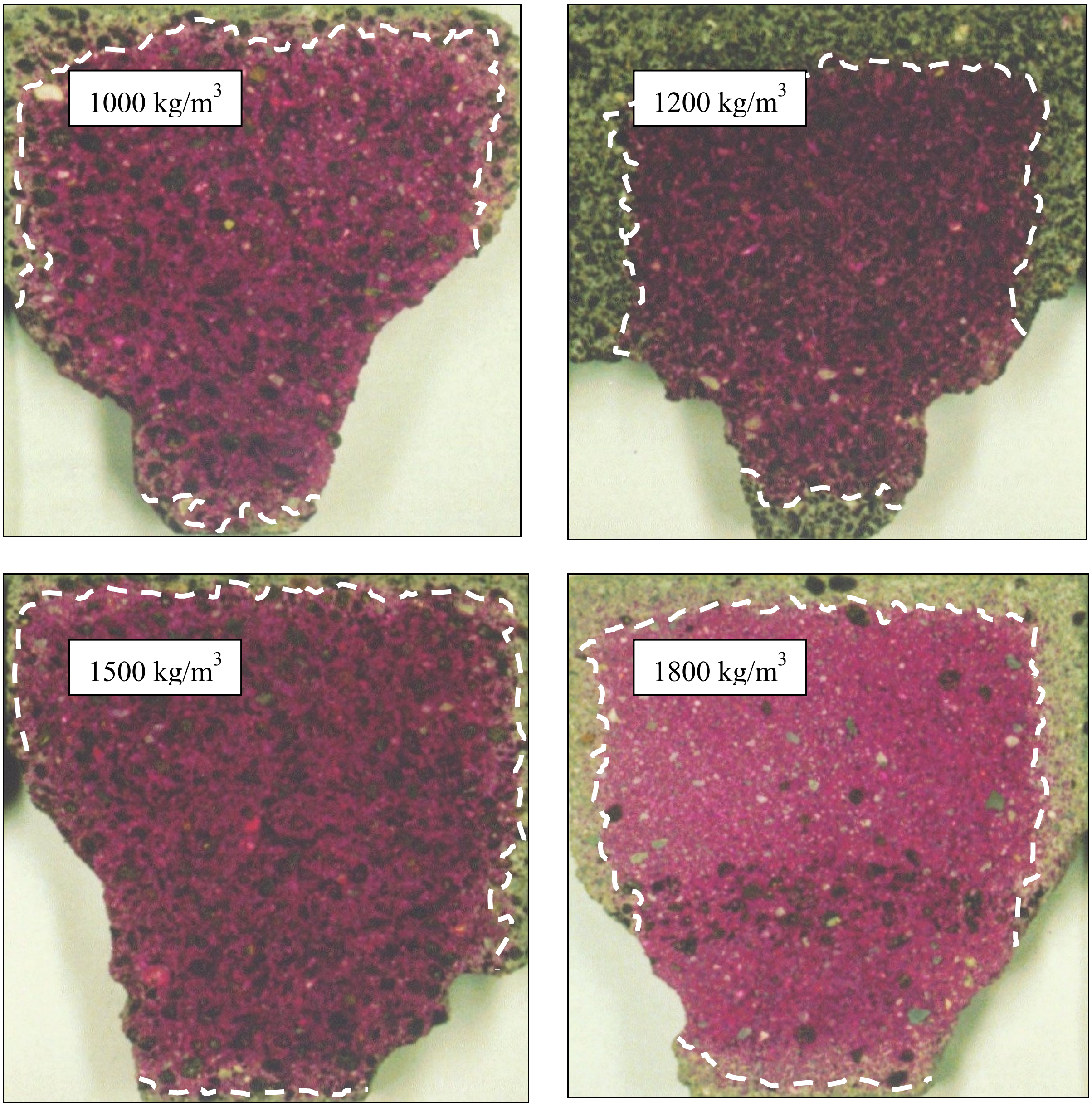

Figure 4. Cross-sections (10 x 10 cm) from long-term testing. Dark (violet) colour marks the non-carbonated parts of the reference samples. The frames indicate the original cross-section before the extraction of the bars and the dashed curves the approximate carbonation front.

4.1 Other results

A few other results of corrosion testing with the same or similar test methods have been obtained from different sources as shown in Table 5. The corrosion protection was approved in all cases.

Table 5. Other test results.

Id	Test method	ρ kg/m^3	Cover mm	Coating	Corrosion	Ref
	84 cycles of 4 hours at 55°C and 4 hours 20°C at 100 % RF	1470	15	No	None	[17]
LBH 8/1.6	DIN 4232, Short-term	1614	18/20	No	Negligible	[18]
LBH 8/1.6	DIN 4232, Long-term	1614	18/20	No	Negligible	[18]
LBH 8/1.8	DIN 4232, Short-term	1848	18/20	No	Negligible	[18]
LBH 8/1.8	DIN 4232, Long-term	1848	18/20	No	Negligible	[18]
LB 5/1.2	DIN 4232, Short-term	1248	20	No	None	[19]
LB 8/1.6	DIN 4232, Short-term	1647	20	No	None	[19]
LB 8/1.8	DIN 4232, Short-term	1818	20	No	None	[19]

5. EVALUATION OF RESULTS

5.1 Rules for classification of degrees of corrosion.

The Danish Code-of-Practice DS 420 prescribes that testing of the corrosion protection should be carried out according to DS 434.8 [13], and that the corrosion degree must be classified according to the Swedish standard SIS 18 51 11 [20] "Europeisk rostgradsskala för rostskyddsfärger (European corrosion scale for protective paints)".

SIS 18 51 11 was published in 1964, but has been withdrawn in 1985 and is not easily obtained. It was, however, replaced by SS 18 42 03 [21], which is identical to ISO 4628-3 "Paint and varnisches - Evaluation of degradation of paint coatings - Designation of intensity, quantity and size of common types of defects - Part 3: Designation of degree of rusting" [22].

ISO 4628-3 uses a scale for the degree of corrosion (from 0 to 5), which does not correspond to the scale in SS 18 51 11 (from 0 to 9). The ISO 4628-3 presents, however, both a typical picture and a percentage of corroded surface for each step in the scale, whereas the SS 18 51 11 only defines the scale by a typical picture for each level.

Table 6. Corrosion degree classification in ISO 4628-3 and the correlation to the scale in SIS 18 51 11 as prescribed in ISO 4628-3 (Corroded area 40/50 indicates 40 to 50 %).

ISO 4628-3	European classification SIS 18 51 11	Corroded area %
Ri 0	Re 0	0
Ri 1	Re 1	0.05
Ri 2	Re 2	0.5
Ri 3	Re 3	1
	Re 4	5 (interpolated)
Ri 4	Re 5	8
	Re 6	10/20 (interpolated)
Ri 5	Re 7	40/50

5.2 Acceptance criteria in DS 420 and prEN 1520

The Danish code DS 420 specifies the following criteria for the reinforcement to be regarded as adequately protected:

- if the degree of corrosion for one or more of the non-corrosion tested reference steels is 0-2, the degree of corrosion for the steel in the corresponding corrosion tested prim(s) should not exceed 3, or
- if the degree of corrosion for one or more of the non-corrosion tested reference steels is 3-6, the degree of corrosion for the steel in the corresponding corrosion tested prism(s) should not exceed this value by more than 1.

The test standard DS 434.8 specifies that the degree of corrosion is determined by comparison to the pictures in the European corrosion degree scale for corrosion protection measures SIS 18 51 11 [20].

The European standard prEN 1520 requires testing according to at least one of the three short-term test methods in EN 990 and approves the corrosion protection in the following situations:

- if the steel surface is free from corrosion or if only first signs of corrosion (no flaky rust or pitting) are visible in separate places which are approximately uniformly distributed over the bars and cover not more than 5 % of the steel surface, or
- if the area of corrosion does not exceed by more than 5 % that observed on bars of the corresponding reference specimens stored in a non-corrosive atmosphere at a relative humidity $\leq$ 70 %, or
- if the reduction of the rust grade number is not greater than 1.

It is clearly specified in EN 990 that the corrosion is primarily described by the percentage of the surface, which shows sign of corrosion, whereas the use of the European scale is only mentioned in a footnote: ”In some countries the effect of the corrosion test is judged by the reduction of the rust grade according to the European Scale for degree of rusting. The rust grade of the reference bars and that of the exposed bars are determined. The reduction in rust grade number is calculated by subtracting the rust grade of the exposed bars from that of the reference bars. The effect of the protective system is assumed to be satisfactory if the reduction of the rust grade number is not greater than 1”.

5.3 Evaluation of test results

The evaluation of the test results has been carried out on the basis of the measured percentage of corroded area, as required in EN 990. The Table 6 has been used for the classification according to SIS 18 51 11 and ISO 4628-3.

The evaluations of the results of the short-tem testing is presented in Table 7 and the similar evaluation of the results of the long-term testing is presented in Table 8.

Table 7. Evaluation of the short-term testing.

Series	ρ (kg/m^3)	Cover (mm)	Coa-ting	Classification by ISO 4628-3		Classification by SIS 18 51 11		DS420	PrEN1520
				S	SR	S	SR		
1	1911	12.3	No	Ri 4	Ri 4	Re 5	Re 4	Passed	Passed
2	1949	21.5	No	Ri 3/4	Ri 3/4	Re 4	Re 5	Passed	Passed
3	1938	18.1	C-L	Ri 2	Ri 2	Re 2	Re 2	Passed	Passed
4	1577	13.6	No	Ri 3	Ri 3	Re 3	Re 3	Passed	Passed
5	1563	18.2	No	Ri 3	Ri 3	Re 3	Re 3	Passed	Passed
6	1586	22.4	C-L	Ri 0	Ri 0	Re 0	Re 0	Passed	Passed
7	1134	12.2	No	Ri 4/5	Ri 3/4	Re 6	Re 4/5	Rejected	Rejected
8	1166	20.4	C-L	Ri 2/3	Ri 2/3	Re 2/3	Re 2/3	Passed	Passed
9	1133	19.0	No	Ri 4	Ri 4	Re 4/5	Re 4/5	Passed	Passed
10	1048	7.9	No	Ri 4/5	Ri 3	Re 5	Re 3	Rejected	Rejected
11	1074	17.6	C-L	Ri 1	Ri 1	Re 1	Re 1	Passed	Passed
12	1065	18.2	No	Ri 3/4	Ri 1	Re 4	Re 1	Rejected	Rejected

Table 8. Evaluation of the long-term testing.

Series	ρ (kg/m^3)	Cover (mm)	Coa-ting	Classification by ISO 4628-3		Classification by SIS 18 51 11		DS420	PrEN1520
				L	LR	L	LR		
1	1918	12.2	No	Ri 3	Ri 3	Re 3	Re 3/4	Passed	Passed
2	1941	21.6	No	Ri 3/4	Ri 3	Re 3/4	Re 3/4	Passed	Passed
3	1933	18.9	C-L	Ri 2	Ri 2	Re 2	Re 2	Passed	Passed
4	1576	11.9	No	Ri 3/4	Ri 3	Re 3/4	Re 3	Passed	Passed
5	1568	18.0	No	Ri 3/4	Ri 3	Re 3/4	Re 3	Passed	Passed
6	1588	23.7	C-L	Ri 0	Ri 0	Re 0	Re 0	Passed	Passed
7	1129	12.1	No	Ri 3/4	Ri 3/4	Re 4	Re 4	Passed	Passed
8	1162	20.8	C-L	Ri 3	Ri 3	Re 3	Re 3	Passed	Passed
9	1130	18.4	No	Ri 4	Ri 3/4	Re 5	Re 4	Passed	Passed
10	1063	10.3	No	Ri 3	Ri 3	Re 3	Re 3	Passed	Passed
11	1077	21.0	C-L	Ri 0	Ri 0	Re 0	Re 0	Passed	Passed
12	1069	20.8	No	Ri 1	Ri 1	Re 3	Re 1	Passed	Passed

The evaluation according to DS 420 in Tables 7 and 8 is independent of which of the corrosion classification systems, that has been used. The evaluations after prEN 1520 are all based on corrosion percentage and the ISO-classification.

The results of the short-term testing as a function of the cover and the density are shown in Figure 5. The results of the long-term testing are not illustrated, as all types passed the long-term testing.

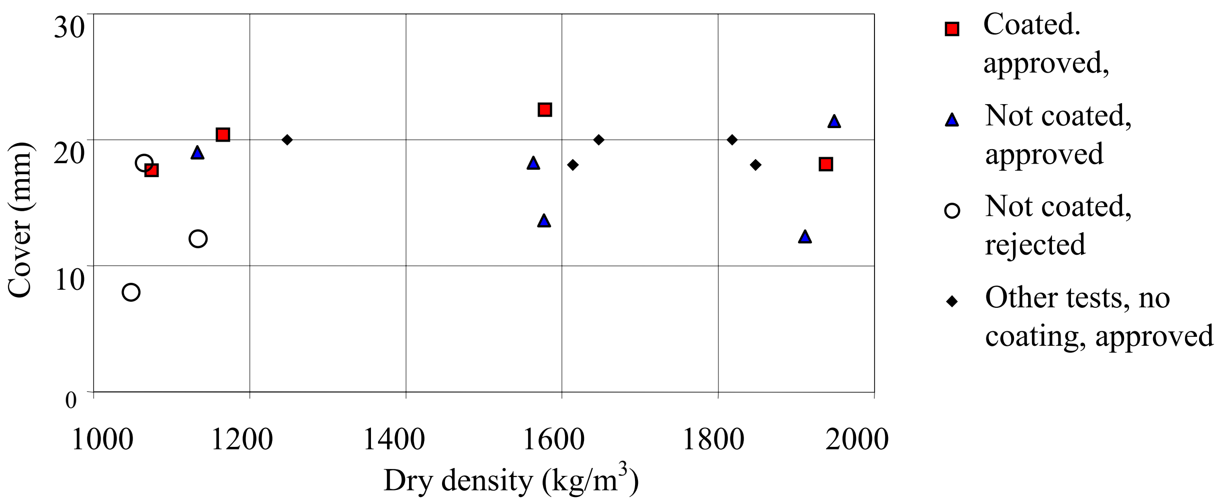

Figure 5. Result of short-term testing and evaluation of the corrosion protection.

6. CONCLUSIONS

The rules for classification of corrosion degrees and the acceptance criterias in DS 420 and in prEn 1520 are quite different, but lead to the same assessments in each of the tests and show that the corrosion protection is sufficient when the reinforcement is protected by a LAC-cover of at least 10-15 mm and a density of more than 1200-1500 kg/m^3 or when the reinforcement is coated with a cement-latex coating. The DS 420 and the prEN 1520 do, however, still prescribe a mandatory initial testing and an annual testing of the corrosion protection, in order to prevent corrosion problems due to changes in the production, mix design or coating.

The corrosion classification rules and the acceptance criterias in DS 420 can therefore be replaced by the use of the percentage of corroded surface areas, when the acceptance criterias in prEN 1520 are used.

The results of the short-term testing (EN 990, method 2) corresponds well with the current practice and the few observations from practice.

The long-term testing (EN 990, method 4) have so far approved the corrosion protection in all the tests, independent of coating, cover or density of the concrete. This indicates that the long-term testing may be un-conservative and should not be used.

The test method EN 990 is currently under revision and the enquiry version prEN 990 [23] has actually removed the long-term testing. The revision has also removed the corrosion classification by a certain corrosion degree class and uses solely the corroded surface area to describe the test results with.

7. ACKNOWLEDGEMENT

The work has been funded by the Danish Association of Full-wall Element Producers (BIH). The production of elements and the preparation of samples have been carried out by the producers H+H FIBOMENT and Betonelement.

8. REFERENCES

1 DS 420 “DIF’s norm for letbetonkonstruktioner af letbetonelementer (The Association of Danish Engineers Code of practice for the structural use of lightweight concrete)”, 1983.
2 prEN 1520 “Prefabricated reinforced components of lightweight aggregate concrete with open structure”, Final draft January 2001.
3 Goltermann, P.: “Prefabricated floor slabs in roller-compacted lightweight aggregate concrete”, 2nd International Symposium on Structural Lightweight Concrete, 18-20 June, 2000, Norway
4 Goltermann, P.: ”Design by Testing”, pp.22-28, 44. Ulmer Beton- und Fertigteil Tage, February 1-3, 2000, FBF Betondienst Gmbh, Germany.
5 Larsen, H.; Goltermann, P. and Ingholt, N.U.: "Lightweight aggregate concrete beams. Load-bearing capacity", pp.42-58, Nordic Concrete Research, No.20, 1997.
6 Goltermann, P., Larsen, H. and Ingholt, N.U.: "Strength and stiffness relations in lightweight aggregate concrete with open structure", Nordic Concrete Research, pp.35-46, No.15, 1994.
7 Letter from Dantest to Dansk Leca A/S, Dantest B 20212N, 1985.
8 Letter from the Danish Lightweight Concrete Control (LBK), 02-09-1987.
9 Moen, T.I. : ”Korrosjon på armering i letklinkerbetong”, Norsk Leca, September 1991.
10 Tuutti, Kyösti: “Corrosion of steel in concrete”, CBI, 1982
11 EN 990 “Test methods for verification of corrosion protection of reinforcement in autoclaved aerated concrete and lightweight aggregate concrete with open structure”, 1985
12 DIN 4232 “Walls of no fines lightweight concrete, design and construction”, 1987
13 DS 434.8 “Lightweight aggregate concrete. Testing of corrosion protection of reinforcement”, 1985.
14 Product from A/S Sygros, Køvervej 12, Seest, 6000 Kolding, tel. +45 7552 3200
15 Goltermann, P.: “Korrosionsbeskyttelse i letklinkerbeton. Testreport.”, January 1999, RAMBOLL.
16 Goltermann, P.: “Korrosionsbeskyttelse i letklinkerbeton. Konkluderende rapport”, March 1999, RAMBOLL
17 Testing attestation from Dantest for Midtjydsk Leca, Dantest B 20069, 1986.
18 Testing of corrosion protection in walls. A/S FIBO, July 1993 to August 1994.
19 Testing report from IBMB, 2 May 1996.
20 SIS 18 51 11 “Europeisk rostgradsskala för rostskyddsfärger”, 1964
21 SS 18 42 03 “Färg och lack - Bedömning av nedbrytning af färgskikt - Beteckning för intensitet, mängd och storlek av vanliga typer av fel - del 3: Beteckning för rostgrad”, 1985
22 ISO 4628-3 “Paint and varnisches - Evaluation of degradation of paint coatings - Designation of intensity, quantity and size of common types of defects - Part 3: Designation of degree of rusting”, 1982
23 prEN 990: ”Test methods for verification of corrosion protection of reinforcement in autoclaved aerated concrete and lightweight aggregate concrete with open structure”, Enquiry version, January 2001.

TEMPERATURE DEPENDENCY OF THE HYDRATION OF DENSE CEMENT PASTE SYSTEMS CONTAINING MICRO SILICA AND FLY ASH

Tommy B. Hansen
Ph.D., Project Manager
AALBORG WHITE® Technical Team
Aalborg Portland A/S
Rørdalsvej 44, P.O Box 165, DK-9100 Aalborg
E-mail: tbh@aalborg-portland.dk

ABSTRACT
The effect of curing temperatures of 5, 25 and 50°C on sealed cured cement paste samples containing between 7.5 and 25 % pozzolanic filler in the form of fly ash and micro silica at a water/powder ratio of app. 0.23 has been studied. The results indicate that the main effect of elevating the curing temperature is densification or crystallization of the hydrates, liberating significant amounts of surface adsorbed water and increasing the amount of chemically bound water.

Key words: Hydration, Temperature, Cement paste, Pozzolans.

1. INTRODUCTION

It is well documented that the amount of chemically bound water and the compressive strength of a Portland cement system decreases, when the curing temperature is increased beyond the usually applied reference temperature of 20°C[1,2,3,4,5]. At least this is the case in the normally used range of water/cement ratios (above 0.35 to 0.50[1,2,3,4,5]). There is some difference of opinion as to whether the addition of pozzolanic fillers like fly ash influences this tendency. Some observe an increase in strength at elevated curing temperatures when more than 10 % of fly ash is added[2], some a decrease for an addition as high as 30 %[4]. The degree of hydration however is reported to increase as a function of temperature, even at a water/cement ratio of 0.56[6].

The reason for the reduced strength at higher curing temperatures is believed to be the rapid formation of dense inner product hydrate layers on the surface of the cement grain, resulting in a reduced hydration rate[4] and an increased porosity. Micro cracks caused by thermal stresses and similar phenomenon may weaken the matrix further.

In denser systems with lower water/cement ratios, the effect of temperature is not as well documented. Some investigations on neat cement pastes have been conducted, suggesting that the main effect of increased curing temperature is visible through a densification of the inner product hydrates[7] and a corresponding increase in general porosity[8]. However, the low water/cement ratio systems are rarely applied using only neat cement pastes, rather they incorporate significant amounts of pozzolanic fillers such as fly ash and micro silica.

As part of an industrial Ph.D. study[9], the relation between curing temperature and chemically bound water content (often used as indicator for the degree of hydration and therefore as indicative for compressive strength) in dense cement pastes containing significant amounts of fly ash and micro silica, was established.

2. MATERIALS AND METHODS

The investigation was conducted on cement paste samples in a sealed cured state (no moisture transfer with the surroundings and therefore allowed to self-desiccate). The mix designs for the mixes are shown in Table 2, and the Bogue composition of the used cements is shown in Table 1. Elkem micro silica and Danaske fly ash were used. As superplasticizer, Glenium 51 was used (in solution, 35 % solids). Normal tap water was used.

Table 1: Chemical composition of the used cement types (Bogue). Both cements where ground to a Blaine fines of app. 400 m^2/kg in the laboratory.

Cement type	C_3S [%]	C_2S [%]	C_3A [%]	C_4AF [%]	Total [%]
"W": White cement	61.7	24.9	4.5	0.9	92.0
"M": Mineralised cement	63.0	10.0	8.0	11.0	92.0

Table 2: Mix designs for the investigated cement pastes. "W" in the beginning of the mix name symbolises white cement and "M" mineralized cement. "f" indicates percentage of fly ash, "s" percentage of micro silica. All percentages of dry powder weight.

Mix	Cement [%]	Fly ash [%]	Micro silica [%]
W-f5-s2.5	92.5	5.0	2.5
M-f5-s2.5	92.5	5.0	2.5
W-f15-s2.5	82.5	15.0	2.5
M-f15-s2.5	82.5	15.0	2.5
W-f5-s10	85.0	5.0	10.0
M-f5-s10	85.0	5.0	10.0
W-f15-s10	75.0	15.0	10.0
M-f15-s10	75.0	15.0	10.0

The mixes consisted of 500 g of powder (cement, fly ash and silica), and 100 g of water (water/powder-ratio 0.20). The super plasticizer was added to the mix without correction for water content (dosages ranging from 2 to 4 % by weight), and the materials contained some water, resulting in slightly varying water/powder ratios around 0.23. The cement pastes were first mixed under vacuum, and then cast and cured in sealed polypropylene micro tubes containing app. 2 ml. of cement paste.

The cured samples were dried to weight constant in a vacuum oven (CO_2-free drying) to establish the content of evaporable water, and subsequently burned at 975°C to weight constant to establish the amount of non-evaporable or chemically bound water. Six samples were cast for each mix/temperature/maturity combination and the average results used.

Since the reaction rate of cement is highly temperature dependent, it is necessary to compare the evaporable and non-evaporable water contents as a function of accumulated maturity M_θ, relative to the fixed temperature, θ, in order to compare the results obtained at different curing temperatures. Thus, the accumulated maturity of the samples is compared to what would have been achieved by curing the samples at 25°C, presuming constant activation energy of 33.5 kJ/mol (corresponding to ordinary Portland cement[10]), according to the Arrhenius function[11]. The curing time expressed in maturity hours is henceforth denominated $\tau(M_{25})$. The samples were allowed to cure to $\tau(M_{25})$: 3, 6, 20, 54 168 and 672 hours (from 0.125 to 28 days) at 5°C, 25°C and 50°C. Selected samples were investigated using Scanning Electron Microscopy (SEM) to determine differences in physical structure as a result of the different curing temperatures.

3. RESULTS

An example of the results is shown in Figure 1. The obtained water phase distribution at 28 days for the investigated mixes are presented in Table 3.

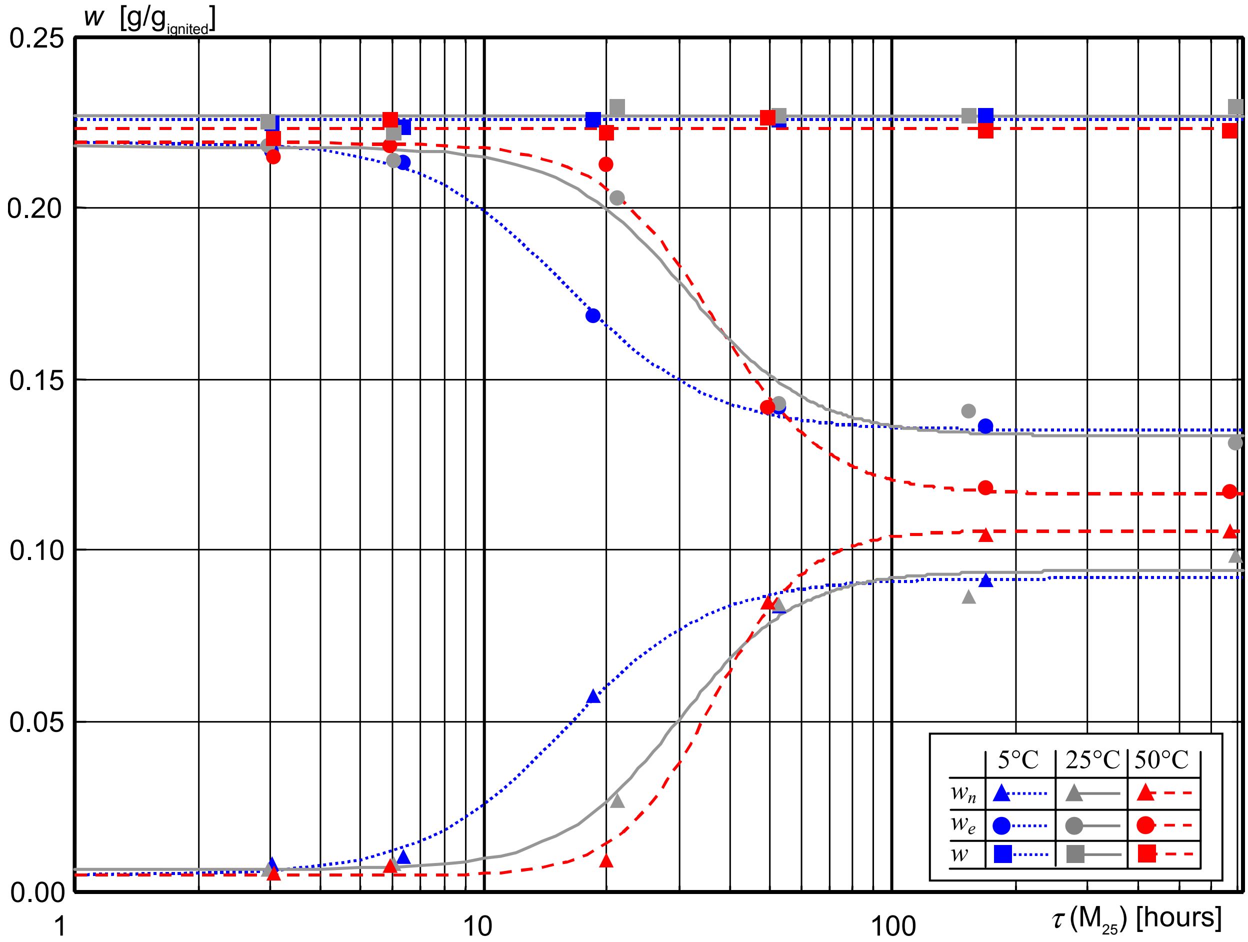

Figure 1: Water phase distribution development up to 28 days for cement paste W-f5-s2.5 cured in a sealed cured state at 5°C, 25°C and 50°C. w_n is the chemically bound water, w_e evaporable or physically bound water and w is total water content.

Table 3: Water phase distribution at 28 days M_{25} for the investigated cement pastes. All values are in gram water per gram ignited powder weight. w_n is the chemically bound water, w_e evaporable or physically bound water and w/p is total water content per gram powder.

	5°C			25°C			50°C		
Sample	w_n [g/g]	w_e [g/g]	w/p [g/g]	w_n [g/g]	w_e [g/g]	w/p [g/g]	w_n [g/g]	w_e [g/g]	w/p [g/g]
W-f5-s2.5	0.0947	0.1324	0.2271	0.0984	0.1312	0.2296	0.1056	0.1172	0.2228
M-f5-s2.5	0.0945	0.1381	0.2326	0.0899	0.1431	0.2330	0.1116	0.1078	0.2194
W-f15-s2.5	0.0859	0.1342	0.2201	0.0907	0.1364	0.2271	0.0971	0.1247	0.2218
M-f15-s2.5	0.0899	0.1385	0.2284	0.0887	0.1388	0.2275	0.1021	0.1216	0.2237
W-f5-s10	0.1004	0.1448	0.2452	0.1015	0.1461	0.2476	0.1039	0.1440	0.2479
M-f5-s10	0.0944	0.1492	0.2436	0.0954	0.1499	0.2453	0.0973	0.1417	0.2390
W-f15-s10	0.0945	0.1485	0.2430	0.0927	0.1555	0.2482	0.0931	0.1487	0.2418
M-f15-s10	0.0985	0.1498	0.2483	0.0970	0.1486	0.2456	0.0919	0.1454	0.2373
Average	**0.0941**	**0.1419**	**0.2360**	**0.0943**	**0.1437**	**0.2380**	**0.1003**	**0.1314**	**0.2317**

The apparent difference in the course of hydration between the curing temperatures in Figure 1 is mainly due to differences between presumed and actual temperature of the samples during the first few hours of curing. The samples were all mixed at 20°C, and it took one to two hours before the samples attained their intended curing temperatures at 5°C and 50°C. Hence the calculated maturities used for the plot deviates from the actually attained. Forthwith only the water phase distribution at 28 days is considered.

4. DISCUSSION

From Figure 1 and Table 3 it is evident that there is little difference between 5°C and 25°C on the final hydration ratio of the cement paste. A curing temperature of 50°C increases the amount of chemically bound water at the expense of physically bound water – additional strength giving hydrates are formed – contrary to the usual assumption regarding the effect of curing at elevated temperature described in section 1.

These tendencies are common to all samples, although not equally pronounced. To illustrate the effect of curing temperature, the amount of chemically bound water in g pr. g cement at 28 days M_{25} is presented in Figure 2. The water/cement ratios for the samples are calculated directly by disregarding the filler content in the mixtures.

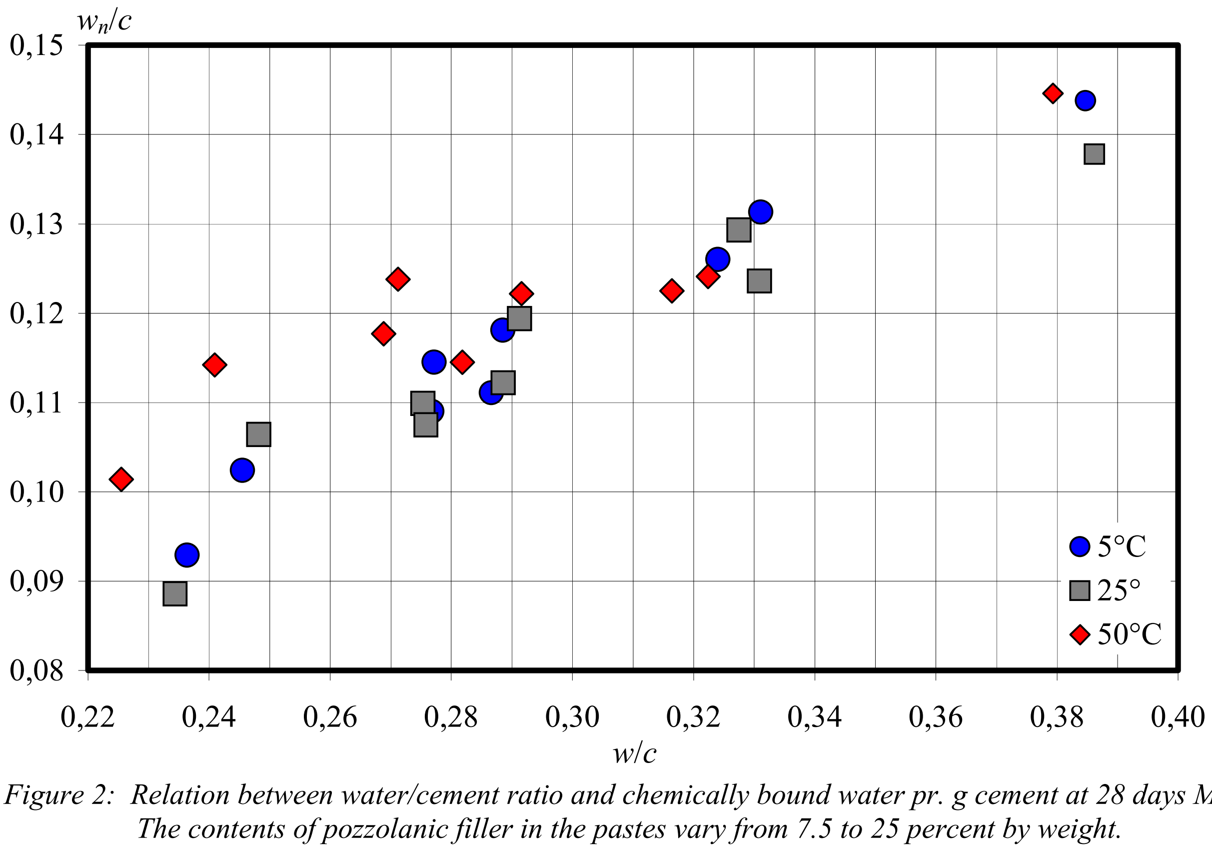

Figure 2: Relation between water/cement ratio and chemically bound water pr. g cement at 28 days M_{25}. The contents of pozzolanic filler in the pastes vary from 7.5 to 25 percent by weight.

For comparison, the expected chemically bound water contents at complete hydration of cement ranges from app. 0.21 to 0.23 g/g cement[12,13,14]. By calculation, the specific theoretical values for the used temperatures were 0.2103 g/g at 5°C, 0.2134 g/g at 25°C and 0.2094 g/g at 50°C[14]. The calculated lower content of chemically bound water at 50°C is a result of the differences in equilibrium temperatures at which different CSH hydrates are stable[15]. At low temperatures all normally found hydrates are stable (or rather meta-stable). At higher temperatures however, the hydrates containing a significant number of water molecules destabilize and may release water. Hence at different temperatures, different hydrates are thermodynamically meta-stable. At low temperatures, the usually assumed average chemically bound water content for the hydrates of 0.23 g/g may well be valid in a system containing sufficient water. However, when the temperature is increased, the meta-stable hydrates will – on average – contain less water, reducing the value to less than 0.23 g/g.

The difference between the observed chemically bound water content around 0.11 g/g cement compared to the usual 0.21 to 0.23 g/g cement at complete hydration, is mainly attributable to the low initial water cement content (below 0.38), making complete hydration impossible. But the addition of pozzolanic fillers, especially micro silica also influences the ratio:

Since pozzolanic hydration reactions cause no significant change of water phase distribution[15,16], the effect of pozzolanic reaction is to bind a large fraction of the accessible water originally in the mix by surface adsorption. Hence the effect of the pozzolans on the water phase distribution is to decrease the *available* water/cement ratio. So although the presence of filler in the system initially increases the water/cement ratio, the ultimate effect is to decrease the amount of water available for cement hydration. The mechanism is schematically illustrated in Figure 3.

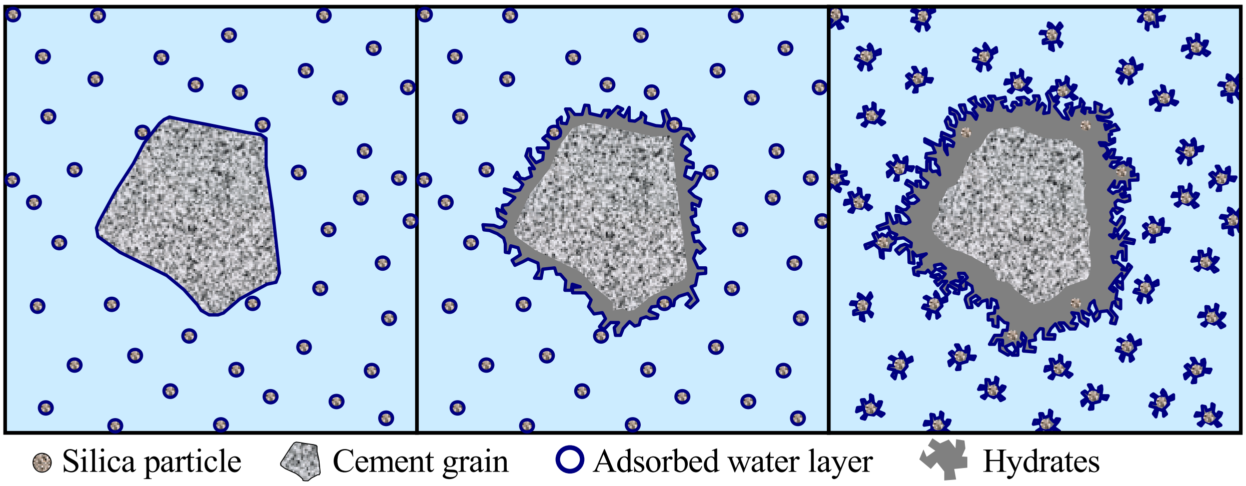

Figure 3: Progressive surface adsorption. Immediately after water addition (left) the cement and silica particles are suspended in water and bind little water physically. Next, cement hydration begins, increasing the surface area and the amount of physically bound water (middle). Finally, the pozzolanic particles react with calcium hydroxide from the cement reactions and the cement hydration continues, both increasing the physical binding of water (right).

Thus, in addition to the temperature effect, the self-desiccation of the cement paste system, accelerated by the physical binding of water on the surfaces formed by pozzolanic reactions, may result in a further redistribution of water within the system. The thermodynamic activity is lowered due to the self-desiccation, forcing some of the more water-containing hydrates to release some of their crystal (or chemically bound) water to the surroundings, where some reacts with unhydrated cement, and some is adsorbed onto the formed surfaces.

To summarize, the attainable chemically bound water content pr. g cement in a dense cement paste containing pozzolanic fillers at increased curing temperatures should be the result of two parallel processes: The water-rich hydrates becomes less stable due to increased temperature, and, the lowered activity of the physically bound water in the system due to self-desiccation accelerates the release of chemically bound water from the hydrates.

How does the above mentioned correlate to the fact that the observations from the measurements indicate an *increase* in chemically bound water in the samples cured at 50°C compared to those cured at 5°C and 25°C, and not a decrease?

Two mechanisms are believed responsible:

A: Some of the water liberated from the hydrates at higher temperatures react to form more hydrates, compensating somewhat for the reduced w_n/c ratio by increasing the amount of reacted cement. This only *reduces* the loss of chemically bound water pr. g. cement compared to normal temperature cured materials, since it also results in the formation of new surfaces.

B: The structure of the hydrates formed at higher temperatures is more crystalline than hydrates formed at lower temperatures (meaning denser, with less surface area). The reduced surface area liberates a significant quantity of otherwise physically bound water for further hydration. This mechanism would also explain the difference between "low" and "normal" water cement ratio systems: In the "normal" range, the liberation of physically bound water is insignificant to the hydration since there is already sufficient free water for complete hydration of the cement. Hence no extra hydration takes place, and the reduced w_n/c ratio and the "blocking effect"[4] governs the final amount of chemically bound water. This mechanism is believed to be the main reason for the observed increase in chemically bound water content at increased curing temperature for the considered cement paste systems.

The conclusion is supported by SEM results, see Figure 4 and 5, showing a significant densification of the hydrates when the temperature is increased, also observed previously[7].

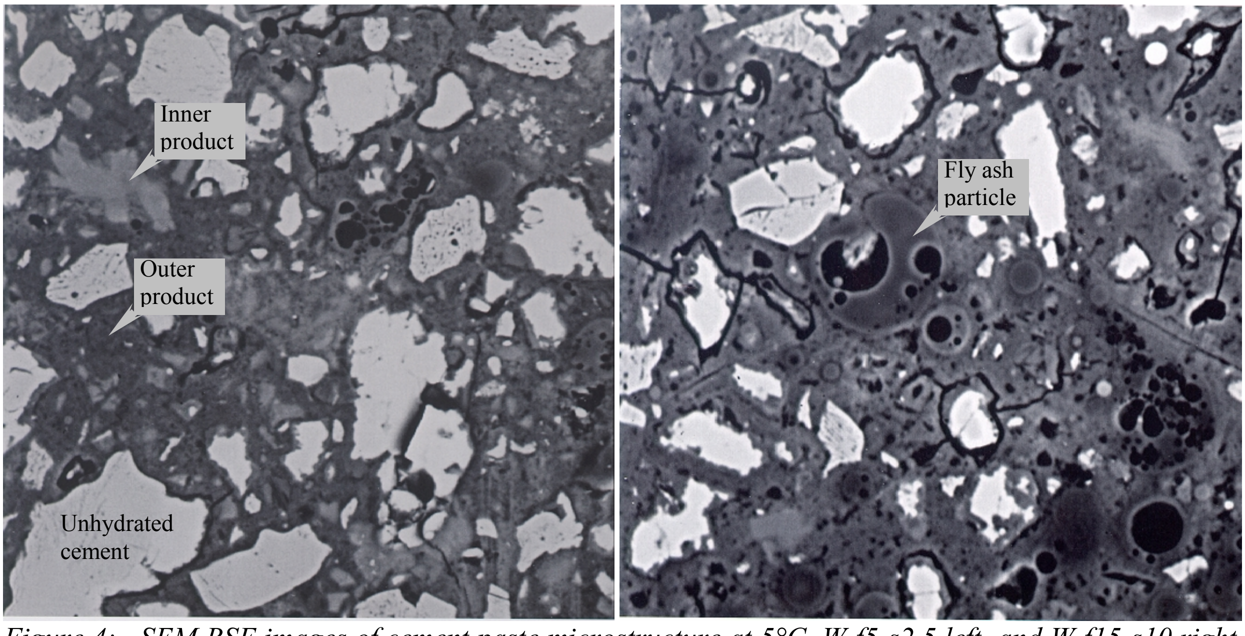

Figure 4: SEM BSE images of cement paste microstructure at 5°C. W-f5-s2.5 left and W-f15-s10 right. The images are 100 μm wide (original magnification 1000×)

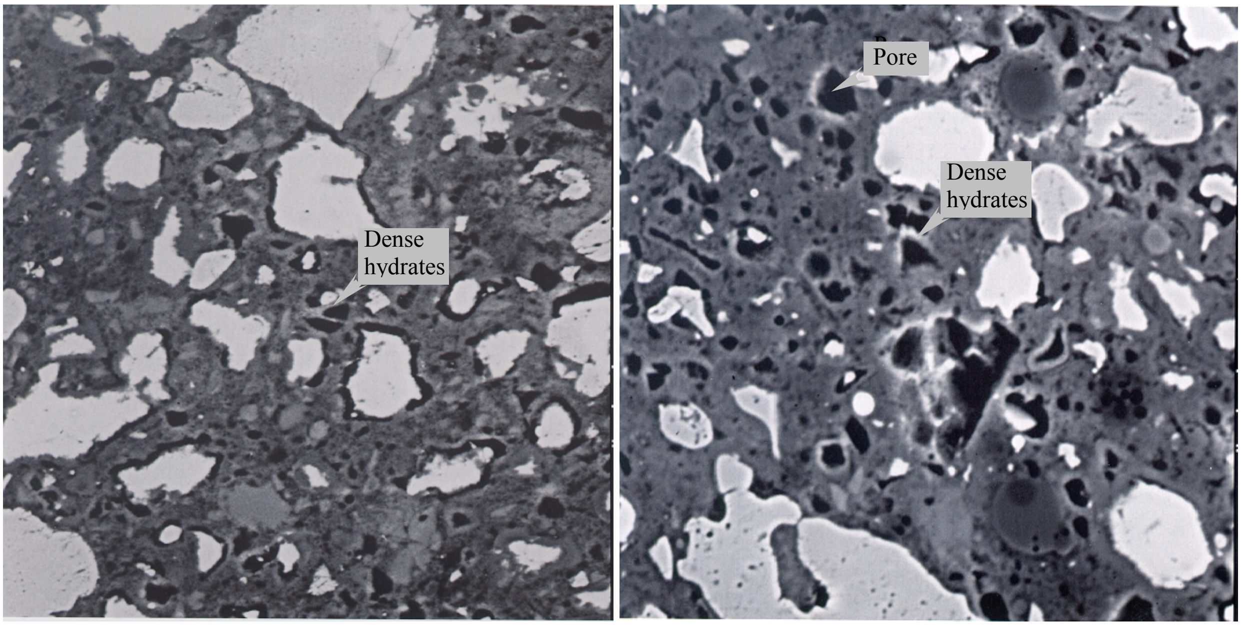

Figure 5: SEM BSE images of cement paste microstructure at 50°C. W-f5-2.5 left and W-f15-s10 right. The images are 100 μm wide (original magnification 1000×)

5. CONCLUSION

It has been demonstrated that the amount of chemically bound water increases with curing temperature for a sealed cured cement paste system containing moderate amounts of pozzolanic fillers at *sufficiently low* water/cement ratios.

This is believed to be the direct result of a more crystalline structure of hydrates formed at higher temperatures, reducing the amount of surface adsorbed water in the system: In the low water/cement ratio system, the available amount of water is limited and the system is self desiccated. The reduced physical adsorption increases the amount of water available to hydration.

This increase in available water counters the effect of reduced w_n/c ratio of the hydrates at higher temperature, and the retaining of water by physical binding on the surfaces of hydrates formed by pozzolanic reactions.

Within the considered composition and curing temperature range the net result of these mechanisms ranges from an increase in chemically bound water content with increased curing temperature at *low to moderate* pozzolanic filler contents (especially micro silica contents appears significant) to a negligible effect at *high* filler contents.

This increase in chemically bound water (and thus formed hydrates) due to the above mentioned mechanisms may be the cause for the increased compressive strengths at increased curing temperatures observed in some low water content systems.

6. ACKNOWLEDGEMENTS

The presented investigation was conducted as part of an industrial Ph.D. study under the Academy of Technical Sciences, ATV, and was as such partially financed by the Danish Agency for Trade and Industry.

7. REFERENCES

1 Kim, J.-K. et. al.: "Compressive strength development of concrete with different curing time and temperature", *Cement and Concrete Research Vol. 28, No. 12*, December 1998.

2 Maltais, Y. & Marchand, J.: "Influence of curing temperature on cement hydration and mechanical strength development of fly ash mortars", *Cement and Concrete Research Vol. 27, No. 7*, July 1997.

3 Mouret, M. et. al.: "Study of the degree of hydration of concrete by means of image analysis and chemically bound water", *Advanced Cement Based Materials, 1997, No. 6*, 1997.

4 Escalanta-García, J.J. and Sharp, J.H.: "Effect of temperature on the hydration of the main clinker phases in Portland cement paste: Part I, Neat cements", *Cement and concrete research, Vol. 28, No. 9*, 1998.

5 Almusallam, A.A.: "Effect of environmental conditions on the properties of fresh and hardened concrete", *Cement and Concrete Composites, Vol. 23, no. 4/5*, August/October 2001.

6 H. Kada-Benameur, E. et. al.: "Determination of apparent activation energy of concrete by isothermal calorimetry", *Cement and Concrete Research, Vol. 30, No. 2*, February 2000.

7 Schrivener, K.L.: "The effect of heat treatment on the inner product C-S-H", *Cement and Concrete Research Vol. 22, No. 6*, June 1992.

8 M. Mouret, A. et. al.: "Microstructural features of concrete in relation to initial temperature – SEM and ESEM characterization", *Cement and Concrete Research, Vol. 29*, 1999.

9 Hansen, Tommy B.: "Physical and thermodynamical properties of water phases in hardening Portland cement systems", *Aalborg University, Ph.D. thesis*, January 2001.

10 Freiesleben Hansen, P.: "Material Physics for Building Engineers – the basis for calculation", *Federal Building Institute, SBI publication 183*, 1995. In Danish.

11 Atkins, P.W.: "Physical Chemistry", *Oxford, 5th edition*, 1997.

12 Powers, T.C. & Brownyard, T.L.: "Studies of the physical properties of hardened Portland cement paste", *American Concrete Institute, ACI Bulletin 22*, March 1948.

13 Soroka, I.: "Portland cement paste and concrete", *MacMillan*, 1979.

14 Sideris, K.K.: "The stoichiometry in the paste hydration of C_3S, alite and β-C_2S cured at 5, 25 and 50°C ", *Advances in Cement Research, Vol. 12, No. 3*, July 2000.

15 Mchedlov-Petrossyan, P.P et. al.: "Thermodynamics of silicates", *Springer*, 1985.

16 Sellevold, E.J. et. al.: "Silica fume – cement pastes: Hydration and pore structure", *Nordic Concrete Research,* proceedings from "Silica in concrete", Trondheim*,* December 1981.

Drying Shrinkage of "Norwegian" Self-Compacting Concrete

Kåre Johansen
MSc Eng., Research Engineer,
E-mail: Kare.Johansen@civil.sintef.no

Tor Arne Hammer
MSc Eng., Research Engineer,
E-mail: Tor.Hammer@civil.sintef.no

SINTEF Civil and Environmental Engineering, 7465 Trondheim Norway

ABSTRACT

Drying shrinkage has been tested on typical Self-Compacting Concretes (SCC) used in Norway (w/b of 0.6). The application for Norwegian practice with respect on SCC has focused at maintaining the paste content and composition as close to equivalent traditional concretes as possible. Consequently, the risk of cracking of the SCC is not significantly different either as demonstrated by the results presented in this paper. However, reduced w/b and/or increased paste volume is occasionally required and contributes to increased shrinkage.

Key words: self-compacting concrete, type of co-polymer, grain size distribution and drying shrinkage.

1. INTRODUCTION

SCC recipes are often associated with high contents of binder, fillers and plasticizing admixtures, which all may contribute to increased drying shrinkage. Thus, questions have been raised about cracking of SCC due to drying shrinkage. The application for Norwegian practice with respect on SCC focused at maintaining the paste content and composition as close to equivalent traditional concretes as possible, mainly from a cost point of view. Thus, the main agents to make a SCC are fillers, especially in concretes with higher w/b than 0.45, which increases the need of plasticizers, and use of co-polymer plasticizing admixtures with a stabiliser included (thickening agent) [1]. Also, the focus on cost entails not to use lower w/b than required for e.g. environmental reasons. In Norway the major volume of concrete is in the “Moderately Aggressive Environment” class, requiring a w/b lower than 0.60 (according to Norwegian Standard 3420). Therefore, the research and development work includes development of SCC with w/b = 0.60.

It is important to consider that the risk of cracking is not solely linked to the shrinkage. Cracks develop when the shrinkage leads to stress equal to the tensile strength of the concrete. The stress is dependent on the product of **shrinkage**, **modulus of elasticity** and **creep /**

relaxation (provided that the structure is 100% restrained). Nevertheless, shrinkage is the most important indication as to ranking of concrete in view of risk of cracking.

2. TESTS AND CONCRETES

2.1 Tests

The drying shrinkage was tested as the length change of 100/100/500 mm beams. The beams were cured in water for six days from the time of de-moulding (24 hours after casting) and then exposed to drying at 50 % RH and 22°C.

The measurements were done with an extensiometer and with measuring points of steel studs cast in the ends of the beams. The scale corresponds to 0.005 mm (i.e. 0.01 ‰).

2.2 Concretes without silica fume

The concretes, all with w/c = 0.60, were designed for a parameter study on fresh concrete properties. The parameters tested were:

- Co-polymer type (three types available in Norway)
- Paste-aggregate volume-ratio (27/73 and 30/70)
- Grain size distribution

A total of ten mixes were tested. All concretes fulfilled the Norwegian definition of SCC; a slumpflow at least 650 mm without separation. The nominal recipes are given in Table 1. The aggregate was composed of Norwegian glacifuvial gneiss/granite aggregate with dry density 2650 kg/m^3 plus limestone filler with dry density 2700. Three different grain size distributions between 0.125 and 8 mm were used, composed by combining of fine sand, 0-2 mm, and a coarse sand 0-8 mm, see also Figure 1, where Modulus of Fineness (MF) is defined in [2].

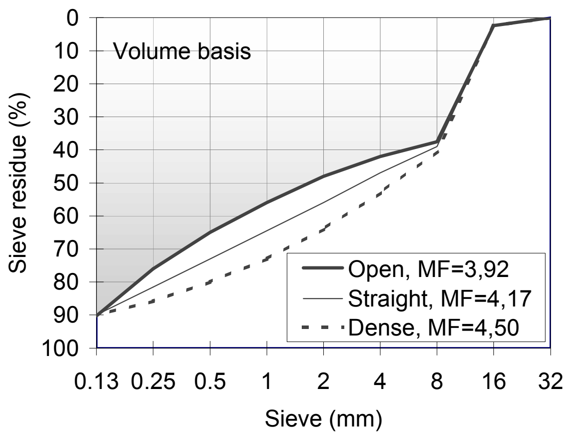

Figure 1 - Grain size distribution

1. **"Open"** distribution: Surplus of grains between 0.125 mm and 2.0 mm and with natural filler (< 0.125 mm).
2. **"Straight"** distribution: The reduced amount of filler due to less fine sand, was compensated by increased amount of limestone filler, 0-0.5 mm (49 % lime stone filler = 82 kg/m^3).
3. **"Dense"** distribution: Surplus of grains between 4 and 8 mm. The reduced amount of filler due to less fine sand, was compensated by increased amount of lime stone filler, 0-0.5 mm (96 % limestone filler = 179 kg/m^3).

Fly ash cement, type CEM II A-V 42.5 R with density 2950 kg/m^3 was used in all the mixes.

For each of the three curves (open, straight and dense) three different co-polymers, which normally are used in self-compacting concrete in Norway, were used. The three co-polymers were:

MBT Norge AS	Glenium 51	(about 35 % dry substance)
Scancem Chemicals AS	SSP 2000	(about 25 % dry substance)
	Scancem VMA	
Sika Norge AS	ViscoCrete 3	(about 28 % dry substance)

2.3 Concretes with silica fume

The silica fume content was 4, 7 and 10% by cement weight respectively. The other materials were similar to those used in the concretes without silica fume, except for the sand (included natural filler) which was another type with a nearly straight distribution.

2.4 Recipes

The recipes without silica fume are given in Tables 1, and 2. The nominal constituents are given in Table 1, and the real content of admixtures is given in Table 2:

Table 1 - Nominal recipes kg/m^3 (water-binder ratio 0.60 without silica fume):

Grain size distribution: Materials composition		Open	Straight	Dense[1)]	Dense
Paste content, l/m^3 [2)]		282	282	282	259
Matrix content, l/m^3, [3)]		350	350	350	340
Norcem Standard cement FA,		300	300	300	275
Norcem Limestone Powder, Brevik 0-0,5 mm		0	92	179	220
Årdal aggregates,	0-2 mm	726	354	0	0
dry weight	0-8 mm	392	672	941	935
	8-11 mm	372	372	373	386
	11-16 mm	372	372	373	386
Water, (water in additives included)		180	180	180	165

[1)] Only tested with copolymer SSP 2000
[2)] Paste = volume of cement + water + additives
[3)] Matrix = volume of paste and filler < 0,125 mm

Table 2 - Amount of admixtures and fresh concrete characteristics for all mixes without silica fume:

Grain size distribution: Materials and measurements		Open	Straight	Dense[1)]	Dense
Nominal paste content, l/m^3 [2)]		282	282	282	259
Nominal matrix content, l/m^3, [3)]		350	350	350	340
Co-polymer, kg/m^3:	Glenium 51	1.5	1.3		2.1
	ViscoCrete 3	2.8	2.3		3.3
	Scancem SSP 2000	3.6	3.0	2.8	4.6
Stabilizer: Scancem VMA[4)]		3.0	3.0	3.0	3.0
Slump Flow, mm:	Glenium 51	675	675		665
	Viscocrete 3	725	665		600
	Scancem SSP 2000	725	650	690	655
Density, kg/m^3:	Glenium 51	2365	2325		2389
	Viscocrete 3	2405	2375		2385
	Scancem SSP 2000	2380	2380	2385	2425
Air content, %:	Glenium 51	1.9	3.1		1.1
	Viscocrete 3	0.7	1.2		2.1
	Scancem SSP 2000	1.0	0.6	1.2	1.0

[1)] Only tested with copolymer SSP 2000
[2)] Paste = volume of cement + water + additives
[3)] Matrix = volume of paste and filler < 0,125 mm
[4)] Stabilizer was used only in combination with copolymer SSP 2000

The recipes with silica fume is given in Table 3:

Table 3 - Recipes kg/m^3 (water-binder ratio 0.60) and fresh concrete characteristics with silica fume. Nominal values except for the admixtures that are real :

Amount of silica fume in % cement weight		4	7	10
Paste content, l/m^3		280	278	276
Matrix content, l/m^3		350	350	350
Norcem Standard FA		279	265	250
Condensed silica fume, CSF		11.2	18.6	25.2
Årdal	0-2 mm	132	133	152
aggregate [1)]	0-8 mm	827	815	796
	8-11 mm	376	379	379
	11-16 mm	376	379	379
Grefsrud filler 0-0.5 mm		169	190	190
Co-polymer SSP 2000		3.03	3.58	4.03
Stabilizer, Scancem VMA		1.39	1.33	1.26
Free water [2)]		180.8	182.2	182.4
v/(c+2csf) – ratio		0.601	0.602	0.604
Slump Flow, SU in mm		647	650	680
Density, kg/m^3		2365	2375	2370
Air content, %		1.8	1.6	1.1

[1)] Oven dry weight of aggregate
[2)] Water in additives included, but absorbed water in aggregate excluded

3. RESULTS AND DISCUSSION

3.1 Influence of co-polymers, paste content and grain size distribution

Drying shrinkage was measured until 49 days of drying. This is a relatively short period of time, but still, it gives a strong indication about the influence of the parameters on the drying shrinkage. The results at 56 days (49 days drying) are given in Table 4.

Table 4 - Measured drying shrinkage, mm/m (49 days). Each number represents the average of two prisms.

Aggregate / Copolymer		Glenium 51	ViscoCrete 3	SSP 2000
Open (300)	Shrinkage 56 days	0.55	0.53	0.48
Straight (300)	Shrinkage 56 days	0.54	0.50	0.48
Dense (300)	Shrinkage 56 days	-	-	0.40
Dense (275)	Shrinkage 56 days	0.31	0.31	0.34

In general, the results for open and straight grain size distribution showed values quite similar to normal concretes with the same cement type and w/b, [3]. The results showed that the type of co-polymer did not have any significant influence on the drying shrinkage, see Table 4. The grain size distribution, however, showed apparently a large influence, i.e. the dense distribution had significantly lower shrinkage, see Figure 2. This is supported by the weight measurements of the specimens, Figure 3) showing that the evaporation decreases in the order: “Open” > “Straight” > “Dense”. This is quite unexpected since the paste composition is unchanged and the amount of admixture is fairly equal. According to Neville "The size and grading of aggregate per se do not influence the magnitude of shrinkage" /4/. Another difference is the composition of the filler, i.e. the ratio between natural and lime stone filler. The concrete with the highest content of limestone filler (“Dense”) had the lowest shrinkage and evaporation, see Figure 3. We have not found other results showing this effect of limestone filler. New tests will be performed in order to verify the results.

The concrete with less cement content (corresponding to less paste volume of 25 litres/m^3 or 8 % by volume) showed less shrinkage, as expected. The reduction, at 49 days of drying, corresponds to approximately 15 %.

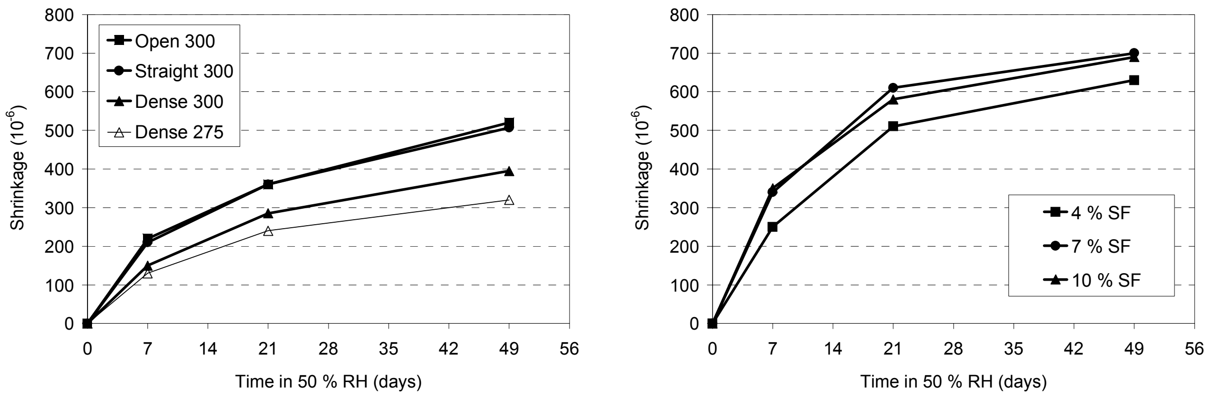

Figure 2 - Left: Drying shrinkage of SCC with “Open”, “Straight” and “Dense” grain size distribution and cement contents of 300 and 275 kg/m^3, respectively. Right: Drying shrinkage of SCC with w/b = 0.60 and different silica fume (SF) contents

The weight loss of SCC with “Open”, “Straight” and “Dense” grain size distribution is shown in Figure 3. (average of three mixes with Glenium 51, Viscocrete 3 and SSP 2000, respectively). The weight increase between 1 and 7 days when the prisms are stored in water was not measured.

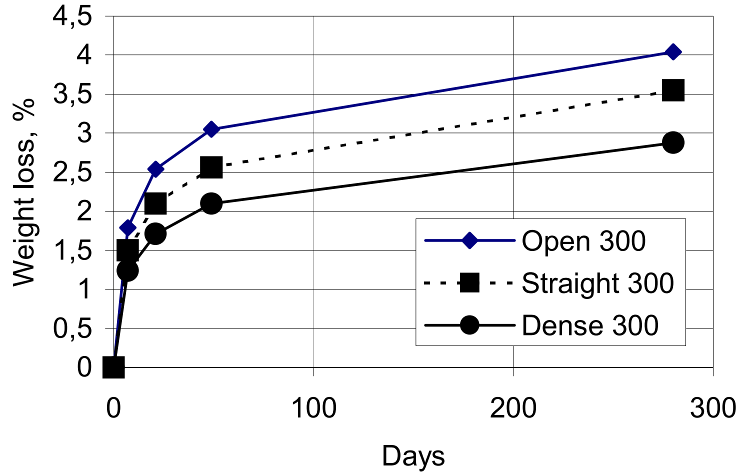

Figure 3 - Weight loss of SCC with “Open”, “Straight” and “Dense” grain size distribution and cement contents of 300 kg/m³.

3.2 Effect of silica fume

Silica fume is a very good aid in order to attain sufficient resistance against separation of SCC, especially when using relatively high w/b-ratio. The silica fume was added as replacement for cement using an efficiency factor of 2. The investigation did not include a reference without silica fume, see section 2.3. The paste volume was kept constant. The results indicate that the silica fume content between 4 and 10% does not influence significantly the drying shrinkage, see Fig 2. However, a comparison with the results from investigation of concretes without silica fume (with similar cement type, w/b and admixture, but different sand), see Figs 2 and 3, indicates that the addition of silica fume increases drying shrinkage the first 2 to 3 weeks of drying. The conclusion from a review on the influence of silica fume [5] is that there is no uniform influence of silica fume on drying shrinkage.

4. CONCLUSIONS

In general, the risk of cracking of concrete due to drying shrinkage is linked to the paste content, w/b and binder type as the main material parameters. The application for Norwegian practice on SCC has focused on maintaining these parameters as close to equivalent traditional concretes as possible, mainly from a cost point of view. Consequently, the risk of cracking of SCC as mentioned, is probably not significantly different from equivalent traditional concretes. The present results confirm that the drying shrinkage is not significantly different, and the type of copolymer admixtures did not have significant influence on the drying shrinkage. Reduced w/b and/or increased paste volume are effective, and thus, tempting tools in order to fulfil workability requirements, but one should keep in mind that the consequence may be increased cracking risk, as demonstrated in the present investigation.

REFERENCES

1. Smeplass S. and Mørtsell E: The particle matrix model applied on SCC. The Second International Symposium on Self-Compacting Concrete, 23-25 October, 2001, Tokyo, Japan.

2. prEN 12620

3. Arne Vatnar: "Concrete used in floors - Effect of constituents upon fresh and hardened properties. Testing of shrinkage reducing agents". Norcem report 9D4R01010 in the project "Competetive concrete solutions for industrial- and residential buildings", task Concrete Floors. Norcem R&D, 03.10.2001. In Norwegian.

4. Neville A.M., "Properties of Concrete" Forth and Final Edition, 1995, Addison Wesley Longman Limited, p 429.

5. Sellevold E.J.: Condensed Silica Fume in Concrete. FIP State-of-the-art Report. 1987.

Finite Element Study of Concrete-Filled Steel Tubes Using a New Confinement-Sensitive Concrete Compression Model

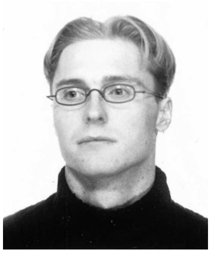

Mathias Johansson,
Lic. Sc., Research Assistant
Department of Structural Engineering, Concrete Structures, Chalmers University of Technology, SE-41296 Göteborg, Sweden
E-mail: mathias.johansson@ste.chalmers.se

Magnus Åkesson,
Ph. D.
Swedish Meteorological and Hydrological Institute, SE-60176 Norrköping, Sweden
E-mail: magnus.akesson@smhi.se
(Formerly Department of Structural Engineering)

ABSTRACT

The constitutive model in this paper addresses the influence of confinement on the compressive response in concrete structures, which is one issue when dealing with their compressive failure. The elasto-plastic model is based on the Drucker-Prager yield criterion having a confinement-sensitive hardening sub-model. To examine the predictive capacity of the model, it was applied to study a series of laboratory experiments where a number of concrete cylinders were exposed to an active confinement pressure. Furthermore, the model was used in a FE study of concrete-filled steel tubes, in which the state of stress is more complex and the confining stresses on the concrete core are induced by passive confinement provided by the steel tube.

Key words: confined concrete, constitutive modeling, non-linear finite element analyses, concrete-filled steel tube.

1. INTRODUCTION

Concrete in compression is usually characterized with a stress-strain relationship obtained from uniaxial standard compression tests. However, most concrete structural elements are subjected to a multiaxial stress state. A uniaxial stress state represents only one of an infinite number of multiaxial stress conditions to which an element of concrete in a structure may be subjected throughout the loading history of the structure; see Kotsovos (1987). The response of concrete varies widely for different stress states and it is therefore important to know how the concrete behaves for different multiaxial stress states. As an example, Kotsovos shows the variation of the peak axial compressive stress sustained by a concrete cylinder with increasing confining pressure. It was noted that a small confining pressure of about 10 percent of the uniaxial cylinder compressive strength was sufficient to increase the load-bearing capacity of the specimen by as much as 50 percent.

A confinement-sensitive compression model to be used in FE analyses of concrete structures has been developed. Various methods of introducing confinement or pressure dependence have been proposed in the literature. One solution was reported by Malvar *et al.* (1997) where the compressive strength was made dependent on the hydrostatic pressure. Another way of dealing with the problem was suggested by Chen and Han (1987) who defined the plastic modulus as a function of the hydrostatic pressure through a modification factor. However, it is the authors' opinion that in order to simulate the confinement dependence completely it is necessary to make both the strength and the plastic modulus dependent on the confinement. This way of introducing confinement sensitivity in both the strength and the plastic modulus is believed to be a novel feature. Furthermore, it is believed that the hydrostatic pressure is an unfortunate choice of controlling parameter as two different stress situations can share the same hydrostatic pressure.

The proposed model is fundamentally an elasto-plastic model based on flow theory, i.e., it consists of a yield surface, a hardening rule, a yield law and reliance on the assumption of strain decomposition. What makes this model different from conventional elasto-plastic models is its capability to incorporate confinement into the integration of the internal state. It is a well-known fact that the response for a general stress situation cannot be captured with a conventional elasto-plastic model calibrated with only a limited set of strength data. That is, frequently used data for calibration of such models are a uniaxial stress-strain relation together with some factor giving the relation between uniaxial and biaxial compressive strength. With these data at hand, it is explicitly assumed that the hardening rate for all loading histories is the same. This is not the case, as can easily be observed by performing a numerical simulation of a situation outside the calibration data range. Such a simulation will reveal too soft behavior; see Figure 1. To resolve this discrepancy when simulating a general situation calls for a more complete set of material data.

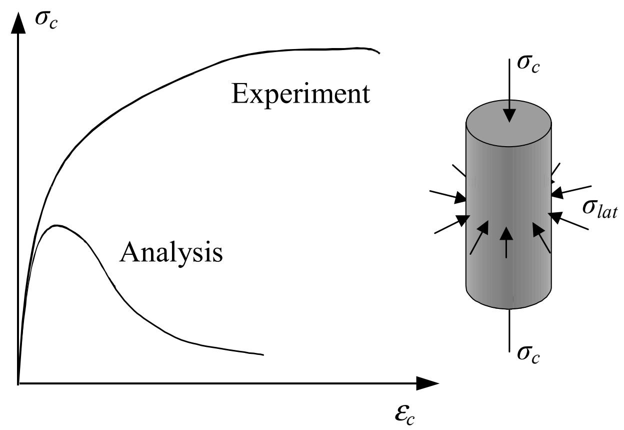

Figure 1 – Typical difference of experimental and analysis result for confined concrete.

The first section of this paper gives a brief description of the fundamental behavior and theories of confined concrete, for the cases of both active and passive confinement. The second section gives a description of the constitutive formulation of the model. Apart from the classical formulation, it consists of a discussion about the concept of confinement-sensitive hardening. Further, the section includes a description of the application of this model and a verification of it. The last section shows an example of an application of the model in a study of concrete-filled steel tubes with some comments on the results. Finally, some remarks and conclusions are presented.

2. CONFINED CONCRETE

2.1 Active confinement of plain concrete

Richart *et al.* (1928) were the first to observe that confined concrete showed greatly increased maximum compressive strength, increased stiffness, and extended strain at which the peak stress was reached; see Figure 2. The concrete can sustain large deformation without substantial reduction of the load-bearing capacity and fails gradually in a ductile way. A number of experimental and theoretical studies on normal-strength concrete subjected to multiaxial states of stress have been performed, for example by Richart *et al.* (1928), Mills and Zimmerman (1970), Pantazopoulou (1995) and Imran and Pantazopoulou (1996). To consider the increased concrete strength due to confinement Richart *et al.* (1928) proposed the well-known empirical formula:

$$f_{cc} = f_{co} + k\sigma_{lat} \tag{1}$$

where f_{cc} is the axial compressive strength of concrete confined by the lateral stress σ_{lat}, f_{co} is the uniaxial compressive strength of the concrete, and k is the so-called triaxial factor and is found to be 4.1. Although newer test results have suggested a modification of this relation, the basic approach for determining the confined strength remains the same. To calculate the axial compressive strain at peak stress ε_{cc} they also proposed the following equation:

$$\varepsilon_{cc} = \varepsilon_{co}\beta_1\left[\frac{f_{cc}}{f_{co}} - \beta_2\right] \tag{2}$$

where ε_{co} is axial compressive strain at peak uniaxial stress, $\beta_1 = 5$ and $\beta_2 = 0.8$. Using equation (1) it can be written as a function of the lateral confining pressure as:

$$\varepsilon_{cc} = \varepsilon_{co}\beta_1\left[\left(1 + \frac{k\sigma_{lat}}{f_{co}}\right) - \beta_2\right] \tag{3}$$

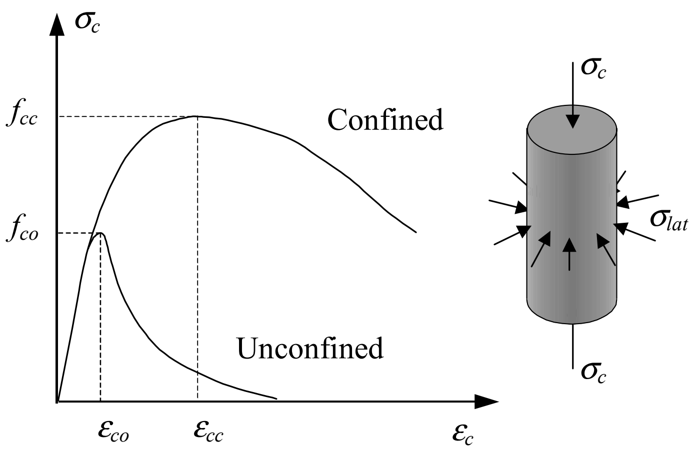

Figure 2 – Schematic stress-strain relations for unconfined and confined concrete.

The experimental data for high-strength concrete under multiaxial states of stress are less extensive than those for normal-strength concrete. However, Attard *et al.* (1996) performed a test series of high-strength concrete subjected to low confining pressure and Ansari and Li (1998) carried out a comprehensive experimental program with high confining pressure, ranging up to $1.0f_{co}$. They found that the influence of confining pressure on the maximum compressive strength of high-strength concrete is not so pronounced as on that of normal-strength concrete. According to Cederwall (1988), can the factor k in equation (1) be assigned a value of 3 to 4 for high-strength concrete.

2.2 Passive confinement in concrete-filled steel tubes

Triaxial stresses in concrete-filled steel tubes have been studied by several researchers, for example Gardner and Jacobson (1967), Tomii *et al.* (1977), Orito *et al.* (1987) and Schneider (1998). In a composite column consisting of a concrete-filled hollow steel section, compressive confining stresses on the concrete core are induced by passive confinement provided by the steel tube. In the case of passive confinement, the confining pressure is not constant as is the case for active confinement, and it also depends on the lateral deformation of the concrete core under axial load and the stress-strain relationship of the confining steel. However, it has been found that the concrete behavior is similar irrespective of whether the confining pressure is active or passive; see Attard *et al.* (1996).

Short concrete-filled steel tubes concentrically loaded on the entire section are significantly affected by the difference between the values of Poisson's ratio of the steel tube, ν_a, and the concrete core, ν_c. In the initial stage of loading, Poisson's ratio of concrete is lower than for steel; therefore, the steel tube expands faster in the radial direction than the concrete core, i.e. the steel does not restrain the concrete core. As the load increases and the compressed concrete starts to plasticize, the lateral deformations of the concrete catch up with those of the steel and, for further increase in load, the steel tube restrains the concrete core and the hoop stresses in the steel become tensile (σ_{ah}). At this stage and later, the concrete core is stressed triaxially and the steel tube biaxially; see Figure 3.

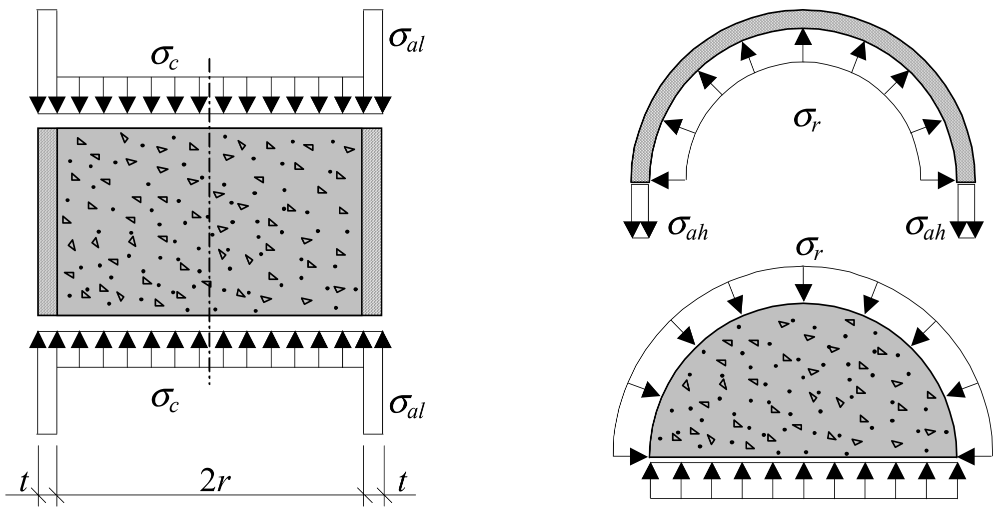

Figure 3 – Stress conditions in the steel tube and the concrete core.

From the equilibrium of the forces acting on the half tube, it is possible to establish a relation between the hoop tensile stresses σ_{ah} and the internal pressure σ_r:

$$\sigma_r = \frac{t}{r}\sigma_{ah} \tag{4}$$

where r and t are the radius and thickness of the steel tube, respectively. By setting $\sigma_{lat} = \sigma_r$ and using equations (1) and (4), the ultimate compressive strength of the concrete core confined by a steel tube can now be calculated as:

$$f_{cc} = f_{co} + k\frac{t}{r}\sigma_{ah} \tag{5}$$

In equation (5) it can be observed that increased hoop tensile stresses in the steel tube give a higher compressive strength of the concrete. However, because of the presence of hoop tension, the steel tube cannot sustain the plastic resistance in the axial direction according to the von Mises yield criterion:

$$\sigma_{ah}^2 + \sigma_{al}\sigma_{ah} + \sigma_{al}^2 = f_y^2 \tag{6}$$

where σ_{al} is the longitudinal compressive stress in the steel and f_y is the yield strength of the steel. This means that when the circumferential tensile steel stress increases due to lateral deformations of the concrete core, the axial compressive steel stress has to decrease.

When the load is applied only to the concrete section, the steel tube has a restraining effect on the concrete core as soon as lateral deformations of the core develop, and the confinement of the concrete core can be most pronounced. In this case, any bond at the steel-concrete interface induces longitudinal compression in the steel tube; i.e. the behavior is influenced by the bond strength. However, when the load is applied to the entire section the bond strength has no or little influence on structural behavior because there is no relative movement between the concrete core and the steel tube.

The total load on the stub column can normally be written as the sum of the contributions from the concrete and the steel:

$$P_{cal} = P_{c,cal} + P_{a,cal} = (f_{co} + k\frac{t}{r}\sigma_{ah})A_c + \sigma_{al}A_a \tag{7}$$

where A_c and A_a are the areas of the concrete core and steel tube, respectively. Assuming that the steel is yielding when the concrete fails, it is possible to find two extreme bounds for the load resistance. The lower bound is obtained by assuming the axial steel stress equal to the yielding stress ($\sigma_{al} = f_y$) and the circumferential steel stress equal to zero ($\sigma_{ah} = 0$). The upper bound, known as the Lohr principle (Lohr 1934), is instead obtained with the steel only acting as an encasement, i.e. setting the axial steel stress equal to zero ($\sigma_{al} = 0$) and the circumferential steel stress equal to the yielding stress ($\sigma_{ah} = f_y$). However, in practice the real situation will be somewhere inbetween and the stress pattern in the structure can be very complex.

3. CONFINEMENT-SENSITIVE CONCRETE COMPRESSION MODEL

3.1 Constitutive formulation

The material model designed for modeling concrete crushing is fundamentally a classical elasto-plastic model, but it is extended to include a confinement-sensitive hardening behavior by means of two adjustment functions connected to the strength and the plastic modulus. The underlying model was chosen as the Drucker-Prager model with associative evolution laws, see Chen and Han (1987). Figure 4 shows the yield surface in the principal stress space. This was a choice guided by the aim of just demonstrating a principle for introducing the confinement sensitivity into the constitutive formulation, but also guided by the fact that the main contributing factor for capturing the confinement sensitivity is given by the hardening rule. That is, the shape of the yield surface only comes into play at onset of yielding and its contribution to the response is not as dominant as the effect of the hardening rule. Another factor affecting the choice of underlying plastic model, though less important, was the ability to produce correct and efficient numerical algorithms for integrating the state. With this model, it is also simple to establish the algorithmic tangent stiffness tensor at a low computational cost, which is a major concern when dealing with implementation issues.

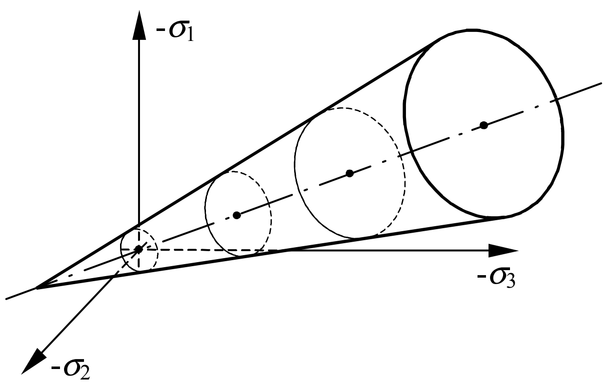

Figure 4 – The Drucker-Prager yield surface in the principal stress space.

The yield surface for the Drucker-Prager model is a linear function in both the deviatoric stress q and the hydrostatic pressure p:

$$F(\boldsymbol{\sigma}, K) = q + p\tan\alpha - K = 0 \tag{8}$$

where K is the strength representing the cohesion and α is the frictional angle. The hydrostatic pressure is defined as:

$$p = -\frac{1}{3}\boldsymbol{\sigma} : \mathbf{I} \tag{9}$$

where $\boldsymbol{\sigma}$ is the stress tensor and $\mathbf{I}$ is the unit tensor. The deviatoric stress is defined as:

$$q = \sqrt{\frac{2}{3}(\mathbf{S} : \mathbf{S})}, \tag{10}$$

where $\mathbf{S}$ is the deviator stress tensor, defined as:

$$\mathbf{S} = \boldsymbol{\sigma} + p\mathbf{I} \,. \tag{11}$$

The next component in the model is the flow rule, expressing the evolution of plastic strains:

$$d\boldsymbol{\varepsilon}^p = d\lambda \frac{\partial Q}{\partial \boldsymbol{\sigma}} = d\lambda \frac{\partial F}{\partial \boldsymbol{\sigma}} = d\lambda \left(\sqrt{\frac{3}{2}} \frac{\mathbf{S}}{|\mathbf{S}|} + \frac{\tan\alpha}{3} \boldsymbol{\delta} \right) \tag{12}$$

where $d\lambda$ is the plastic multiplier and $\boldsymbol{\delta}$ is the Kronecker delta. Relation (12) is called the associated flow rule because the plastic flow potential function Q is associated with the yield criterion ($Q = F$); see Chen and Han (1987). Although it is common practice to use a non-associative flow rule ($Q \neq F$) when modeling concrete crushing, again with the aim of investigating a principle, associativity was chosen for the sake of simplicity. The last component of the model, also associative, is the hardening rule, which consists of two parts describing the evolution of the hardening parameter and the strength hardening parameter dependence, i.e.

$$d\kappa = d\lambda \frac{\partial F}{\partial K} = -d\lambda \qquad \text{and} \qquad K = -H d\lambda \tag{13}$$

where H is the isotropic hardening modulus. Introduction of a confinement dependence on both the hardening parameter and the strength will also make the plastic modulus a function of the confinement. What would be desirable would be to introduce a hyper-surface defined by the three principal stress components and the hardening parameter describing the material strength. This would make it possible to have smooth transitions between different confinement situations. However, this requires that there exists such a surface and from a numerical point of view that it must be reasonably simple in its definition.

It can be argued that a non-associative yield law and a proper yield criterion can be used for achieving the same effect as a confinement-sensitive hardening rule. By just using a non-associative yield law together with a linear yield criterion, the only effect will be a translation of the response curve, keeping the same tendency for different confinement situations. On the other hand, by using a more complex yield criterion in combination with an associative yield law, the dominant effect will simply be a better simulation of onset of crushing. To find the right combination of a non-associative yield law and a complex enough yield criterion seems to be an impossible task; hence, it is a much more straightforward solution to resort to the proposed approach with a confinement-sensitive hardening rule.

The method chosen to introduce the confinement dependence into the hardening sub-model is by means of two adjustment functions f and g. These two functions are defined as polynomials of arbitrary power, i.e.

$$f(\sigma_{lat}) = \sum_{i=0}^{n} a_i \cdot \sigma_{lat}^i \tag{14a}$$

$$g(\sigma_{lat}) = \sum_{i=0}^{n} b_i \cdot \sigma_{lat}^i \tag{14b}$$

The first function scales the strength K according to the current confinement while the second function scales the hardening parameter κ; see Figure 5. In equations (14a) and (14b) the constants a_i and b_i have to be calibrated from pertinent test data. That is, the confinement influence varies depending on what concrete quality used. With these two adjustment functions, an approximation of the "true" strength hyper-surface is achieved.

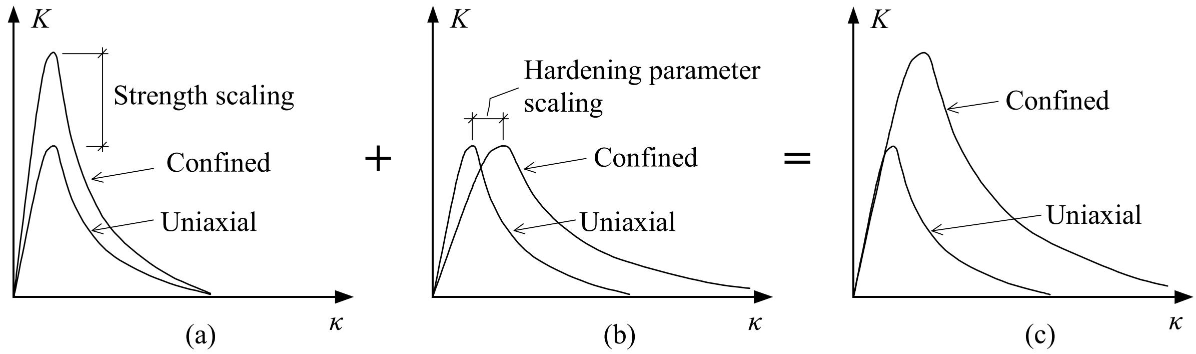

Figure 5 – Strength scaling (a), hardening parameter scaling (b) and resulting confined strength-hardening parameter relation (c).

The confinement value σ_{lat} in an element is taken as the mean value of the two smallest principal stresses under the condition that it is compressive –otherwise it is set equal to zero; see Figure 6. This restriction is due to uncertainties of how the compressive strength is influenced by transverse tensile stresses. Before the model can be extended to include this situation, further experimental investigation has to be done.

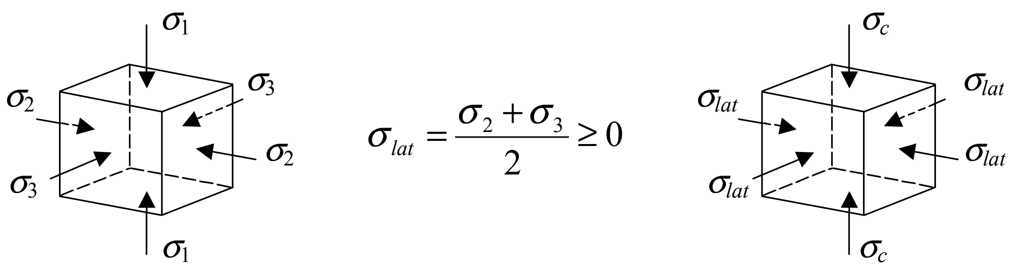

$$\sigma_{lat} = \frac{\sigma_2 + \sigma_3}{2} \geq 0$$

Figure 6 – Definition of stress state in an element when the confinement value is calculated.

To reach a broader public, the model has been implemented in ABAQUS/Standard. Although ABAQUS only offers a Fortran interface for user-defined material models a choice of using the programming language C++ was made; for reference see Lippman (1991). By using C++, it was possible to implement the model in terms of an object-oriented approach, which makes it possible to combine a well-structured code with numerical robustness and efficiency.

3.2 Application and verification

To exemplify the application and verify the confinement-sensitive compression model, an experimental series performed by Imran and Pantazopoulou (1996) was used. In total the experimental series consisted of 130 triaxial tests where the influence of confinement, loading path and moisture content on the stress-strain relation was examined. In this study a part consisting of 42 specimens were chosen to be used in the verification of the material model. The test specimens were of cylindrical shape with a height of 108 mm and a diameter of 54 mm. The peak strength, f_{cc}, and the corresponding strain, ε_{cc}, at given lateral confinement were recorded from the test results and compared with the values calculated according to equations (1) and (3); see Figure 7.

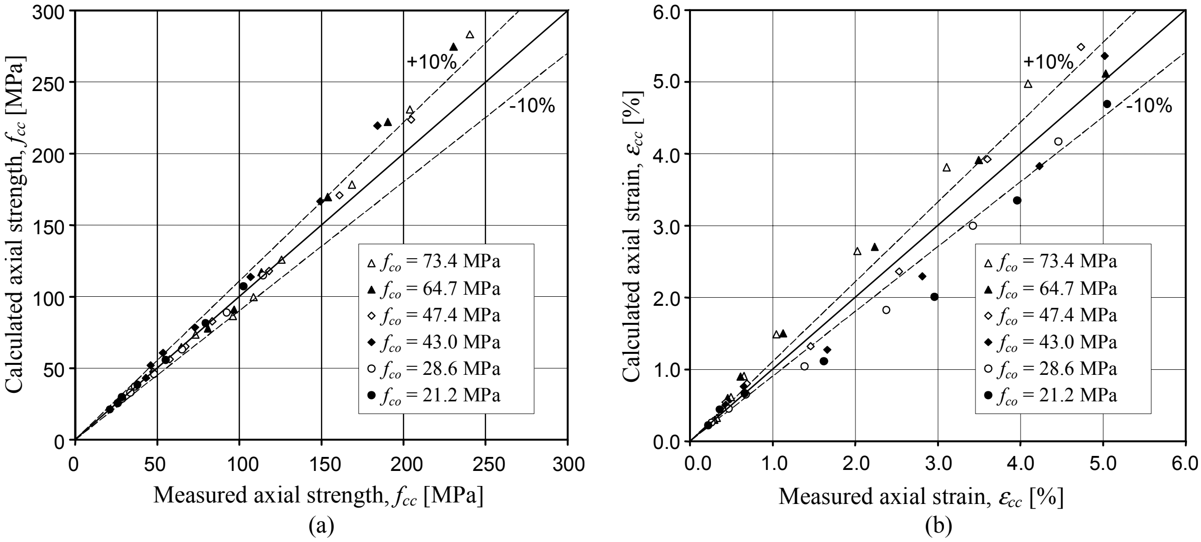

Figure 7 – Comparison of measured and calculated values for (a) the peak strength f_{cc} and (b) the corresponding strain ε_{cc}.

It can be observed that there are rather good agreements between the measured and calculated results for both the strength and the strain. Hence, in absence of triaxial tests it is possible to use the equations in order to derive the two scaling functions used in the material model. However, triaxial tests are more reliable and should be used if possible.

Instead of a relation between stress and strain for the uniaxial behavior, the confinement-sensitive compression model uses a relation between the cohesion and the hardening parameter. The cohesion is calculated as:

$$K = \sigma_c(\varepsilon^p)(1 - \frac{\tan\alpha}{3}) \tag{15}$$

where $\sigma_c(\varepsilon^p)$ is the compressive stress as a function of the plastic strain, ε^p, in the direction of the uniaxial stress. The plastic strain is recalculated into the hardening parameter as:

$$\kappa = \frac{\varepsilon^p}{\left(1 - \frac{\tan\alpha}{3}\right)} \tag{16}$$

The stress-strain relation can be determined by standard uniaxial tests on concrete cylinders. However, it is often not possible to record the stress-strain relation after the maximum strength is reached. Therefore, the post-peak behavior of the concrete can be derived according to the recommendations in CEB-FIP Model Code, CEB-FIP (1993) or CEB Bulletin d'Information 228 (1995). In absence of material tests, the entire stress-strain relation can be derived according to these models. To derive the strength scaling function, $f(\sigma_{lat})$, the peak cohesion, K_{max}, is calculated for a number of values of the lateral confinement, σ_{lat}, according to:

$$K_{\max} = f_{cc}(1-\frac{\tan\alpha}{3}) - \sigma_{lat}(1+\frac{2\tan\alpha}{3}) \tag{17}$$

The function simply describes the increase of cohesion with changes in lateral confinement. Correspondingly, the hardening parameter scaling function, $g(\sigma_{lat})$, is derived from the hardening parameter corresponding to the peak cohesion, κ_{max}, for a given lateral confinement and calculated as:

$$\kappa_{\max} = \frac{f_{cc}(\varepsilon_{cc} - \frac{f_{cc}}{E_c})}{f_{cc}(1-\frac{\tan\alpha}{3}) - \sigma_{lat}(1+\frac{2\tan\alpha}{3})} \tag{18}$$

The values of f_{cc} and ε_{cc} correspond to a specific value of σ_{lat}, and are either taken from triaxial material tests or calculated according to equations (1) and (3), respectively.

To investigate the predictive capacity of the constitutive model in simulating the response under various confinement situations, a set of numerical analyses were carried out simulating the experimental series performed by Imran and Pantazopoulou (1996). Out of this vast material, a test series with $f_{c,cyl}$ = 43.5 MPa was chosen. For this sub-series, seven different levels of confinement were applied. The peak strength, f_{cc}, and the corresponding strain, ε_{cc}, recorded from the seven stress-strain relations obtained in the tests are given in Table 1, and corresponding cohesion and hardening parameters were calculated according to equations (17) and (18).

Table 1 – Investigated experimental series.

Lateral confinement, σ_{lat} [MPa]	Measured		Calculated		FEA	
	f_{cc} [MPa]	ε_{cc} [%]	f_{cc} eq. (1) [MPa]	ε_{cc} eq. (3) [%]	f_{cc} [MPa]	ε_{cc} [%]
0.0	43.1	0.25	43.1	0.25	42.8	0.23
2.2	46.0	0.43	51.9	0.51	50.4	0.46
4.3	53.5	0.65	60.7	0.76	58.5	0.76
8.6	73.0	1.66	78.4	1.27	74.3	1.80
17.2	107.0	2.81	114.0	2.29	105.8	2.81
30.1	149.3	4.23	167.0	3.83	153.0	4.30
43.0	184.2	5.02	219.0	5.36	198.3	5.00

In Figure 8 the obtained values of the cohesion and hardening parameter are plotted against the level of confinement. The values are normalized with respect to maximum values obtained in uniaxial compression, i.e. zero confinement. Also the derived scaling functions for the cohesion and the hardening parameter are shown. Both scaling functions are chosen to be represented by a linear relation. For comparison the results obtained by using equations (1) and (3) to calculate f_{cc} and ε_{cc} are also given in Table 1 and Figure 8.

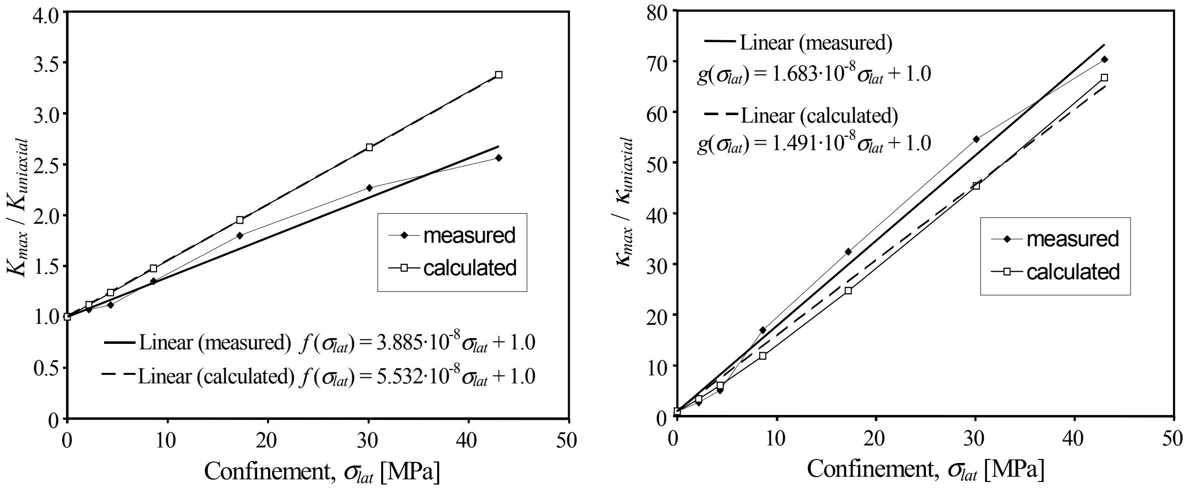

Figure 8 – The normalized values of (a) cohesion and (b) hardening parameter plotted against the level of confinement.

The results from the comparative FE analyses are shown in Figures 9 to 12 where the axial stress is plotted against the total axial strain. The peak strength, f_{cc}, and the corresponding strain, ε_{cc}, obtained in the FE analyses are compared with the test results in Table 1. As can be seen, the correspondence between the numerical results and the experimental data is fairly good. However, this is perhaps not surprising since it is a simple problem regarding both geometry and response.

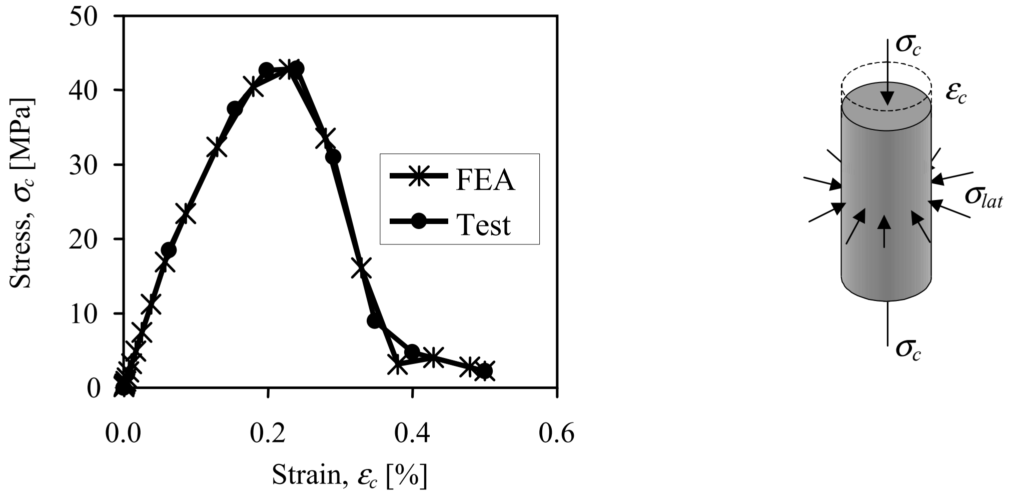

Figure 9 – Results for confinement 0.0 MPa (uniaxial) and the concrete cylinder specimen with a height of 108 mm and a diameter of 54 mm.

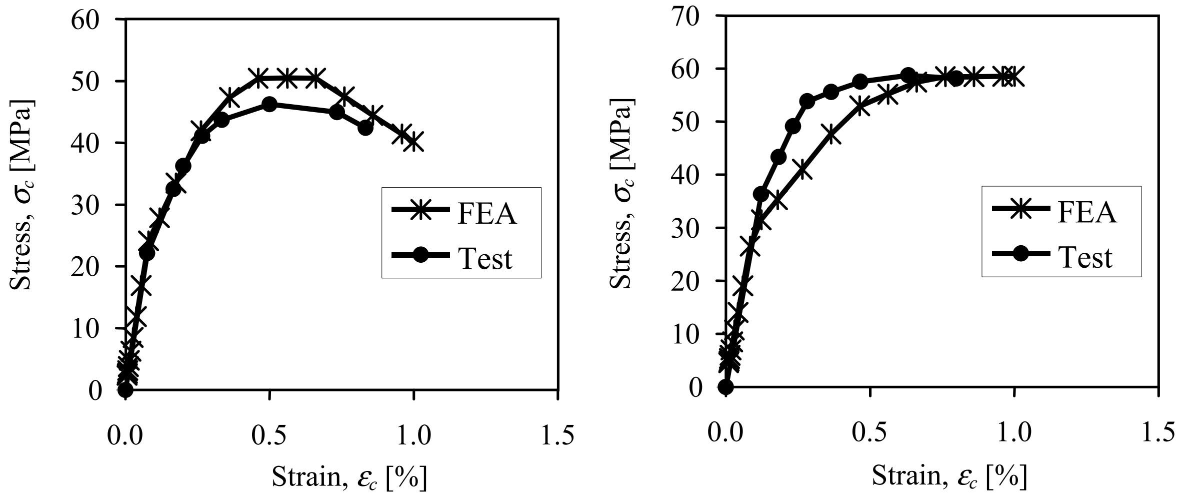

Figure 10 – Results for confinement 2.2 MPa and 4.3 MPa respectively.

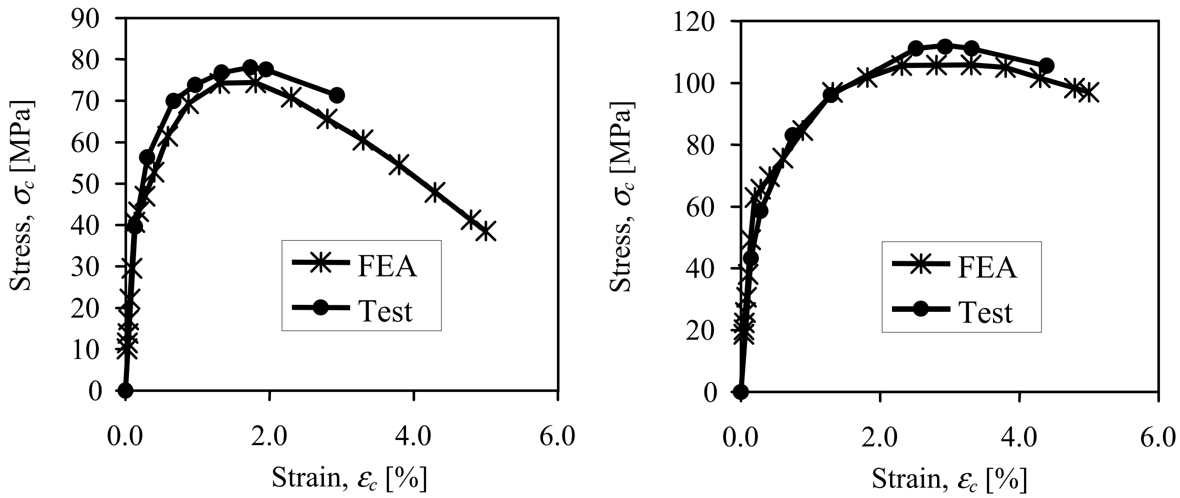

Figure 11 – Results for confinement 8.6 MPa and 17.2 MPa respectively.

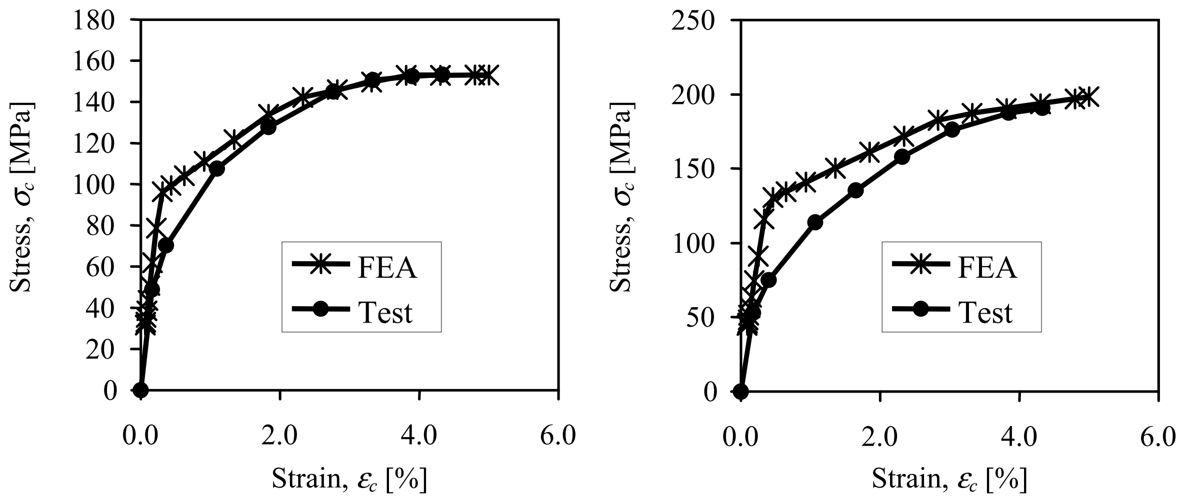

Figure 12 – Results for confinement 30.1 MPa and 43.0 MPa respectively.

4. STUDY OF CONCRETE-FILLED STEEL TUBES

4.1 Experiment

The emphasis of this paper is non-linear finite element analyses and application of the new confinement-sensitive concrete compressive model described in section 3; therefore, the tests are only briefly described. More detailed information about the tests can be found in Johansson (2000). The experimental study consisted of 13 short stub columns with the length of 650 mm and circular cross sections with a 159 mm outer diameter. The thickness of the steel tubes was 4.8 mm. Nine columns were circular hollow steel sections filled with concrete, while four columns, which were to be used as reference columns, were tested unfilled. The load was applied concentrically to the concrete section, to the steel section or to the entire section. Since no effect of increased concrete strength due to confinement is achieved when the load is applied only to the steel section, this loading situation will not be further discussed. The average values of the material properties of the concrete and the steel are summarized in Tables 2 and 3. These values are also used in the following FE analyses.

Table 2 – Material properties of the concrete at the age of 28 days.

$f_{c,cube}$ [MPa]	$f_{c,cyl}$ [MPa]	ε_{co} [‰]	E_c [GPa]	G_F [N/m]
79.4	64.5	3.0	38.5	157

Table 3 – Material properties of the steel.

f_y [MPa]	f_u [MPa]	ε_{ah} [‰]	ε_{au} [‰]	E_a [GPa]
433	568	29	136	206

4.2 Finite element analysis

An established FE model should be able to simulate the columns in a realistic way; such phenomena as the bond between the concrete core and the steel tube, and the increase in concrete compressive strength due to confining effects, have to be taken into account. The non-linear finite element analyses were made with ABAQUS/Standard 5.7; see HKS (1997). Three symmetry planes were used and only one eighth of the column was modeled since the same concentric load was applied in the same way at both ends; see Figure 13. The steel tube, the concrete core and the loading plates had to be separated from each other to simulate the bond between them: therefore they were defined as individual bodies using a three-dimensional finite element model based on solid elements. The confinement-sensitive compression model described in section 3 was used to model the concrete. The uniaxial stress-strain relations in compression, used in the analyses, were derived from standard cylinder tests with concrete from the same batch as the columns; see Table 2. In these tests the stress-strain relation could be recorded only up to the maximum stress. The remaining part of the stress-strain relation was determined in accordance with the CEB Bulletin d'Information 228 (1995). The relation between the cohesion and the hardening parameter was calculated according to equations (15) and (16). The scaling functions for the cohesion and the hardening parameter are represented by linear relations; see Figure 14.

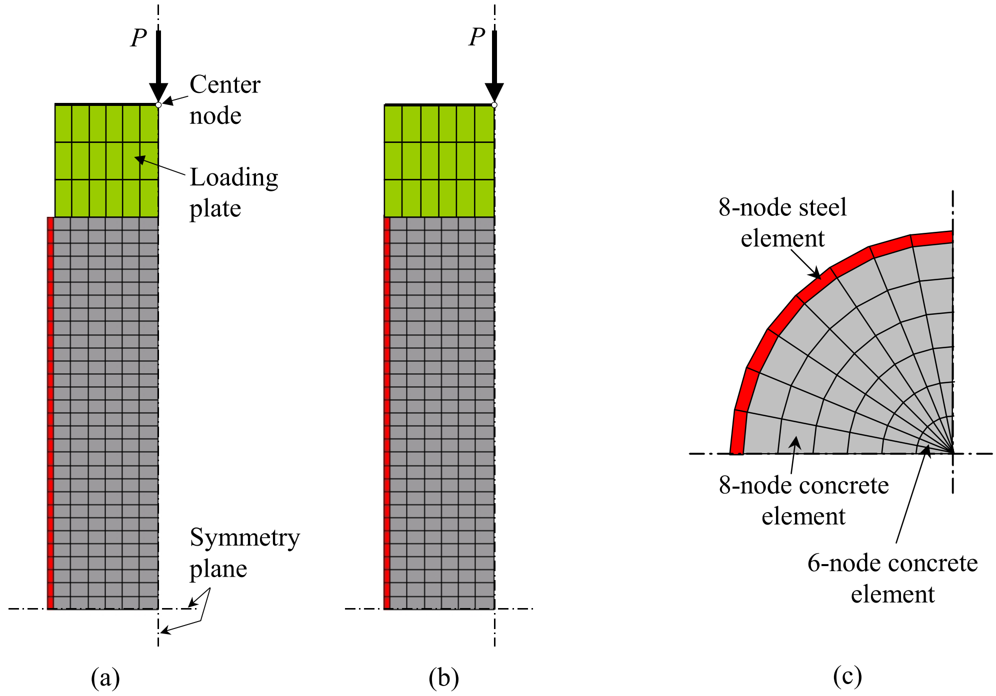

Figure 13 – The FE model: load on (a) concrete section and (b) entire section. The section of the columns in the FE model (c).

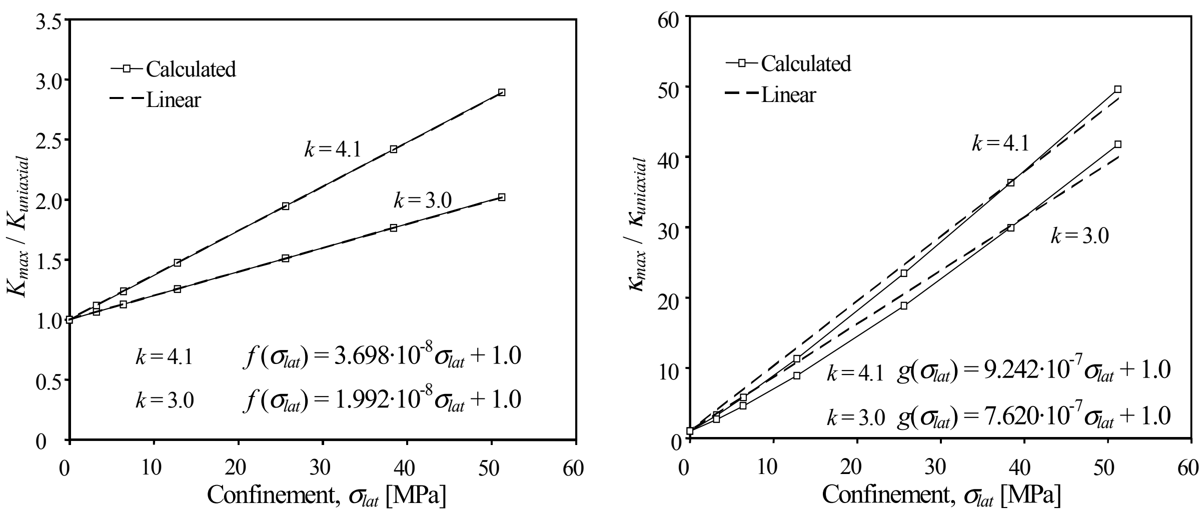

Figure 14 – The normalized values of (a) cohesion and (b) hardening parameter plotted against the level of confinement. (The results for k = 4.1 are shown only for comparison.)

The values for f_{cc} and ε_{cc} were calculated using equations (1) and (3) and corresponding values of K_{max} and κ_{max} according to equations (17) and (18), respectively. The triaxial factor k was set to 3.0 and the friction angle α to 30°. Poisson's ratio for the concrete in the elastic part was approximated as $\nu_c = 0.2$.

An elastic-plastic model, with the von Mises yield criterion, associated flow rule and isotropic strain hardening, was used to describe the constitutive behavior of the steel; see HKS (1997).

The complete stress-strain relation obtained from uniaxial tensile tests on specimens taken from the steel tubes was used in the FE analyses. Poisson's ratio in the elastic part was set to $v_a = 0.3$. To simulate the bond between the steel tube and the concrete core, surface-based interaction with a contact pressure-overclosure model in the normal direction, and a Coulomb friction model in the directions tangential to the surface, were used. In this way the surfaces could separate and slide relative to each other, as well as transmit contact pressure and shear stresses between the concrete core and the steel tube. According to Baltay and Gjelsvik (1990) the coefficient of friction, μ, between concrete and steel has a value between 0.2 and 0.6. The load was applied as an increased deformation at the center node of the loading plate to model the load of the structure. To distribute the load, all other nodes at the top surface of the loading plate were forced to have the same vertical translation as the center node. The Newton-Raphson iteration method was used to find equilibrium within each load increment. Furthermore, the geometric non-linear behavior, i.e. the local buckling of the steel tube, was taken into consideration.

4.3 Results and discussion

To verify the FE model, a comparison of the load-deformation relationships obtained from tests and those obtained in the FE analyses was made; see Figure 15. When the load was applied only to the concrete section (SFC) the best agreement was obtained when a coefficient of friction of 0.6 was used. Furthermore, as expected for this loading situation, the load resistance increases and the stiffness decreases with a lower value on the coefficient of friction. For the columns with the load applied to the entire section (SFE) a changed value of coefficient of friction did not affect the structural behavior. These observations are also according to what should be expected; see section 2.2. For the SFE column the maximum obtained concrete strength is approximately $1.3f_{c,cyl}$ and for the SFC column it depends on the coefficient of friction and varies from $1.3f_{c,cyl}$ up to $2.2f_{c,cyl}$ when μ is 1.0 and 0.0, respectively. As a further comparison the upper and lower bounds calculated according to equation (7) are shown in Figure 15. It can be observed that the load resistance of all columns falls within these two bounds. In absence of bond strength (μ = 0.0) between the steel and the concrete with the load applied only to the concrete section, there will be no axial stresses ($\sigma_{al} = 0$) in the steel tube and the tube is only used as lateral confinement of the concrete core. Hence, as can also be seen in Figure 15a, this situation corresponds well with the upper bound.

Figure 16 shows how the total axial load is distributed between the steel tube and the concrete core at the midsection of the SFC and SFE columns, when the coefficient of friction is set to 0.6. Although the structural behavior is approximately the same for both the SFE and SFC columns, it can be observed, when comparing the distribution of the axial force during loading, that there are differences in how the load is carried in the columns. In the former, the concrete core and the steel tube are loaded simultaneously; consequently, the load is already distributed from the beginning of the loading; see Figure 16b. In the SFC column, though, the concrete core carries almost the entire load in the initial stage of the loading. As the total load is increased, the concrete core expands in the lateral direction, and contact pressure and shear stresses develop between the concrete and the steel; hence the force carried by the steel tube increases; see Figure 16a. Further, this results in a lower stiffness for the SFC column than for the SFE column where the steel contributes to carrying load from the beginning.

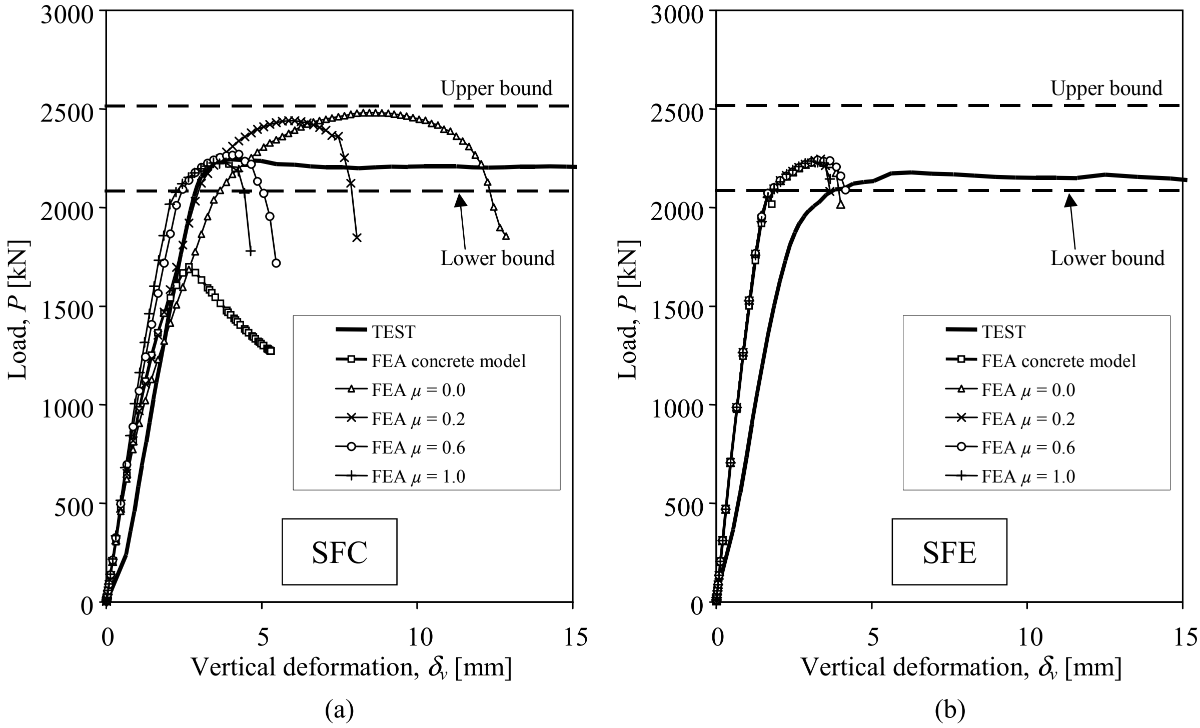

Figure 15 – Comparison of results of FE analyses and tests. Load (a) on concrete section and (b) on entire section.

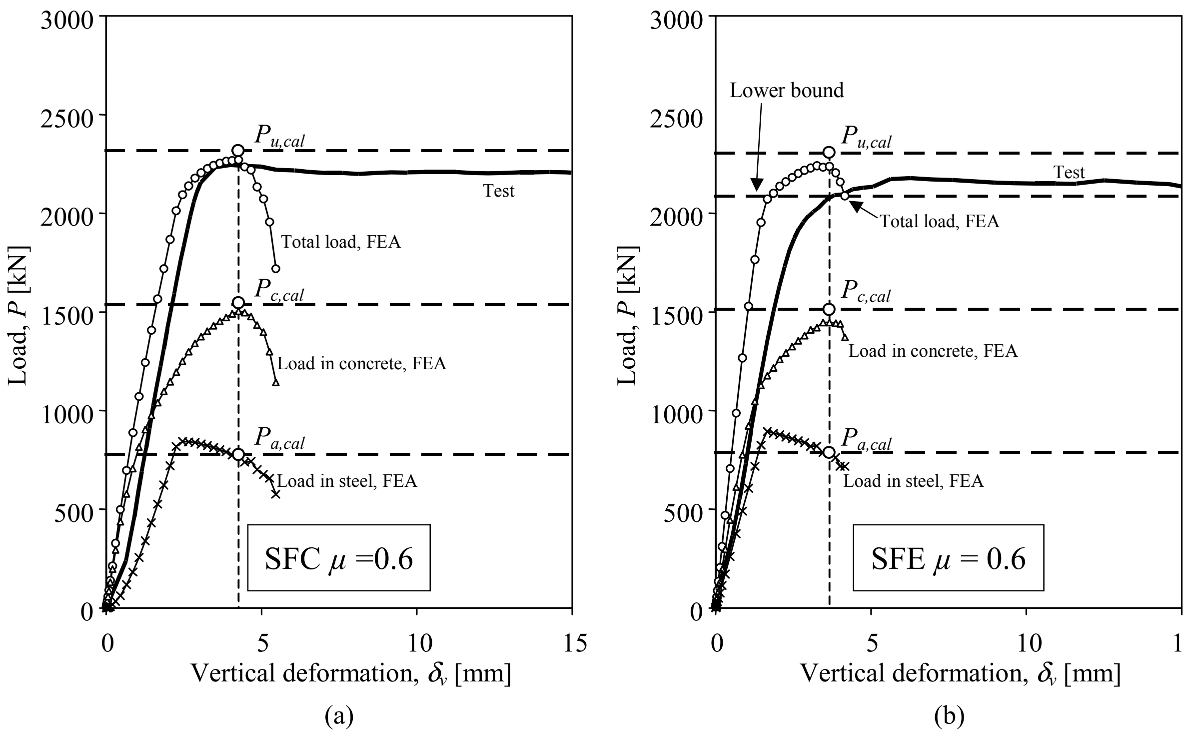

Figure 16 – Distribution of the axial force between concrete and the steel in the midsection of (a) the SFC and (b) the SFE column (μ = 0.6).

Figure 17 shows how the stresses (σ_{al}, σ_{ah} and σ_{at}; see also Figure 18) in a steel element, in the midsection of the SFC and SFE columns, vary during the loading (σ_{at} is the steel stress perpendicular to σ_{al} and σ_{ah}). Also the lateral confinement pressure σ_{lat} is shown, calculated from circumferential steel stress according to equation (5) (observe different scale). First, it can be noticed that the assumption of biaxial state of stress in the steel tube is true, since there is no stress over the thickness of the steel tube, i.e. $\sigma_{at} = 0$. Further, for the SFE column it can clearly be seen that there exists no circumferential steel stress before a vertical deformation of approximately 1.2 mm, when the lateral deformations of the concrete core catch up with those of the steel and a contact pressure is introduced. It can also be observed that because of the presence of circumferential steel stress, the yield strength is not reached in compression; and due to increasing circumferential steel stress, the axial steel stress decreases after the maximum stress is obtained; see Figure 17.

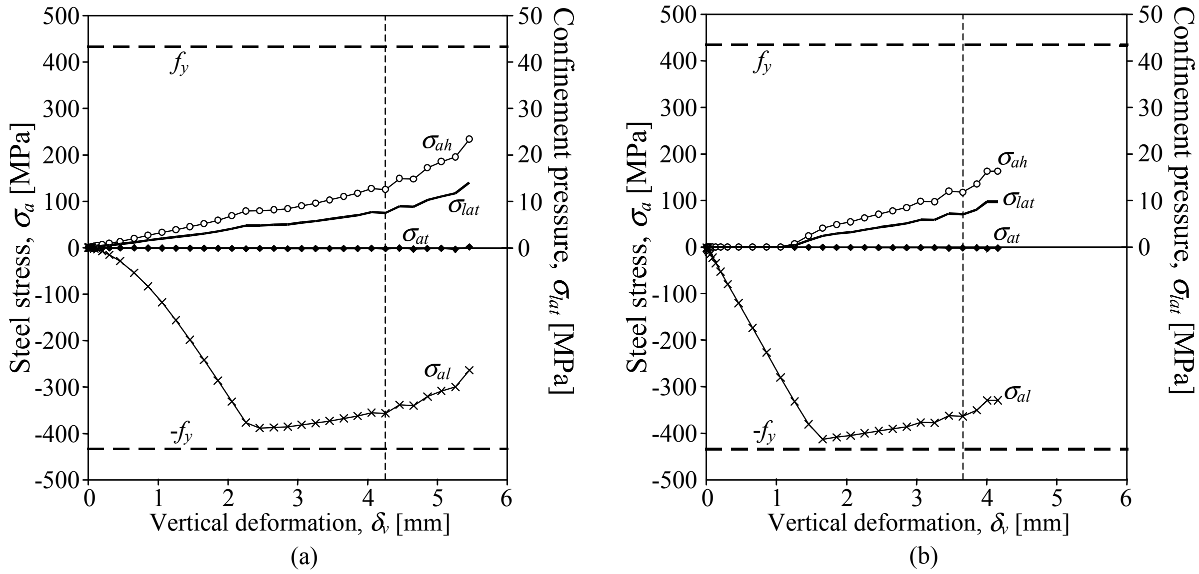

Figure 17 – The stresses for a steel element in the midsection of (a) the SFC and (b) the SFE column (μ = 0.6).

This effect is even more clear in Figure 18 where the stress path for the steel element of the SFC (μ = 0.0, 0.2, 0.6 and 1.0) and SFE columns (μ = 0.6) is shown, i.e. the relation between σ_{al} and σ_{ah}. As long as no hardening of the steel is obtained, this stress path can never go outside of the von Mises yield curve (see equation (6)); consequently the axial compressive steel stress has to decrease when the circumferential tensile steel stress increases. For the SFC column it is possible to see how the coefficient of friction affects the mechanical behavior of the steel tube, by means of the axial to circumferential steel stress ratio. For the higher value (μ = 1.0) the steel tube is mainly subjected to compressive stresses in the axial direction. Meanwhile, in absence of friction (μ = 0.0) only circumferential tensile stresses are present, thus, the steel tube is used only to provide lateral confinement of the concrete core. The latter situation provides the most effective use of the materials; however, it is hard to realize in practical use. For the SFE column, the ratio between axial and circumferential steel stresses is the same independently of the coefficient of friction.

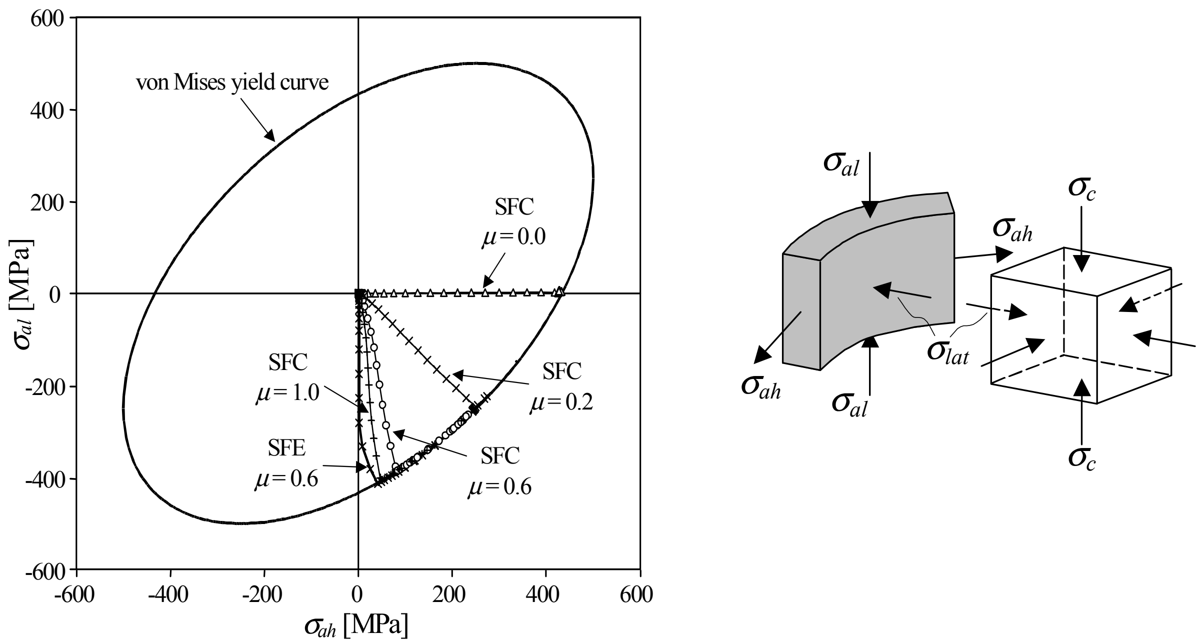

Figure 18 – The stress path for a steel element in the midsection of the SFC (μ = 0.0, 0.2, 0.6 and 1.0) and SFE columns (μ = 0.6).

If the steel stresses (σ_{al} and σ_{ah}) at the ultimate load obtained in the FE analyses (see Figure 17) are used in equation (7), it is possible to calculate the "theoretical" value of the ultimate load resistance $P_{u,cal}$ and its components $P_{a,cal}$ and $P_{c,cal}$. In Figure 16 these values are compared with the results obtained from the FE analyses and it can be seen that there is rather good agreement. However, the problem with using only the theoretical expression still remains, because it is necessary to know the relation between σ_{al} and σ_{ah}, which is hard to find without the FE analyses. This relation depends on the ratio of concrete to steel areas as well as the strength of the two materials. To be able to estimate the resistance and deformation capacity of a concrete-filled steel tube section, it is necessary to know how σ_{al} (i.e. the confinement pressure on the concrete core) and σ_{ah} develops during loading. Therefore, a simple analytical model that takes this into account needs to be developed.

Although the correspondence up to the load resistance between the numerical and experimental results is fairly good, and the structural behavior of the columns is in agreement with theories and previous studies, the post-peak behavior of the columns is not captured satisfactorily. To overcome this problem, not only the strength and hardening parameter needs to be confinement-sensitive; also the shape of the descending branch of the concrete stress-strain relationship should depend on the confinement stress level, i.e. increased confinement should give a more ductile behavior of the concrete; see Figure 2.

5. CONCLUSIONS

An object-oriented implementation of a confinement-sensitive compression model using the programming language C++ was presented. The confinement sensitivity affected both the strength and the hardening parameter and thereby also the plastic modulus. The confinement dependence is introduced by means of two adjustment functions, which can be derived either from triaxial material tests or by the presented theoretical expressions. The applicability of the model was shown in an example. Here results from the model were compared with experimental data from triaxial compression tests on concrete cylinders exposed to an active confinement pressure. The results showed that the model was capable, in an acceptable way, of reproducing the experimental data.

Furthermore, the model was used in a finite element study of composite columns consisting of concrete-filled steel tubes. There is a rather good correspondence up to the load resistance between the numerical and experimental results. Hence, the model is able to simulate the confining effects on the concrete also when the confining pressure is changing during the load history, i.e. passive confinement. Since the shape of the descending branch of the concrete stress-strain relationship is not confinement-sensitive, the post-peak behavior of the composite columns was not captured adequately. For the columns with the load applied to the entire section, the bond strength did not affect the structural behavior. However, when the load is applied only to the concrete section the load resistance increases and the stiffness decreases with lower bond strength.

6. REFERENCES

Ansari, F. & Li, Q. (1998): "High-Strength Concrete Subjected to Triaxial Compression." *ACI Materials Journal*, Nov.-Dec., Title no. 95-M75, pp. 747-755.

Attard, M. M. & Setung, S. (1996): "Stress-Strain Relationship of Confined and Unconfined Concrete." *ACI Materials Journal*, Sep.-Oct., Title no. 93-M49, pp. 432-442.

Baltay, P. & Gjelsvik, A. (1990): "Coefficient of Friction for Steel on Concrete at High Normal Stress." *Journal of Materials in Civil Engineering*, Vol. 2, No. 1, February, pp. 46-49.

CEB-FIP (1993): *CEB-FIP Model Code 1990, Design Code*. Thomas Telford, Lausanne, Switzerland, May, 437 pp.

CEB Bulletin d'Information 228 (1995): *High Performance Concrete, Recommended Extensions to the Model Code 90, Research Needs*. Lausanne, Switzerland.

Cederwall, K. (1988): "Some Ideas and Studies Concerning the Ultimate Capacity of Composite Steel and Concrete Elements." *Nordic Concrete Journal*, 1988:5, Stockholm, 7 pp.

Chen, W. F. & Han, D. J. 1987: "Plasticity for Structural Engineers." Springer-Verlag, Berlin, Germany, 606 pp.

Gardner, N. J. & Jacobson, E. R. (1967): "Structural Behavior of Concrete Filled Steel Tubes." *ACI Journal*, July, pp. 404-413.

HKS (1997): *ABAQUS/Standard User's Manual, version 5.7*, Hibbit, Karlsson & Sorensen, Inc. Pawtucket.

Imran, I. & Pantazopoulou, S. J. 1996: "Experimental Study of Plain Concrete under Triaxial Stress." *ACI Materials Journal*, Vol. 93, No. 6, pp. 562-573.

Johansson, M. (2000): “Structural Behaviour of Circular Steel-Concrete Composite Columns.” Licentiate thesis, Chalmers University of Technology, Div. of Concrete Struct., Göteborg, Sweden.

Kotsovos, M. D. (1987): “Consideration of Triaxial Stress Conditions in Design: A Necessity.” *ACI Structural Journal*, May-June, Title no. 84-S29, pp. 266-273.

Lippman, S. B. (1991): *C++ Primer*, *2nd Edition*, Addison-Wesley Publishing Company, reading, USA, 614 pp.

Malvar, L. J., Crawford, J. E., Wesevich, J. W. and Simons, D. (1997): “A Plasticity Concrete Material Model for DYNA3D.” *Int. J. Impact Eng*., Elsevier Science Ltd, Great Britain, Vol. 19, pp. 847-873.

Mills, L. L. & Zimmerman, R. M. (1970): “Compressive Strength of Plain Concrete under Multiaxial Loading Conditions.” *ACI Journal*, Vol. 67, No.10, Oct., pp. 802-807.

Orito, Y., Sato, T., Tanaka, N. & Watanabe, Y. (1987): “Study on the Unbonded Steel Tube Concrete Structures.” *Engineering Foundation Conference on Composite Constructions*, Henniker, New Hampshire, USA, June, 16 pp.

Pantazopoulou, S. J. (1995): “Role of Expansion on Mechanical Behavior of Concrete.” *Journal of Structural Engineering*, Vol. 121, No. 12, December, pp. 1795-1805.

Richart, F. E., Brandtzaeg, A. & Brown, R. L. (1928): *A Study of the Failure of Concrete under Combined Compressive Stresses*, Bulletin No. 185, University of Illinois, Engineering Experimental Station, Urbana, Illinois, USA, November, 104 pp.

Schneider, S. P. (1998): “Axially Loaded Concrete-Filled Steel Tubes.” *Journal of Structural Engineering*, Vol. 124, No. 10, October, pp. 1125-1138.

Tomii, M. Y., Yoshimura, K. & Morishita, Y. (1977): “Experimental Studies on Concrete Filled Steel Tubular Columns under Concentric Loading.” *Proc. Int. Colloquium on Stability of Structures Under Static and Dynamic Loads*, pp. 718-741.

ENVIRONMENTAL ACTIONS AND RESPONSE – REINFORCED CONCRETE STRUCTURES EXPOSED IN ROAD AND MARINE ENVIRONMENT

Anders Lindvall
Ph.D.-student
Department of Building Materials
Chalmers University of Technology
SE-412 96 Göteborg
E-mail: lindvall@bm.chalmers.se

ABSTRACT

In this paper a recently published licentiate-report is presented and summarised. The report deals with environmental actions on and response from reinforced concrete structures and how they influence and limits the service life. It is described how the degradation of reinforced concrete structures takes place and how it can be predicted with mathematical models. A methodology to assess the environmental actions is presented, where they are divided into four different levels depending on the dimensional scale. Finally a survey of environmental actions and response on seven road bridges around Göteborg is presented.

Key words: Environmental actions, Service life design, Chloride penetration, Moisture conditions, Road exposure, Reinforcement corrosion

1. INTRODUCTION

1.1 General

In this paper a recently published licentiate-report [1], written by the author, is presented and the content is summarised. The emphasis of the paper is put on environmental actions and response from reinforced concrete structures. To describe the environmental actions on a concrete structure a division is made into four levels depending on dimensional scale. The most accurate way to describe the environmental actions is to describe them as surface temperature, humidity, wetness and chloride conditions. The response from the concrete can be expressed as temperature and moisture conditions, carbonation depths and chloride penetration. The response from concrete structures is exemplified in a field survey of moisture and chloride conditions and frost action in seven concrete bridges around Göteborg have been performed.

1.2 Background

The expenses for repair, maintenance and remediation of existing reinforced concrete structures have significantly increased during the last decade. A large part of these expenses can be related to problems with lacking durability of the structure. Thus, to reduce the expenses there is a need to design for service life, where the total lifetime for the structure is designed. In the design for service life it is also included how the properties of the reinforced concrete change over time due to degradation. Examples of degradation processes, which change the properties of reinforced concrete, are reinforcement corrosion, initiated by chloride ingress or carbonation, frost attack and alkali-aggregate reactions (AAR).

The degradation of reinforced concrete is influenced by a number of parameters. It is possible to identify three principal parameters: (1) Material properties, (2) Execution during construction and (3) Environmental actions. The designer can choose the material properties and how the execution during construction should be made. However, the environmental actions mainly follow from the location of the (future) structure and are only possible to influence in a limited way. Additionally the material properties and environmental actions change over time, due to continuous cement hydration and seasonal variations respectively. Thus, to design for service life it is required to have sufficiently realistic mathematical models that describe how the material properties and environmental actions vary over time.

The service life can be designed with two principal methodologies: deem-to-satisfy rules, and performance-based design. The deem-to-satisfy rules are usually based on rules-of-thumb, e.g. by specifying a certain concrete composition and/or concrete cover, and the result will be a long but not specified service life. The performance-based design is based on requirements of performance from the structure, e.g. load-bearing capacity or aesthetic appearance, and the result will be a long and specified service life. The performance requirements are specified with so-called limit-states.

Until now large research-efforts have been made to clarify which influence the material properties, and to some extent the execution during construction, have on the degradation of concrete. However, good data about the influences from the environmental actions and the response from the concrete are lacking. Since data on the environmental influence are lacking the result may be that the service life designs have large statistical uncertainties. Thus there is a need to further investigate and quantify the environmental actions and response from concrete structures.

My work has been concentrated on to make an investigation of available models to determine the environmental actions on concrete structures and the response from the concrete. The investigation has been made both as a literature review and field studies. The literature review has been focused on environmental actions and response and degradation of concrete. The data from the field studies have been used to develop and quantify models.

1.3 DuraCrete

The PhD-project described in this paper was initiated during the DuraCrete-project, summarised in [2]. In the DuraCrete-project a new performance based service life design methodology for reinforced concrete structures has been developed. With this design methodology it is possible to model the complete service life for a reinforced concrete structure, i.e. from casting, until degradation has put the structure into an adverse state, e.g. when the bearing-capacity is insufficient. The project has been partly financed by the European community and 12 partners around Europe have been involved.

In the DuraCrete-project the service life has been modelled with a performance based methodology and determined with probabilistic methods. The service life is modelled as initiation and propagation of reinforcement corrosion, consequences of reinforcement corrosion and finally structural consequences. The different models consist of three principal parameters describing the influence from material properties, execution during construction and environmental actions. The probabilistic methods make it possible to also consider statistical uncertainties related to the parameters used to describe the influence from material properties, execution during construction and environmental actions.

2. SERVICE LIFE FOR REINFORCED CONCRETE STRUCTURES

In this section a short introduction of how the service life of reinforced concrete structures can be made is given. For a more detailed description see [1].

2.1 General

The degradation of reinforced concrete structures takes in a number of chemical and physical processes. The most common are: (1) Reinforcement corrosion, (2) Frost attack, (3) Alkali-aggregate reactions (AAR), (4) Sulphate attack, (5) Leaching and (6) Seawater attack.

To be able to explicitly predict the degradation of concrete in a quantitative way there is a need for mathematical models. Usually a division is made between physical and empirical models:

- **Physical models.** Physical models are based on theories on how reactions and transport of different substances takes place in a material. Together with knowledge about initial and boundary conditions, it is possible to make careful predictions of how different substances are transported into a material. The models are often quite complicated and they require an extensive validation before they can be used to make practical predictions. The predictions with physical models usually require numerical methods, e.g. finite difference or element methods to be made, which means that computers have to be used.
- **Empirical models.** Empirical models are based on observations of response from structures, exposed either in field or in laboratory. The observations are used to derive and quantify the parameters in the models. The models are often quite simple and observations are used to derive and quantify the parameters. This means that the models do not need that much validation before they can be used for practical predictions. Since the models often are quite simple they usually can be solved without computers.

However, there is a danger to use observations from already built structures, which is the case with empirical models, since they are influenced both by the materials, environments and the workmanship during construction. All these factors may change, e.g. if a new concrete composition is introduced, which means that the old observations cannot be applied on a structure where a new material will be used. Additionally data from long-term exposure are missing.

Example of a physical model to predict chloride penetration is ClinConc (Chlorides in Concrete) [3], where the predictions are based on mass balance relations that can be defined for concrete. Examples of empirical models to predict chloride penetration are Fick's 2nd law of diffusion (when applied on concrete), DuraCrete-model [4] and Mejlbro-Poulsen-model [5].

2.2 Service life design

There are two principal methods to determine the service life of reinforced concrete structures, namely deem-to-satisfy rules and performance based design.

Deem-to-satisfy rules are usually based on experiences from previously built structures, expressed as rules-of-thumb. The rules-of-thumb usually specify that a required service life can be reached by using a certain concrete mix and concrete cover. The result will be a structure with sufficiently long but not specified service life. Furthermore the rules-of-thumb only work with known materials, since they are based on experiences from previously built structures, which makes it hard to make service-life designs for structures built with new materials.

In a performance based design, the performance of the structure is specified with so-called limit-states. The limit states can be defined by for example authorities and/or the owner of the structure. To determine the probability that the structure is able to meet the performance requirements, with a specified level of reliability, a probabilistic model is formulated. The probabilistic model is based on (sufficiently) realistic mathematical models, where the different behaviour of the concrete structure is modelled, e.g. chloride penetration, consequences of reinforcement corrosion and load-bearing capacity. The results from the probabilistic calculations are given as probabilities that the structure is in an adverse state (according to what is defined from the limit states), i.e. the required performances are not fulfilled, during the desired service life. The result will be a structure with sufficiently long and specified service life.

3. ENVIRONMENTAL ACTIONS AND RESPONSE

In the following section a brief description of the environmental actions and response on concrete structures is given. A more extensive description is given in [1].

3.1 General

The general approach when the environmental actions on a concrete structure are described and modelled is to separate the actions from the response of the structure. With this approach the environmental actions can be described without knowledge about the nature of the surface and the properties of the bulk concrete. The most correct way to describe the environmental actions on a concrete structure is to express them as surface conditions.

The environmental actions can mostly be described from processes in the atmosphere. When the processes in the atmosphere are studied a division is made into two sciences, [6]:

- **Meteorology**. Meteorology is the science of atmospheric physics where atmospheric processes are analysed, explained and predicted. The weather is the current state of temperature, precipitation and wind in the nearest atmosphere.
- **Climatology**. Climatology is the science of how the climate varies between different areas and on different time-scales. The climate is the history of the weather and it gives a picture of what is normal and the probability of a certain type of weather.

It is convenient to divide the environmental actions into different dimensional scales. These scales have both different horizontal dimensions and time-scales. The following four scales can be defined: (1) **Global climate** – Macro scale, (2) **Regional climate** – Meso scale, (3) **Local climate** and (4) **Surface climate** – Micro scale. These four dimensions are explained further later.

However, it is not enough to know the environmental actions outside a concrete structure to predict the surface climate, since the surface climate is also influenced by the surface conditions. Thus, it is desirable to have knowledge about the response from the structure. The response from a concrete structure can be determined in terms of, with variations in three dimensions and time:

- **Temperature conditions**. T(x,y,z,t).
- **Moisture conditions**. RH(x,y,z,t), TOW (Time of wetness).
- **Chloride conditions**. Cl(x,y,z,t).
- **Carbonation.** CO_2(x,y,z,t).

The environmental actions can be quantified with data measured at a meteorological station. Since a meteorological station usually has somewhat different surrounding conditions compared to the location of a (future) structure the data have to be transformed to this location before they can be used. In [6] a procedure to select climate data for a determination of the surface climate is given. The procedure is divided into four steps: (1) Collection and preparation of weather data, (2) Choice of representative weather data, (3) Choice of specific format for the simulation and (4) Transformation of climate data from a weather station to the surface of the construction. The collection of weather data is standardised and the procedure is described in [7]. How weather data can be collected, prepared and characterised is described in [8].

3.2 Global climate – Macro scale

The global climate can be described with energy and mass balances in the Earth-Atmosphere system. The main parts of the energy balance is incoming solar radiation and outgoing long wave radiation. Energy of importance for the earth-atmosphere system exists in four different forms: radiant, thermal, kinetic and potential energy. The energy is all the time transformed from one form to another within the system.

In a similar way to the energy balance it is possible to establish a water-balance for the Earth-Atmosphere system. There is an exchange of water, in different phases, between the surface of the earth and the atmosphere. This is possible due to the fact that water can exist in three different states of aggregation (phases): vapour (gaseous phase), water (liquid phase) and ice (solid state).

3.3 Regional climate – Meso scale

GENERAL
The regional climate is the climate for a relatively small area, e.g. a town or a valley. It is influenced by the properties of the ground, e.g. type of terrain and vegetation, the topography, by large water bodies the location in relation to urban areas and by the exposure to marine environments. Individual buildings or structures do not influence the regional climate. Special conditions occur in urban areas and areas close roads, where de-icing salts are spread (road environments), and oceans (marine environments). The marine and road environments have influences both on the regional and local climate.

URBAN CLIMATE
In urban areas the climate is influenced from changes in the surface properties and the atmosphere caused by urban activities, e.g. air pollution and release of heat and water to the atmosphere. If the conditions in an urban area are compared with the conditions in a surrounding rural area, the urban climate is usually rougher, warmer and drier. Compared with a surrounding rural area the solar radiation in an urban area may be reduced with up to 20% depending on the topography and the amount of pollutions in the air. The differences in air temperature between urban and surrounding rural areas can be up to 5-6°C, with a maximum difference of up to 12°C [9]. The magnitude of the urban influence on the climate is hard to estimate, since observations of the climate in a region before and after urbanization are very rare.

MARINE ENVIRONMENT
A marine environment is the prevailing environment in and in the vicinity of an ocean or sea. Coastal areas, which can be characterized to have a marine climate, normally reach some 10 km from the coastline, due to wind-blown salt mist. However, at special occasions, e.g. during severe storms, the area influenced by the marine climate can be over 100 km from the coastline. The marine environment is characterized by, [10]: (1) Chemical composition of the seawater, (2) Temperature in the seawater, (3) Wave heights, (4) Hydrostatic pressure, (5) Tidal actions, (6) Water levels, (7) Fog and spray and (8) Currents.

In [11] it is proposed to divide the marine environment into four different zones depending on the position to the water level:

- **Submerged zone**. The zone below the water level, which means that the concrete is subjected a constant moist environment.
- **Tidal zone**. The zone between low and high tide, which means that the concrete is subjected to periodical moistening and drying (with an approximately twelve hour cycle).
- **Splash zone**. The zone over the tide level influenced by the waves, which means that the concrete is subjected to randomly moistening and drying, due to wave-actions.
- **Atmosphere zone**. The zone over the splash zone where the concrete is subjected to humid and saline marine air.

ROAD ENVIRONMENT
The road environment is to large extent influenced by if the road is thaw-salted or not. The road environment is influenced by: (1) The amount and types of de-icing salts spread on the road (2) The amount and types of traffic on the road (frequency of heavy traffic), (3) The geometry of

the road and the surroundings, and (4) The distance to the road. De-icing salt can be spread in five different forms on a road depending on the temperature of the road surface: dry salt, wetted dry salt, salt solution, sand mixed with salt and crushed aggregate and sand mixed with salt. The amount of chlorides spread on the road varies depending on the form the de-icing salt is spread, where dry salt gives the highest amount of chlorides.

The de-icing salt spread on the road can be transported into four principal processes, [12] and [13]:

- **Drainage**. De-icing salts are soluble with water and the brine, formed on the road, is forced to the side by gravitation and/or traffic movements. The drainage increases with rainfall
- **Ploughing**. When the road is ploughed, salt-laden snow is pushed to the roadside.
- **Splash**. Splash is produced by the drainage system of vehicle tyres. It consists both of water and snow-slush. The splash is directed from the car towards the side of the road. It is characterized of relatively large droplets that are not easily caught by wind-streams around vehicles.
- **Aerosols (Spray)**. Aerosols, like splash, originate from the drainage system of vehicle tyres. The aerosols are formed when water is thrown outwards by centrifugal action tangential from the tire tread and it breaks down into small droplets when it hits other parts of the vehicle. It is transported by air streams and may persist in the air behind a vehicle for a long time. The amount of aerosols formed is dependent on the speed of the vehicles.

The transport of de-icing salts from the road can be divided into initial loss and loss with time, [13]. The initial loss depends on the state of the road (mainly wetness condition), the application method and the traffic intensity. Several investigations have been made on how de-icing salt spread on a road is transported into the surroundings. The influence from the de-icing salt spread on a road can be detected up to 100 meters from the road, [14]. The transport of salt from a road is in large extent a function of the car-speed on the road. Another important factor is the duration of the slush on the road surface, where a long time of duration results in larger transport of chlorides and thus larger chloride load. The transport of chlorides is also dependant of the orientation of the road in relation to prevailing winds etc.

In [15], where a survey of 200 motorway bridges in Great Britain is presented, three main sources for exposure of chlorides on concrete road bridge are given:

- **Leakage of chlorides through joints**. The chloride-contaminated slush on the surface on the road may leak through joints and reach for example the underside of the bridge slab.
- **Splash from passing traffic**. The traffic on the road produces splash that hits the parts of the structure that are facing towards the traffic.
- **Spray from passing traffic.** The traffic on the road produces spray (aerosols) that is transported with air-streams towards the structure. This means that the chloride-contaminated spray may reach parts of the structure that are not directly facing towards the traffic.

3.4 Local climate

The local climate is the climate for a structure or a certain part of a structure. It follows from the large-scale geometry and the orientation of the (future) structure. The local climate is influenced by for example the radiation exchange between the ground and/or structure and the sky and air streams, with or without precipitation, around structures. Influencing factors are the surface properties of the ground and/or structures, the large-scale geometry of the structure, providing possible shelter against radiation and wind, the distance to larger urban areas and exposure of seawater and spread de-icing salt.

3.5 Near-surface climate – Micro scale

The microclimate, or near-surface climate, for a structure is influenced by the geometry and surface properties of the structure in question. The microclimate can be expressed in terms of:

- **Temperature conditions.** Expressed as equivalent surface temperatures, $T_{s,eq}$, where effects due to radiation (solar and long-wave radiation), evaporation/condensation, heat transfer (convection and conduction) and material and surface properties are considered. The equivalent surface temperatures are calculated by establishing an energy budget for a surface.
- **Moisture conditions.** Expressed as equivalent surface humidities, $RH_{s,eq}$, and TOW (Time Of Wetness). The equivalent surface humidity follows from the equivalent surface temperature conditions and the TOW is achieved by combining wetness due condensation, precipitation and running water. Both the equivalent surface humidity and the TOW depend on the material and surface properties for the structure in question.
- **Chloride conditions**. Expressed as an equivalent surface chloride concentration, $C_{s,eq}$, which is a combination of the exposure environment, the geometry of the structure and the material and surface properties.

3.6 Response from concrete

The environmental actions on a concrete structure result in a response from the concrete, described in terms of:

- **Temperature conditions**. The temperature conditions in a concrete structure can be predicted with the law of energy conservation. However, since concrete is an excellent heat conductor, which means that temperature gradients are usually small and will disappear rapidly. The temperature conditions are decisive for many deterioration processes.
- **Moisture conditions**. The moisture conditions in a concrete can be determined by solving the law of mass conservation, where the moisture content is expressed as evaporable and non-evaporable water. For porous materials there is a relationship between the evaporable moisture and the RH in the pores called sorption-isotherms. Moisture plays a significant role in chemical reactions in concrete and in parts of physical and chemical processes in concrete.
- **Chloride conditions**. The chloride conditions in a concrete can be determined as chloride penetration profiles. The chloride penetration into concrete is a complicated process, influenced by number parameters, e.g. the chloride concentration in the surrounding environment, the temperature and moisture conditions, wind-streams around the structure etc.
- **Carbonation**. Carbonation in concrete can be determined in terms of carbonation depths.

3.7 Quantification of environmental actions

To be able to make service life designs with the different mathematical prediction models it is necessary to quantify the parameters in the models. The quantification of environmental influence on the deterioration of a concrete structure can be made in the following ways:

- **Environmental actions.** The quantification is based on information about the environmental actions on the structure, i.e. the surface conditions expressed as temperature, moisture, chloride and carbon dioxide conditions.
- **Response from concrete.** The quantification is based on information about the response from the concrete on the environmental actions, i.e. chloride penetration profiles, carbonation depths and moisture and temperature distributions in the concrete. However, the response from the concrete does not only includes effects from the environmental actions but also effects from the material properties, e.g. concrete composition, and the execution during construction.

The presently used prediction models do not include the environmental actions in an explicit way, which means that the environmental influence must be quantified with the response from the concrete. This requires knowledge about how the environmental actions vary over a structure over time and how this influences the response. Information about these variations is still scarce and it has been shown that there can be significant variations, in environmental actions and response, even on one single structure. Additionally data from long-term exposure are missing, which makes it hard to assess to long-term properties of the concrete.

In [4], a procedure to quantify the parameters in degradation is proposed. The parameters in the mathematical prediction models are divided into the following three classes:

- **Construction influences.** Follow from the execution during the construction phase, e.g. the placement of the reinforcement, concrete composition, curing conditions etc.
- **Environmental influences.** Follow from the conditions at the location of the structure, e.g. temperature and humidity conditions.
- **Material influences.** By choosing different binder types, binder content, w/b, type of aggregate etc, it is possible to control the material influences. The material influence can be determined in the laboratory, as for example chloride diffusivities.

The designer can choose how the material and partly the construction influences the performance of the structure, but the environmental influences follows from the conditions at the location of the structure.

4. FIELD SURVEY – RESPONSE FROM CONCRETE

In the following section a field survey of seven concrete bridges around Göteborg is presented. The survey was made in November and December of 1998 and 1999. In this section a short description of the survey and results is given. More extensive descriptions are given in [1] and [16].

4.1 Determination of response

Cores have been taken from the examined bridges by drilling with water-cooling for further analysis in the laboratory to determine the response from the concrete. The response from the examined bridges have been determined in terms of:

- **Chloride penetration**. Presented as chloride penetration profiles, where the quotient between the chloride and calcium content at different depths is shown. The chloride penetration profiles have been determined with powder samples achieved from profile grinding in depth intervals, with increasing intervals with increasing depths. The powder has been dissolved in acid and soda and analysed for chloride and calcium with potentiometric titration.
- **Concrete cover**. The concrete cover has been determined with an electrical cover meter. It should be noticed that the measured cover-depth with an electrical cover-meter is only an approximate value of the cover-depth. To get accurate figures of the concrete cover, cores should be drilled into the reinforcement and the concrete cover measured directly.
- **Visible signs of reinforcement corrosion**. The examined bridges have been examined for visible signs of reinforcement corrosion, e.g. cracks with precipitation of rust or rust stains on the surface of the concrete. With information about the chloride penetration profiles it is possible to determine the chloride threshold value for reinforcement corrosion.

Apart from the investigations mentioned above the bridges have also been investigated for chloride diffusivity with the CTH-method, described in [3] and NT BUILD 492 [17], moisture conditions, profiles with RH and S_{cap}, and frost resistance determined with NT BUILD 376 [18]. However, the results from these investigations are not presented in this paper. Complete listings of all results are given in [1] and [16].

The cores used to determine the chloride penetration had a diameter of 50 mm and the cores used to determine the chloride diffusivity, the moisture conditions and frost resistance had a diameter of 100 mm. More extensive descriptions of the different methods to determine the response from the concrete are given in [1] and [19].

4.2 Examined bridges

Seven bridges around Göteborg have been included in the study. The bridges have been selected in such way that each of them represents typical Swedish concrete road bridges, with an age between 25 and 35 years. With a typical Swedish bridge means that the bridge was designed and constructed according to valid Swedish concrete standards. This means that the bridges have been built with a K 400 concrete, with a cement content varying between 300-360 kg/m^3 and a w/c of 0.45-0.50. All the examined bridges are motorway-bridges, where the motorway crosses, either above or below, another way.

The following bridges have been included:

- **Bridge N 434**. Bridge, built 1972, over the motorway E6, where E6 crosses the road between Kungsbacka and Onsala, approximately 30 km south of Göteborg. The southern side-beam on the bridge slab and the two southern columns (middle and side) at the eastern roadway (direction Göteborg) have been examined.
- **Bridge O 670**. Bridge, built 1968, where the motorway E6 crosses Nordre Älv in Kungälv approximately 20 km north of Göteborg. The western side-beam and the underside of the bridge slab have been examined.

- **Bridge O 707**. Bridge, built 1968, with a combined exit- and entry-road to the motorway E6. The eastern side-beam at the abutment and a column at a local road have been examined.
- **Bridge O 762**. Bridge, built 1974, where the high Rv40 crosses Landvettervägen at Slamby, approximately 13 km east of Göteborg. The northern side-beam and the southern of the eastern columns have been investigated. Bridge O 762 is situated approximately 2 km west of bridge O 978.
- **Bridge O 832**. Bridge, built 1972, with exit and entry to the motorway E20, approximately 7 km east of Göteborg. The bridge is a part of a roundabout over E20. The northern side-beam and the eastern of the northern columns have been examined.
- **Bridge O 951**. Bridge, built 1972, over the motorway E6, where a local road crosses E6 in Lindome, approximately 20 km south of Göteborg. The southern of the middle columns have been examined.
- **Bridge O 978**. Bridge, built 1974, over the motorway Rv40, where a local road crosses Rv40 at Landvetter centre, approximately 15 km east of Göteborg. The western side-beam and the westerly of the middle-columns have been examined. Bridge O 978 is situated approximately 2 km east of bridge O 762.

The concrete covers of the examined bridges were found to vary between approximately 22 mm (underside of bridge slab) and 45-55 mm (side-beams). The low concrete cover on the underside of the bridge slab has probably occurred probably due to insufficient execution during construction and lack of quality control.

4.3 Environmental conditions

The environmental conditions for the different bridges have been determined as the regional climate for the Göteborg-region and the road climate for each bridge. Examples of the regional climate for the Göteborg-region are given in figure 1, where the monthly mean values and 5%- and 95%-fractiles for the air temperature and air humidity over the year are presented. The road climate for the examined bridges is given in table 1.

Table 1 – The road climate for the examined bridges

Bridge	Built	Traffic		De-icing	Lanes	
		Amount [ÅDT]	Speed limit [km/h]	kg/m^2 year	Number	Safety lane
O 978*	1974	26000	110	3.0	2+2	Yes
O 978^{+}	1974	♦	50	♦	1	Yes
N 434*	1972	27000	110	2.8	3+3	Yes
N 434^{+}	1972	♦	70	♦	1+1	No
O 951*	1972	34000	110	2.8	2+2	Yes
O 670*	1968	40000	110	3.1	2+2	Yes
O 670†	1968	♦	♦	♦	2+2	Yes
O 707^{-}	1968	♦	50	2.3	1+1	No
O 707^{+}	1968	2400	50	♦	1+1	No
O 762*	1974	32000	110	3.0	3+2	Yes
O 762^{+}	1974	♦	70	♦	1+1	No
O 832*	1972	50000	90	2.7	3+3	Yes
O 832$^{+/-}$	1972	13200	50	♦	2	No

* : Motorway.
+ : Local roadway.
- : Exit/entry on motorway.
† : Underside bridge slab.
ÅDT : Mean-traffic during a day.
♦ : not known

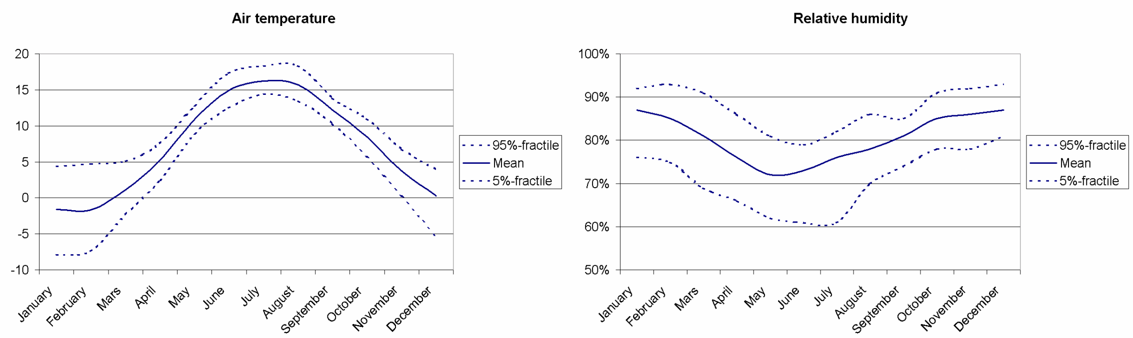

Figure 1 – Variations in monthly air temperatures and humidities in Göteborg. Based on data from [8].

4.4 Results – response from concrete

All chloride penetration profiles are analysed from cores taken during November or December in 1998 or 1999, i.e. before or in the beginning of the season when de-icing salts are applied. When de-icing salts are applied chlorides penetrate into the concrete while during the summer the chlorides in the surface layers of the concrete are washed out. The chloride penetration rate is highest for vertical surface, but the amount total amount of chlorides that penetrate during a winter is higher for horizontal surfaces. This effect is described in [20].

A selection of the chloride penetration profiles from the examined bridges is shown in figure 2. A complete listing of all the chloride penetration profiles is given in [1]. The first index show if the profile comes from a column (C), side-beam (SB) or other part of the structure (Ö), the second index shows which bridge the profile comes from and the third index indicates the name of the profile. The profiles have been analysed after exposure times between 25 and 30 years.

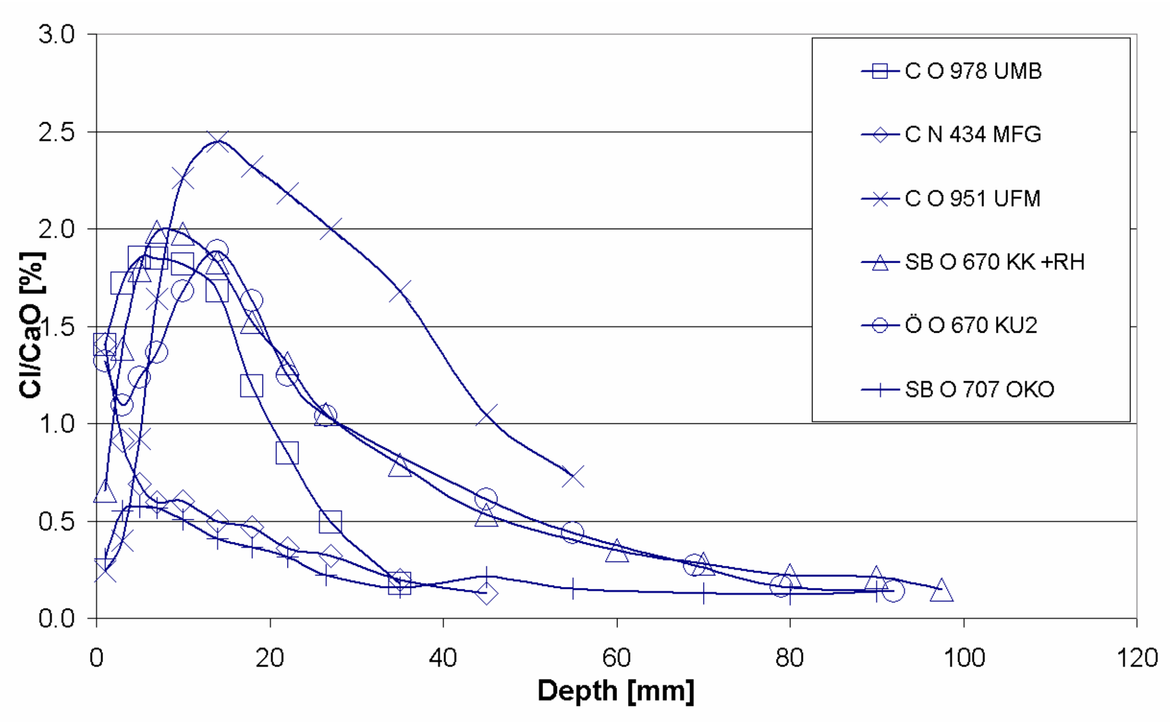

Figure 2 – A selection of typical chloride penetration profiles from the examined bridges.

The chloride ingress in the columns on the bridges O 978, O 951 and N 434 have been investigated on three different heights over the roadway and four different directions towards the traffic. In figure 3a the different sampling spots are presented and in figure 3b the chloride penetration profiles from the column on bridge O 978 are presented. The indexes U, M and Ö show the height over the roadway and the indexes F and M show the orientation towards the traffic. In figure 3b the first letter in the index of each profile shows the height over the roadway and the second and third letters which direction towards the traffic the cores have been taken.

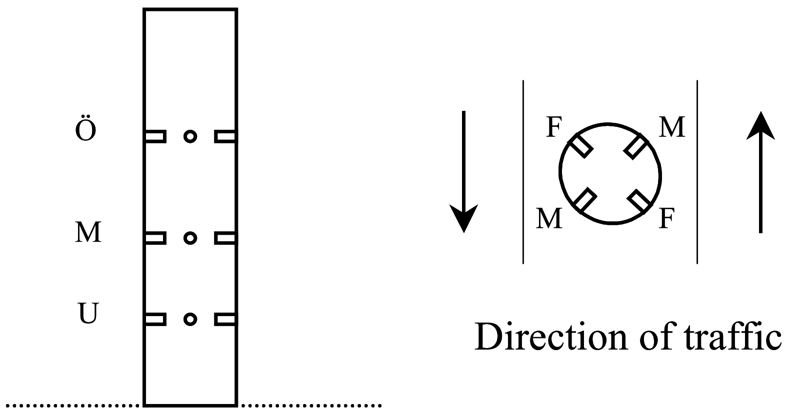

Figure 3a – The different sampling spots in columns on bridge N 434, O 951 and O 978.

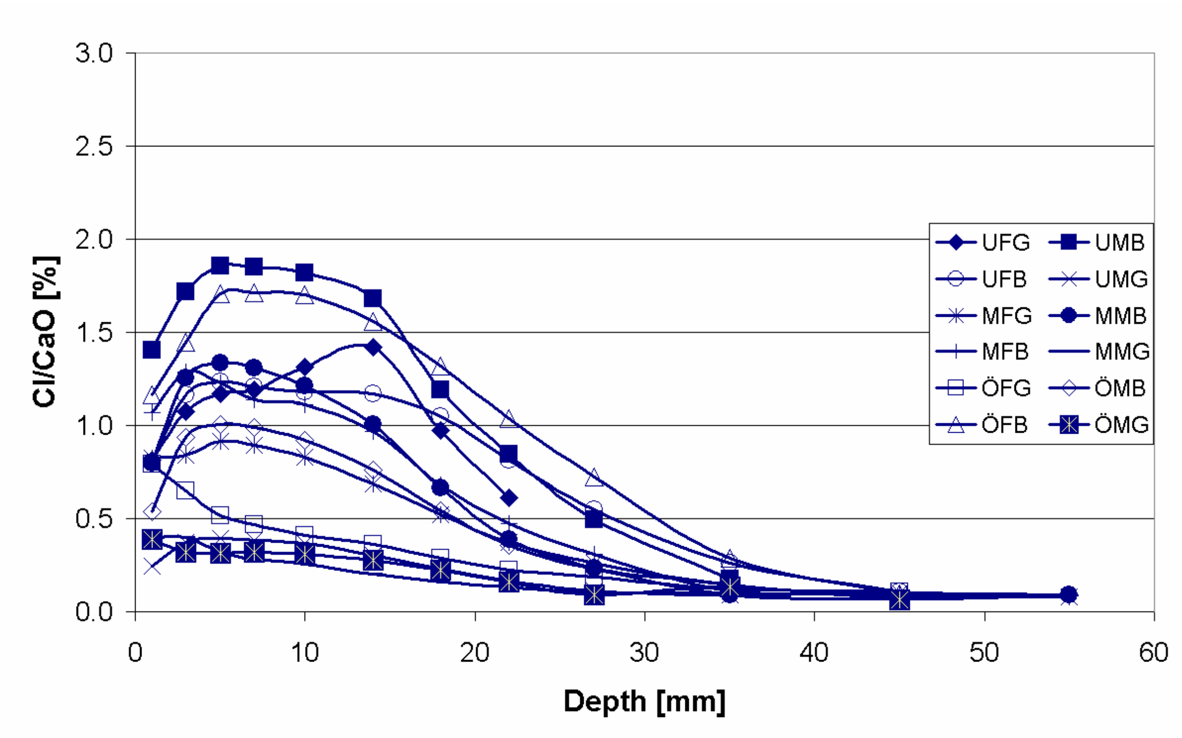

Figure 3b - The chloride penetration profiles from the column on bridge O 978.

5. DISCUSSION AND ANALYSIS

The effect from height over the roadway and orientation towards the traffic has been investigated. Cores have been taken from three different heights in the same orientation direction to determine which effect the height over the roadway has on the chloride penetration on bridge N 434, O 951 and O 978. It is commonly believed that the surface most exposed for chloride penetration is the surface with an orientation of 45° towards the traffic. This is due to the fact that the splash from the traffic on the road usually is orientated with an angle of 45° from the direction of the traffic.

The chloride penetration in bridge N 434 and O 951 was found to agree with the "normal" pattern, with large chloride penetration at the lowest level and little chloride penetration at the highest level. However, on bridge O 978, large chloride penetration was found on the high level, Ö, on a surface orientated towards the traffic. Along the same roadway, on a surface facing from the traffic the chloride penetration is significantly lower on all levels. The chloride penetration profiles are presented in figure 4a, where the profiles from the surface facing towards the traffic from Borås (direction FB) are shown, and figure 4b, where the profiles from the surface facing from the traffic from Borås (direction MG) are shown. The first index indicates the level over the roadway, described in figure 3a.

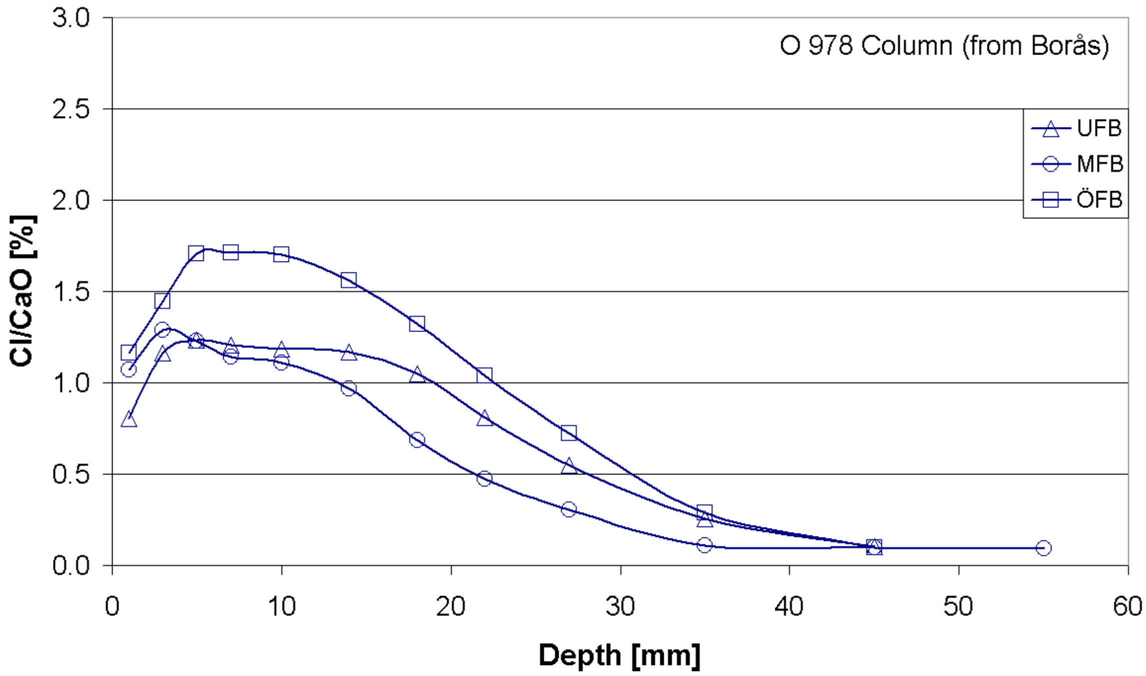

Figure 4a – Chloride penetration profiles from bridge O 978 from the surface facing towards the traffic from Borås (direction FB).

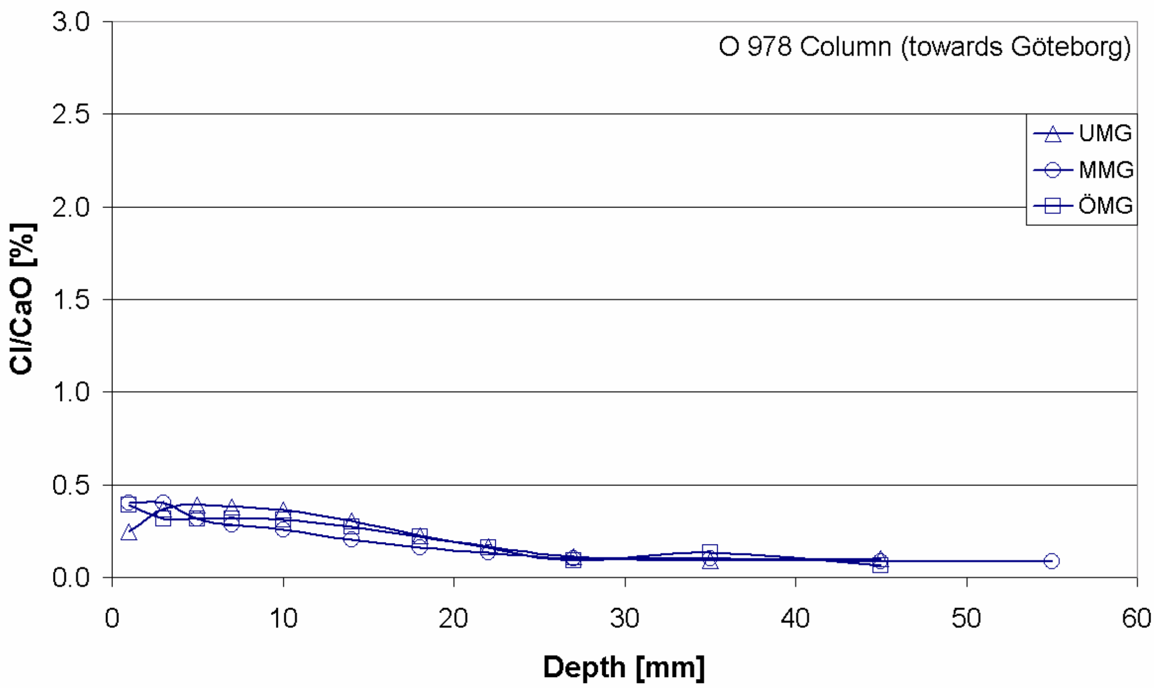

Figure 4b – Chloride penetration profiles from bridge O 978 from the surface facing from the traffic from Borås (direction MG).

A possible explanation to these results can be that the at certain wind directions airborne chlorides, e.g. chloride-contaminated aerosols from the road, will follow air-streams and be deposited on the lee-side (orientation direction FB) of the column. These chlorides will not be washed away but each time with the "right" wind-direction the concentration of chlorides will increase. In orientation direction MG deposited chlorides are constantly washed away on all heights over the roadway, which result in low penetration depths. A schematic pattern for the wind-streams around bridge O 978 is shown in figure 5. The dominating wind-direction is from the west.

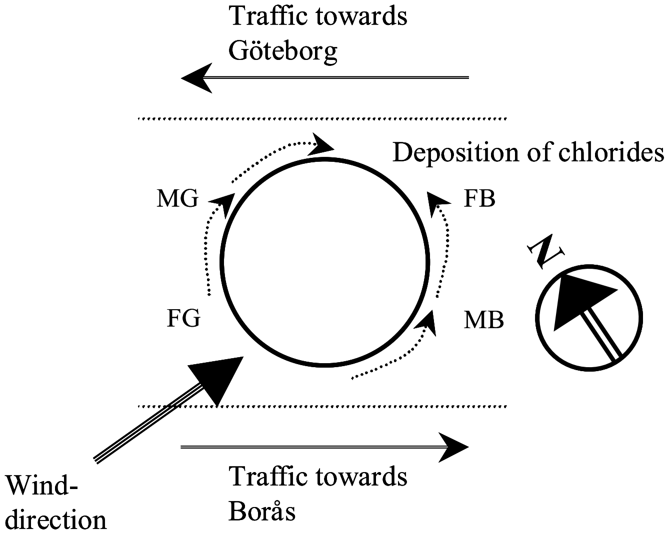

Figure 5 – Schematic picture of the wind-streams around bridge O 978. Dominating wind-direction is from the west.

The application of de-icing salts is normally during the nighttime or early in the morning. Thus, the surfaces on a road concrete structure exposed to splash from the morning traffic should also be the surfaces with the highest chloride exposure. This can be observed on bridge O 951 where the surface orientated towards the traffic towards Göteborg (orientation direction FM) has larger chloride penetration depths compared to the other surfaces. In figure 6a the chloride penetration profiles from the lowest level is shown and in figure 6b the chloride penetration profiles from the middle level are shown. The traffic intensity under bridge O 951 is high towards Göteborg in the morning and from Göteborg in the afternoon/evening.

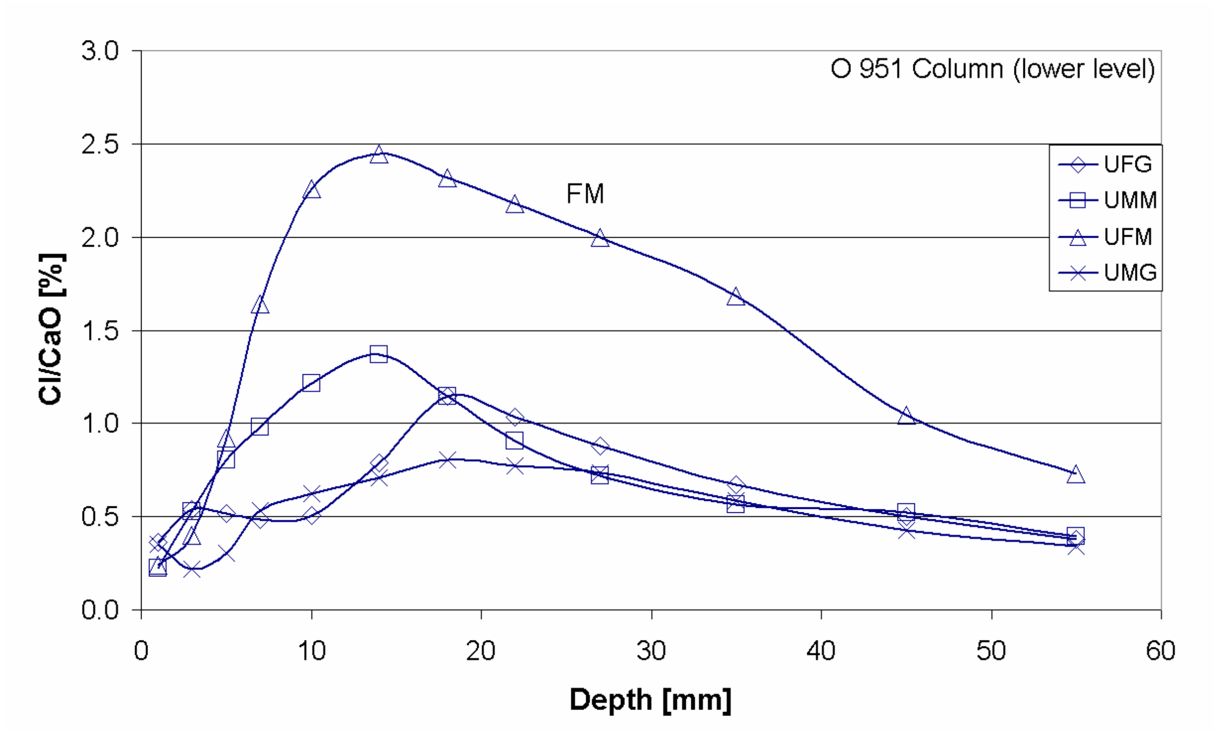

Figure 6 – Chloride penetration profiles from lower level on bridge O 951. The profile in orientation direction FM (facing towards the heavy morning-traffic) has the highest chloride penetration.

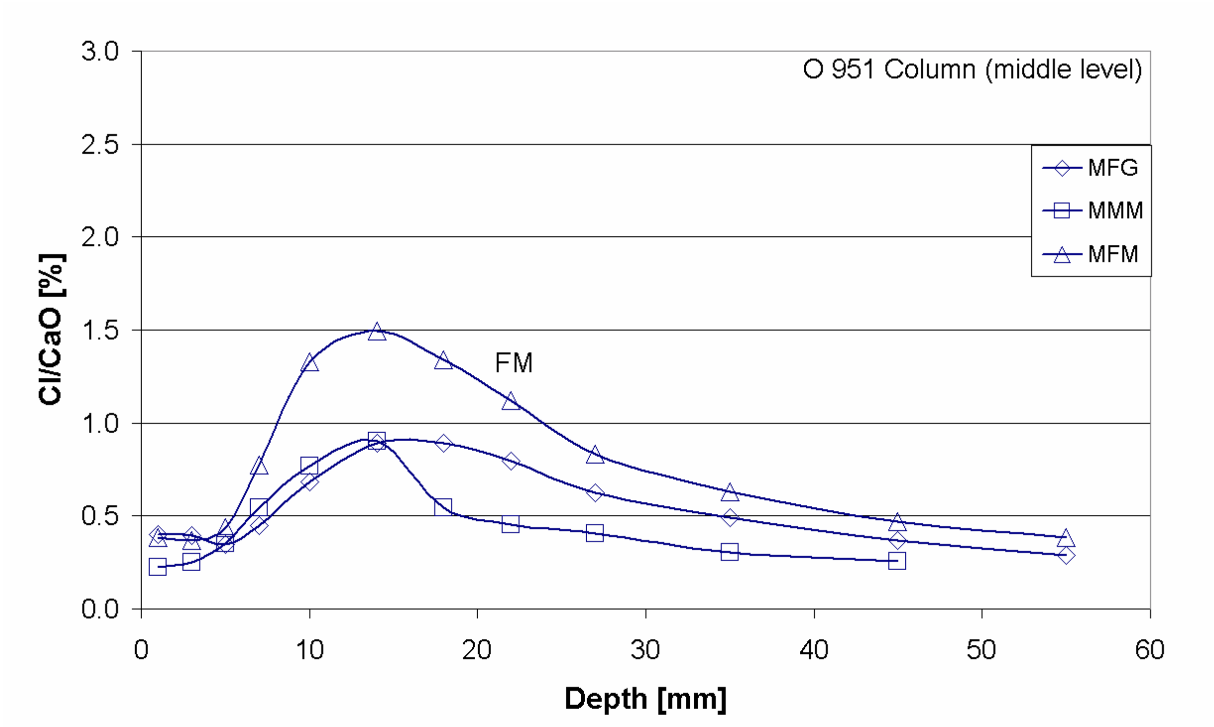

Figure 6 – Chloride penetration profiles from middle level on bridge O 951. The profile in orientation direction FM (facing towards the heavy morning-traffic) has the highest chloride penetration.

6. CONCLUSIONS

The following conclusions can be drawn:

- **Conditions for chloride penetration**. The chloride penetration into concrete is governed by the exposure conditions (chloride- and moisture-conditions) and the concrete properties. From the shape of the chloride penetration profiles it is possible to assess the exposure mechanism for chlorides.
- **Significance of the exposure environment**. The exposure environment has been found to have a large influence on the chloride penetration into a concrete structure. Large variations in the chloride penetration have been found even in one single structure. This implies that the environmental actions on a concrete structure should be determined as surface conditions, to get an as accurate description as possible.
- **Variations in response between bridges**. The results from the survey of the seven bridges have shown that each bridge should be treated separately when the chloride penetration is investigated. This is due to the fact that the chloride penetration is not only influenced by the environmental actions but also the execution during construction, the concrete mix proportions and possible surface treatments, e.g. hydrophobic treatments. This means that before the chloride penetration and moisture conditions in a concrete bridge are evaluated the concrete properties and the effect of possible surface treatments have to be assessed.
- **Quantification of environmental actions**. The statistical quantification in the DuraCrete-project has shown on the difficulties to quantify the environmental actions in mathematical prediction models. It is hard to find data on the same concrete composition exposed in different environments (both marine and road conditions), which makes it hard to quantify differences between different environments. Thus there is need for good data where the same concrete composition is exposed in different environments.

7. FUTURE RESEARCH

The following is proposed for future research:

- **Differences between different marine environments**. Further study how the chloride penetration varies in different marine environments. To avoid effects from execution and concrete composition the same concrete composition should be exposed in different environments. To get well-defined environmental conditions the marine submerged zone should be used for the exposure.
- **Investigate and map the road environment**. Further study how the chloride penetration in bridges varies with the environmental actions. To examine the environmental actions around a bridge, mortar disks can be used. The mortar disks should be used to get a well-defined and homogeneous material.
- **Execution during construction**. Further study the effects that insufficient execution of the concrete during construction has on the durability. To examine this effect the chloride penetration in two bridges, built with board and steel moulds, along the same road can be examined. The chloride penetration profiles are then compared and analysed and the influence from the type of mould can be evaluated.
- **The influence surface treatments**. Further study the effects that surface treatments have on the durability of concrete. To examine this effect chloride penetration profiles from treated and untreated can be compared. The profiles should be taken as close as possible to each other.

REFERENCES

1. Lindvall, A., “Environmental Actions and Response – Reinforced Concrete Structures exposed in Road and Marine Environments”, Publication P-01:3, Department of Building Materials, Chalmers University of Technology, Göteborg, 2001, 320 pp.
2. DuraCrete, “General Guidelines for Durability Design and Redesign”, Document BE95-1347/R15, The European Union – Brite EuRam III, Contract BRPR-CT95-0132, Project BE95-1347, CUR, Gouda, 2001.
3. Tang, L., “Chloride transport in concrete – Measurement and Prediction”, Publication P-96:6, Department of Building Materials, Chalmers University of Technology, 1996.
4. DuraCrete, “Statistical quantification of the Variables in the Limit State Functions”, Document BE95-1347/R9, The European Union – Brite EuRam III, Contract BRPR-CT95-0132, Project BE95-1347, CUR, Gouda, 2000.
5. Poulsen, E., Details of the Mejlbro-Poulsen model, *Chapter 3* in Frederiksen et al (1997), HETEK-report No. 83, Danish road directorate, Copenhagen, 1997.
6. Högberg, A., “Microclimate Description – To Facilitate Estimating Durability and Service Life of Building Components Exposed to Natural Outdoor Climate”, Publication P-98:5, Department of Building Physics, Chalmers University of Technology, Göteborg, 1998.
7. WMO – World Meteorological Organization, “Guide to meteorological instruments and methods of observations”, Secretariat of the World Meteorological Organization, Geneva, 1983.
8. Harderup, E., “Klimatdata för fuktberäkningar – Väderdata från tio meteorologiska mätstationer i Sverige” (Climate data for moisture calculations – Weather data from ten meteorological stations in Sweden), Report 3025, Department of Building physics, Lund Institute of Technology, Lund, 1993. (in Swedish).
9. Oke, T.R., “Boundary Layer Climates”, Routledge, Second edition, London, 1987.
10. Mehta, P.K., “Concrete in the Marine Environment”, Elsevier applied science, London, 1991.
11. CEB – Comité Euro International du Béton, “Durable Concrete Structures”, Bulletin 182, Comité Euro-International du Béton (CEB), Lausanne, 1989.
12. Andersen, A. & Paulsson, J., “Measurements of Seasonal and Diurnal Variations of Environmental Conditions Surrounding a Heavily Trafficked Bridge Structure”, Proceedings International Conference on “Repair of concrete structures – From Theory to Practice in a Marine Environment”, Svolvær, 1997. pp. 143-152.
13. Blomqvist, G., “Impact of De-Icing Salt on Roadside Vegetation – A Literature Review”, VTI rapport 427A, Swedish National Road and Transport Research Institute, Linköping, 1998.
14. Eliasson, Å., ”Spridning av vägsalt kring vägar (The spread of de-icing salts around roads)”, Project work 20p, Naturgeografiska institutionen, Göteborgs universitet, Göteborg, 1996. (in Swedish).
15. Wallbank, E.J.H., “The performance of concrete in bridges – A survey of 200 motorway bridges”, HSMO publication, prepared for the Department of Transport, London, 1989.
16. Lindvall, A. & Andersen, A., “Undersökning av kloridinträngning, armeringskorrosion, frysning och fukttillstånd på sju brokonstruktioner exponerade för tösalter” (Investigation of chloride ingress, reinforcement corrosion, frost and moisture conditions on seven bridge-constructions exposed to thaw-salts), Publication P-00:8, Department of Building

Materials, Chalmers University of Technology, Göteborg, 2000. (in Swedish). 141 pp.
17. NT Build 492, Concrete. Mortar and cement based repair materials: Chloride migration coefficients from non-steady state migration experiments", NORDTEST, Approved 1999-11.
18. NT Build 376, "Concrete testing – Hardened concrete: Frost resistance", NORDTEST, Adopted 1991-09. 6 pp.
19. Andersen, A., "Investigations of chloride penetration into bridge columns exposed to de-icing salt", HETEK-report No. 82, Danish road directorate, Copenhagen, 1997.
20. Nilsson, L.-O., Andersen, A., Luping, T. & Utgennant, P., "Chloride ingress data from field exposure in a Swedish road environment", Publication P-00:5, Department of Buildings Materials, Chalmers University of Technology, Göteborg, 2000. 31 pp.

Partial Coefficient for Thermal Cracking Problems Determined by a Probabilistic Method

Martin Nilsson
Doctoral Student, Tech. Lic.
Department of Civil and Mining Engineering
Division of Structural Engineering
Luleå University of Technology
SE-971 87 Luleå, Sweden
E-mail: Martin.Nilsson@ce.luth.se

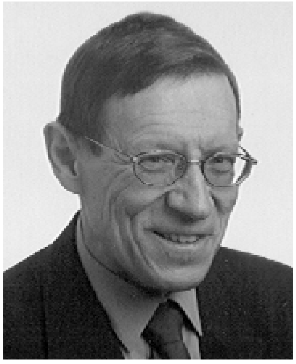

Lennart Elfgren
Professor, Tech. Dr.
Department of Civil and Mining Engineering
Division of Structural Engineering
Luleå University of Technology
SE-971 87 Luleå, Sweden
E-mail: Lennart.Elfgren@ce.luth.se

ABSTRACT

The aim of this work is to calculate partial coefficients for thermal cracking problems of young concrete and to compare the results with the values stated in the Swedish building code for bridges, [1]. The code values are only based on experiences and logical reasoning, whereas the calculated values form a more theoretical base for their determination. The coefficients are calculated with a probabilistic method. Various different possible variations of the used variables have been studied showing the wide range of possible results depending on the input. However, with use of material properties and reasonable assumptions related to thermal cracking problems, fairly good agreement has been found between the stated values in the Swedish code [1] and the values obtained through the probabilistic method.

The calculated values are based on many assumptions and assumed values and should therefor not be seen as what is right but rather more as an indication on the reasonableness of the values stated in the Swedish code. Further investigations, calculations and judgements should be performed before wider conclusions can be drawn.

Keywords: Partial Coefficients, Safety Factors, Young Concrete, Probabilistic method, Cracking

1 INTRODUCTION

A structure or a structural member should be designed in such a way that safety and serviceability are always maintained. This means that no relevant limit state conditions should be exceeded with an in beforehand determined probability. For young concrete structures it is important to prevent surface and through cracks due to e.g. temperature and/or temperature gradients during the hydration phase. Such cracks do not affect the total bearing capacity of a structure, the safety, but can influence the aesthetics and cause leakage and durability problems, the serviceability, and must be taken care of by e.g. injection.

The risk of thermal cracking in young concrete structures is commonly estimated as the ratio between the calculated maximum tensile stress and the actual tensile strength. Alternatively, the ratio between the calculated maximum tensile strain and the actual ultimate tensile strain is used, which will be the case here. If a determined ratio is smaller than a so-called crack safety value, a structure is assumed to fulfil the requirements of no thermal cracking. Depending on the effects of cracking and the accuracy in determining material properties, the Swedish building codes for bridges, [1], states different crack safety values as measures of the risk of cracking.

The risk of cracking due to temperature and temperature gradients can be estimated, according to [1], in three different methods. In Method 1 certain demands are specified on i.e. the casting and the air temperatures, the maximum cement content and the minimum value of the water cement ratio. Demands are also stated on the thickness and height of the structural members, the casting length, and when form stripping is allowed. In Method 2 and Method 3, which is more elaborate, certain values of the crack safety are prescribed depending on the accuracy in the determination of material data. Method 2 implies that requirements in a certain handbook, [2], should be applied. The requirements have been established by numerous thermal stress analyses. Further, material data that should be used are given in the code. In Method 3, the risk of cracking is estimated very accurately with tried and documented computer software and material properties.

The risk of cracking should not be larger than the crack safety values given in Table 1. The environmental classes referred according to [1] in the legend of the first column are according to the Swedish building code for concrete, [3]. Environmental class A2 stands for “Moderately reinforcement aggressive”, class A3 stands for “Very reinforcement aggressive” and class A4 stands for “Extremely reinforcement aggressive”, further see Section 4.2.

Table 1. Crack safety values for Method 2 and Method 3 given in [1]. For Method 2 values from the two right columns are used where C is the cement content [kg/m^3]. Environmental class A2 stands for “Moderately reinforcement aggressive”, class A3 stands for “Very reinforcement aggressive” and class A4 stands for “Extremely reinforcement aggressive”.

Environm. class	Method 3 Complete material data	Method 2 Material data given in the code	
		$360 \leq C \leq 430$kg/m^3	$430 \leq C \leq 460$kg/m^3
A2	1.11	1.25	1.42
A3	1.18	1.33	1.54
A4	1.25	1.42	1.67

The crack safety values can be referred to what usually are called partial coefficients based on probabilistic methods, see e.g. [4], [5], [6], [7] and [8]. Determination of partial coefficients will be presented here. Further, a determination of partial coefficients, that is crack safety values, for thermal cracking problems will follow as an attempt to indicate the reasonableness in the values given in [1]. The method and the results are more thoroughly presented and described in [8]. The determination is based on material properties, assumption on load situations and other conditions typical for thermal cracking problems.

2 PARTIAL COEFFICIENTS

2.1 Limit state function and safety index

The safety against failure can be estimated by a limit state condition in terms of a resistance parameter r and a stress parameter s. The limit state condition, $\Theta(\cdot)$, can be expressed as the resistance parameter r reduced by the stress parameter s as

$$\Theta(\cdot) = r - s \geq 0 \tag{1}$$

Usually, the resistance parameter r is the material strength and the load parameter s is the stresses caused by acting loads. Depending on their relative size, the limit state condition is not exceeded if the resistance is larger than or equal to the stress, $r \geq s$, and it is exceeded if the resistance is smaller than the stress, $r < s$.

The two parameters are regarded as two normally distributed stochastic variables with given probability density functions, $f_r(r)$ and $f_s(s)$, see Figure 1a). From the presumption that the resistance parameter r and the stress parameter s are stochastic variables, the limit state condition is also a stochastic variable. Assuming the resistance parameter r and the stress parameter s being normally distributed also the limit state condition Θ is normally distributed with a probability density function $f_\Theta(\Theta)$, Figure 1b), where β is the so-called safety index.

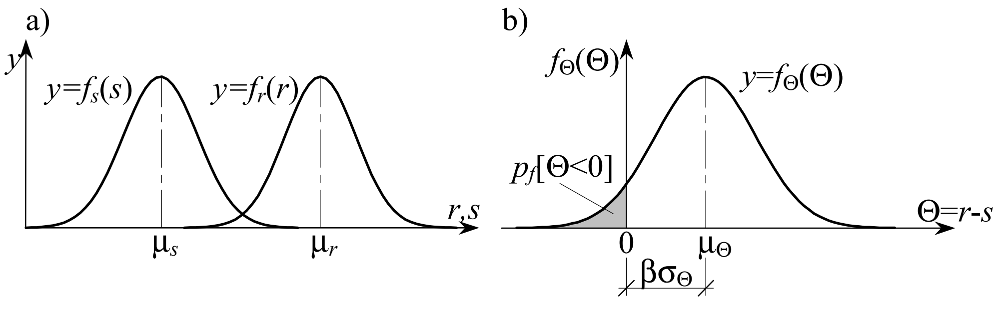

Figure 1. a) Probability density functions for the stress parameter, $f_s(s)$, and the resistance parameter, $f_r(r)$, b) Probability density function for the limit state condition Θ, $f_\Theta(\Theta)$.

The probability of exceeding a limit state condition, $p_f[\Theta = r\text{-}s < 0]$, is equal to the area of the shaded surface in Figure 1b). In the figure, the distance, with the standard deviation σ_Θ as unit, from the mean value μ_Θ to the failure limit, $\Theta = 0$, is written as $\beta\sigma_\Theta$. The coefficient β is the so-called safety index, introduced by Cornell in [9], and is, according to the figure, determined as

$$\beta = \frac{\mu_\Theta}{\sigma_\Theta} \tag{2}$$

How much larger the resistance r should be than the stress s is often specified in building codes in different safety classes and through specified values of the safety index β. The safety index β is defined by a formal probability of failure, that is, of exceeding the limit sate condition. The safety index β is often coupled to safety classes in building codes, see e.g. [6], [7], [10]. If the risk of human injuries is low, often referred to safety class 1, the probability of failure is $p_f = 10^{-4}$ and the safety index $\beta = 3.72$. The same principle applies to safety classes 2 and 3, see Table 2.

Table 2. Correspondence between safety class, safety index and probability of failure, [1], [10].

Safety class	1	2	3
Safety index β Probability of failure, p_f	3.72 10^{-4}	4.26 10^{-5}	4.75 10^{-6}

2.2 Partial coefficients

The partial coefficient method is based on characteristic values and partial coefficients for verification that prescribed safety requirements are fulfilled. Generally, for the limit state condition in Eq. (1), partial coefficients are used as follows

$$\Theta = r_d - s_d = \frac{r_c}{\gamma_r} - \gamma_s s_c \geq 0 \tag{3}$$

where d indicates design values, c indicates characteristic values and γ_r and γ_s are the partial coefficients for the resistance parameter r and the stress parameter s, respectively.

For the risk of thermal cracking of young concrete, the crack safety values in Table 1 are the product of the partial coefficients for the resistance parameter r and the stress parameter s, $\gamma_r\gamma_s$, according to, compare with Eq. (3),

$$\frac{r_c}{s_c} \geq \gamma_r\gamma_s \tag{4}$$

In this case, all partial coefficients have been collected in one coefficient limiting the ratio between the resistance parameter and the load parameter.

3 THE PROBABILISTIC METHOD

3.1 Equations for determination of partial coefficients

A method further referred to as the probabilistic method will be used to determine alternative values of the partial coefficients, safety values, for thermal cracking problems, given in Table 1. The method has the advantage of being consequent but it also includes many approximations.

The results can therefore not be used directly without additional judgements. The following determination of the partial coefficients will be formulated in terms of strains. The procedure in general is based on a method presented by Lars Östlund in [11], reprinted in [12], and adopted on thermal cracking problems in [8]. As design condition with partial coefficients for thermal cracking problems, Eq. (4) will be used as the limit state condition.

3.1.1 Resistance parameter

The resistance parameter r is expressed as, [11]

$$r = C_r a \rho \varepsilon \tag{5}$$

where C_r is a factor describing uncertainties in the calculation method on the resistance parameter such as determination of material properties. C_r is a stochastic variable with mean μ_{Cr} and coefficient of variation V_{Cr}. a is a geometric quantity (eg cross-section area). a is a stochastic variable with mean μ_a and coefficient of variation V_a. ρ is a factor transferring concrete strain from test specimen at failure to concrete strain in real structures. ρ is a stochastic variable with mean μ_ρ and coefficient of variation V_ρ. ε is the actual concrete ultimate strain. ε is a stochastic variable with mean μ_ε and coefficient of variation V_ε. The stochastic variables r, C_r, a, ρ and ε are assumed to be logarithmic normally distributed.

The mean value of the resistance parameter is

$$\mu_r = \mu_{Cr} \mu_a \mu_\rho \mu_\varepsilon \tag{6}$$

and the coefficient of variation, if terms of higher order are neglected,

$$V_r \approx \sqrt{V_{Cr}^2 + V_a^2 + V_\rho^2 + V_\varepsilon^2} \tag{7}$$

Eq. (5) divided by Eq. (6) gives, if using characteristic values,

$$\frac{r_c}{\mu_r} = \frac{C_{rc}}{\mu_{Cr}} \frac{a_c}{\mu_a} \frac{\rho_c}{\mu_\rho} \frac{\varepsilon_c}{\mu_\varepsilon} \tag{8}$$

which will be used further on in the final calculation of the partial coefficients, see Eq. (25) below.

3.1.2 Load parameter

The load parameter s for thermal cracking problems can be formulated, in terms of strains, as

$$s = C_s \gamma_R (b(\varepsilon_{T1} + \varepsilon_{T2}) + c\varepsilon_{sh})$$

where C_s is uncertainties in the calculation method on the load parameter and is assumed to have the same value for all the loads. C_s describes uncertainties in the determination of the strains by e.g. manual methods, see [13] and [14], or by finite element calculations, see [15]. C_s is a stochastic variable with mean μ_{Cs} and coefficient of variation V_{Cs}. γ_R is the coefficient of restraint and is a deterministic coefficient, $0 \leq \gamma_R \leq 1$. For further explanations and the determination of the coefficient of restraint, see [8]. ε_{T1} is the non-elastic strain of volume changes from differences between the casting temperature and the adjacent temperature. ε_{T2} is the non-elastic strain of volume changes from differences between the maximum temperature and the casting temperature. Below, the temperature-induced strains are combined into one parameter, ε_T, which is a stochastic variable with mean μ_T and coefficient of variation V_T. ε_{sh} is the strain of volume changes from shrinkage and is a stochastic variable with mean μ_{sh} and coefficient of variation V_{sh}. b and c are both deterministic coefficients, $0 \le b$ and $0 \le c$. The stochastic variables ε_T and ε_{sh} are assumed to be normally distributed. The deterministic coefficients b and c are used when either the temperature induced strain is of greater importance than the shrinkage strain, or the opposite. Now, the load parameter is

$$s = C_s \gamma_R (b\varepsilon_T + c\varepsilon_{sh}) \tag{9}$$

The variables are put together so that the mean value of the stress parameter is

$$\mu_s = \gamma_R \left(b\mu_T + c\mu_{sh} \right) \tag{10}$$

By introducing the following relation

$$\frac{C_r}{C_s} = C; \quad V_C = \sqrt{V_{Cr}^2 + V_{Cs}^2} \tag{11}$$

the limit state condition is simplified to

$$\Theta(\cdot) = Ca\rho\varepsilon - \gamma_R (b\varepsilon_T + c\varepsilon_{sh}) \tag{12}$$

In the calculation of the partial coefficients for thermal cracking problems of concrete, it is very difficult to give any absolute values of the mean values of the strains of shrinkage and temperature changes. However, the relation between them is easier to estimate. Therefore, a coefficient ν_{sh} is introduced stating the ratio between the mean values of the strains of shrinkage and of the temperature change

$$\nu_{sh} = \frac{c\mu_{sh}}{b\mu_T} \tag{13}$$

3.1.3 Design condition

When calculating partial coefficients by the probabilistic method, the following design values and help values κ are used for the stochastic variables r, ε_T and ε_{sh}.

$$r_d = \mu_r \exp(-\alpha_r \beta V_r) \quad \kappa_r = r_d V_r \tag{14}$$

$$\varepsilon_{T,d} = \mu_T \left(1 - \alpha_T \beta V_T\right) \quad \kappa_T = -b\gamma_R \mu_T V_T \tag{15}$$

$$\varepsilon_{sh,d} = \mu_{sh} \left(1 - \alpha_{sh} \beta V_{sh}\right) \quad \kappa_{sh} = -c\gamma_R \mu_{sh} V_{sh} \tag{16}$$

When using design values in Eq. (3), the equal sign is valid, which together with Eq. (9) gives

$$r_d - b\gamma_R \varepsilon_{T,d} - c\gamma_R \varepsilon_{sh,d} = 0 \tag{17}$$

In the expressions above, α are so-called sensitivity coefficients determined as

$$\alpha_i = \frac{\kappa_i}{\sqrt{\Sigma\kappa_i^2}} = \frac{\kappa_i}{\sqrt{\kappa_r^2 + \kappa_T^2 + \kappa_{sh}^2}}; \quad \text{with } i = r,\ T \text{ and } sh \tag{18}$$

and that must fulfil the condition

$$\alpha_r^2 + \alpha_T^2 + \alpha_{sh}^2 = 1 \tag{19}$$

The sensitivity coefficients take values between -1 and 1 and are positive for favourable factors, the resistance parameters, and negative for unfavourable, the load/stress parameters. The larger the coefficient is, the larger the importance of the uncertainty is in the corresponding variable.

$c\mu_{sh} = \nu_{sh} b\mu_T$ according to Eq. (13) and design values according to Eqs. (14) to (16) inserted in Eq. (17) give

$$\frac{\mu_r}{b\gamma_R\mu_T}\exp(-\alpha_r\beta V_r) - (1-\alpha_T\beta V_T) - \nu_{sh}(1-\alpha_{sh}\beta V_{sh}) = 0 \tag{20}$$

By introducing the help variables

$$Z = \frac{\mu_r}{b\gamma_R\mu_T}$$

and

$$\psi_1 = (1-\alpha_T\beta V_T) + \nu_{sh}(1-\alpha_{sh}\beta V_{sh}) \tag{21}$$

Eq. (20) is simplified to

$$Z\exp(-\alpha_r\beta V_r) - \psi_1 = 0$$

where from

$$Z = \psi_1 \exp(\alpha_r\beta V_r) \tag{22}$$

Z can be determined if the values of α_i (with $i = r$, T and sh), β, ν_{sh}, b, c and V_i are known. The steps for calculating Z can be as follows:

(1) A value of α'_{sh} is assumed

(2) $\alpha'_T = \dfrac{\kappa_T}{\sqrt{\Sigma\kappa_i^2}} = \dfrac{-b\gamma_R\mu_T V_T}{-c\gamma_R\mu_{sh}V_{sh}}\alpha'_{sh} = \dfrac{V_T\alpha'_{sh}}{\nu_{sh}V_{sh}}$ is calculated

(3) ψ is calculated with Eq. (21), α'_{sh} and α'_T

(4) $r_d = \mu_r\exp(-\alpha_r\beta V_r) = \mu_r\dfrac{\psi_1}{Z} = b\gamma_R\mu_T\psi_1$ and $\kappa_r = r_d V_r$ are calculated

(5) $N = \dfrac{\sqrt{\Sigma\kappa_i^2}}{b\gamma_R\mu_T} = \sqrt{(V_T)^2 + (\nu_{sh}V_{sh})^2 + (\psi_1 V_r)^2}$

(6) $\alpha_{sh} = \dfrac{\kappa_{sh}}{\sqrt{\Sigma\kappa_i^2}} = \dfrac{-\gamma_R b\mu_T \nu_{sh} V_{sh}}{\sqrt{\Sigma\kappa_i^2}} = \dfrac{-\nu_{sh} V_{sh}}{N}$ is calculated and compared to α'_{sh}

(7) When $\alpha'_{sh} \approx \alpha_{sh}$, $\alpha_T = \dfrac{-V_T}{N}$ and $\alpha_r = \dfrac{\psi_1 V_r}{N}$ are calculated

(8) Check of $\Sigma\alpha_i^2 = 1$

(9) Z is calculated by Eq. (22).

The value of Z is used below in the calculation of the partial coefficients.

3.1.4 Partial coefficients

The design values in Eqs. (14) through (16) can alternatively be expressed with partial coefficients as

$$r_d = \frac{r_c}{\gamma_r} = \frac{\mu_r}{\gamma_r}\exp(-k_r V_r) \tag{23}$$

$$s_d = \gamma_s\gamma_R\left(b\varepsilon_{T,c} + c\varepsilon_{sh,c}\right) = \gamma_s\gamma_R\left(b\mu_T(1+k_T V_T) + c\mu_{sh}(1+k_{sh}V_{sh})\right) \tag{24}$$

which in the limit state condition, Eq. (3), give

$$\frac{\mu_r}{\gamma_r}\exp(-k_r V_r) - \gamma_s\gamma_R\left(b\mu_T(1+k_T V_T) + c\mu_{sh}(1+k_{sh}V_{sh})\right) \geq 0$$

With $Z = \mu_r/b\gamma_R\mu_T$, $\nu_{sh} = c\mu_{sh}/b\mu_T$ and $\psi_2 = (1+k_T V_T)+\nu_{sh}(1+k_{sh}V_{sh})$ it can be re-written as

$$\gamma_s\gamma_r \leq \frac{Z}{\psi_2}\exp(-k_r V_r) = \frac{Z}{\psi_2}\frac{r_c}{\mu_r} \tag{25}$$

giving the partial coefficients $\gamma_r\gamma_s$. Z is calculated according to Section 3.1.3 and r_c/μ_r is calculated from Eq. (8) with $x_{i,c}/\mu_i = \exp(-\alpha_i\beta V_i) = \exp(-k_i V_i)$. k_i depends on actual fractile value.

3.2 Numerical values

Calculations of partial coefficients for thermal cracking problems of young concrete have been performed by varying the variables shown in Table 3 and keeping all others constant.

ν_{sh} are defined by to Eq. (13) and states the ratio between the mean values of the strains of shrinkage and of the strains of temperature change. b and c are varied to simulate situations when one of the two strain components has smaller or larger influence. Especially in high strength concrete the shrinkage is considerable implying larger values of c. V_ε is the coefficient of variation of the actual concrete (actual ultimate strain ε_{cu}). V_C is the coefficient of variation of the methods used for estimating the risk of thermal cracking. Compare V_C with Methods 1 to 3 in Section 1 where e.g. V_C = 0.15 for Method 1, V_C = 0.10 for Method 2 and V_C = 0.05 for Method 3. These values are just an attempt to estimate the accuracy in the methods and should not be seen as what is right. The safety index β is varied to coincide with safety classes 1 and 3 with probabilities of failure of 10^{-4} and 10^{-6}, see Table 2.

Table 3. Variables varied in the determination of partial coefficients for thermal cracking problems.

Variable	Values				
ν_{sh}	$0.01\frac{c}{b}$	$0.20\frac{c}{b}$	$0.50\frac{c}{b}$	$1.00\frac{c}{b}$	$2.00\frac{c}{b}$
b	1/3	1	3		
c	1/3	1	3		
V_ε	0.05	0.10	0.15	0.20	0.25
V_C	0.05	0.10	0.15	0.20	0.25
β	3.72	4.75			

The coefficient of variation of the temperature induced strains is given the value $V_T = 0.08$ according to [16]. The coefficient of variation of the shrinkage is given the value $V_{sh} = 0.20$. This value is a bit smaller than what can be determined from [17]. The values of k_T and k_{sh} are 1.65 coinciding with 95 % fractile values of the temperature and shrinkage induced strains, respectively, see Table 4.

The coefficients of variations of the geometry parameter V_a and of the factor transferring strength in test specimens and in real structures V_ρ are both given the value 0, that is $V_a = 0$ and $V_\rho = 0$. The coefficient of variation of the geometry is assumed to be very low since in civil engineering structures, any divergences from the right measures do not affect the risk of thermal cracking. For the concrete ultimate strain, $k_\varepsilon = 0.13$, is chosen assuming a 45% fractile value. The high value of the ultimate strain for the concrete is chosen bearing in mind that thermal cracking only causes flaws and costs for repair and reduction of the life of the structure but not total failure. For the accuracy in design method, C, for the geometry parameter, a, and for the factor transferring the ultimate strain in test specimens and in real structures ρ, the coefficient k is chosen $k_C = k_a = k_\rho = 1.65$ assuming 5% fractile values, see Table 4.

Table 4. Constant values for the resistance parameters C, a, ρ and ε and the load parameters T and sh used in the determination of the partial coefficients.

k_C	V_a	k_a	V_ρ	k_ρ	k_ε	V_T	k_T	V_{sh}	k_{sh}
1.65	0	1.65	0	1.65	0.13	0.08	1.65	0.20	1.65

3.3 Calculation of partial coefficients

The following presumptions and values are used to illustrate the calculation of partial coefficients. Let the influence of the imposed volume changes be equal, $b = c = 1$. The mean value of the volume change due to shrinkage is one hundredth of the mean value of the imposed volume change due to the temperature change, $\nu_{sh} = 0.01 \cdot 1/1 = 0.01$. Further, the variation coefficients of the strength of the concrete and the calculation method are assumed to be five percent, $V_\varepsilon =$

V_C = 0.05. The safety index β = 3.72 corresponding to safety class 1 and corresponding to a probability of exceeding the limit state condition $p_f = 10^{-4}$. The following values for the resistance parameter, the sensitivity values α and the help values ψ, N and Z are obtained, Table 5 and Table 6.

Table 5. Calculated values for the resistance parameter.

V_r	C_c/μ_C	a_c/μ_a	ρ_c/μ_ρ	$\varepsilon_c/\mu_\varepsilon$	r_c/μ_r
0.071	0.921	1.000	1.000	0.994	0.915

Table 6. Calculated sensitivity values α and help-values ψ_1, N and Z.

α'_{sh}	α_T	ψ_1	N	α_φ	α_T	α_r	Z
-0.017	-0.682	1.213	0.117	-0.017	-0.682	0.731	1.470

The partial coefficient for this case is then calculated as, Eq. (25)

$$\gamma_r\gamma_s = \frac{Z}{\psi_2}\frac{r_c}{\mu_r} = \frac{1.470}{(1+1.65\cdot 0.08)+0.01(1+1.65\cdot 0.20)}0.915 = 1.174 \tag{26}$$

implying that the resistance parameter must be about 1.174 times larger than the load parameter for not exceeding the limit state condition.

All the partial coefficients calculated with values according to the description and Table 3 above are presented in Figure 2 to Figure 6 below. In all the diagrams, the curves from the lowest to the upper most represent V_C = 0.05, 0.10, 0.15, 0.20 and 0.25, respectively. See [8] for more descriptions of the calculations and the results.

In Figure 2 to Figure 6 it can be seen that with increased safety index β, the partial coefficient $\gamma_r\gamma_s$ increases and is varying over a larger range depending on the values of V_C. When the coefficient b increases also the partial coefficient increases, and when b decreases the partial coefficient decreases, compare Figure 3 and Figure 4 with Figure 2. For the coefficient c, the opposite is valid. When c increases, the partial coefficient decreases and when c decreases, the partial coefficient increases, compare Figure 5 and Figure 6 with Figure 2.

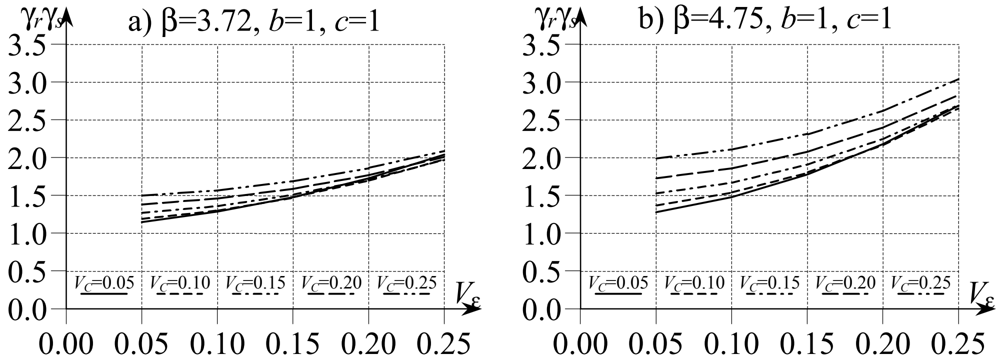

Figure 2. Partial coefficient $\gamma_r\gamma_s$ for a) β=3.72, b=1 and c=1, b) β=4.75, b=1 and c=1.

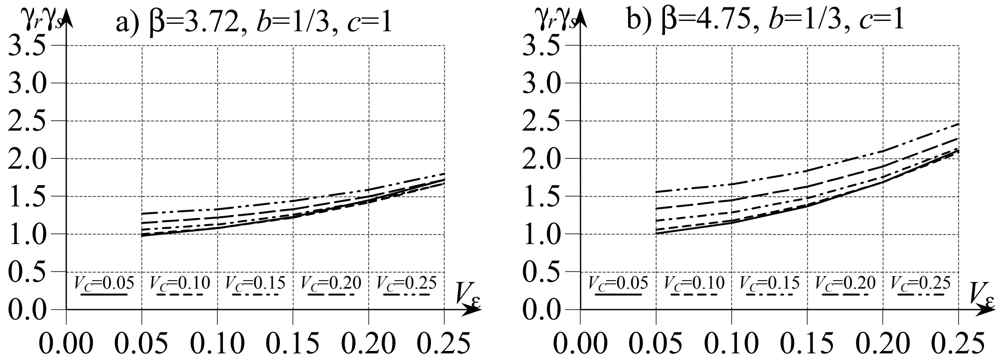

Figure 3. Partial coefficient $\gamma_r\gamma_s$ for a) β=3.72, b=1/3 and c=1, b) β=4.75, b=1/3 and c=1.

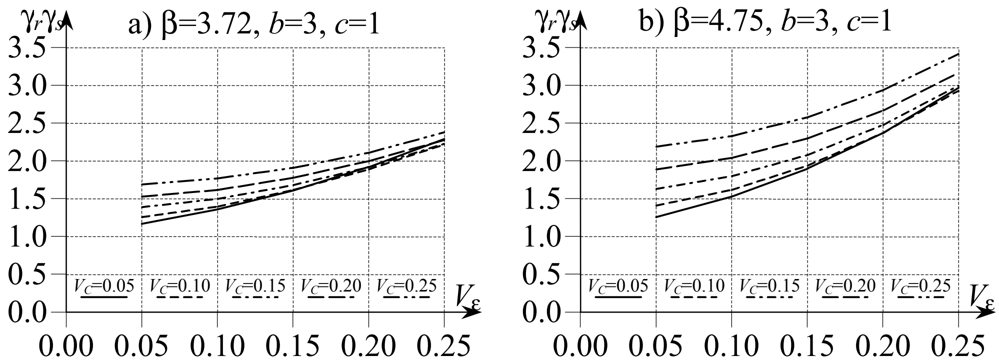

Figure 4. Partial coefficient $\gamma_r\gamma_s$ for a) β=3.72, b=3 and c=1, b) β=4.75, b=3 and c=1.

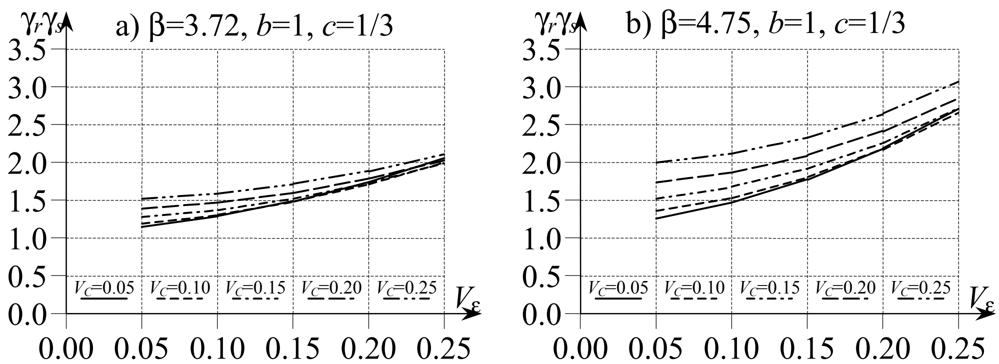

Figure 5. Partial coefficient $\gamma_r\gamma_s$ for a) β=3.72, b=1 and c=1/3, b) β=4.75, b=1 and c=1/3.

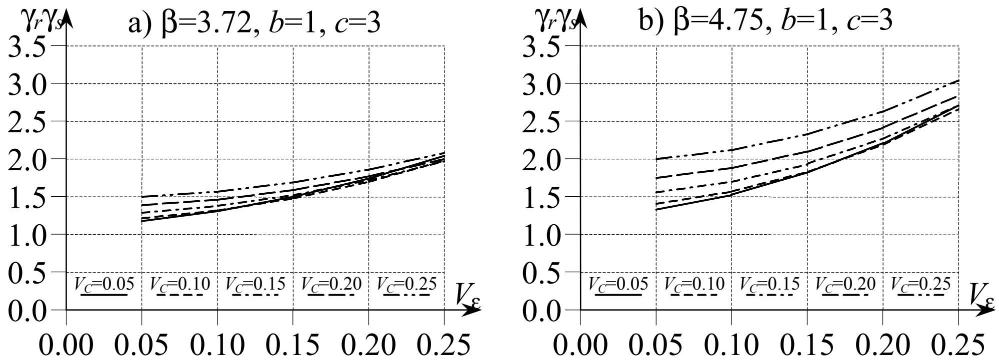

Figure 6. Partial coefficient $\gamma_r\gamma_s$ for a) β=3.72, b=1 and c=3, b) β=4.75, b=1 and c=3.

4 RESULTS

4.1 Final values of partial coefficients

Final values of the partial coefficient $\gamma_r\gamma_s$ are determined from the previous calculations with $b = c = 1$, $\beta = 3.72$ (probability of failure, $p_f = 10^{-4}$) and with coefficients of variation, $V_C = 0.05$ and $V_\varepsilon = 0.05$, 0.10 and 0.15. The values are chosen to coincide with the first row in Table 1. That is, for Method 3 (the column of complete material data) the models of analysis (computer software) are very well documented and tried and should give results not varying much from reality. Therefore, the coefficient of variation for the method of calculation is chosen to be small, $V_C = 0.05$. For Method 2, (columns for material data given in [1]) lots of calculations and judgements are behind, [2], implying good accuracy of the analyses, again $V_C = 0.05$. The differences in accuracy of material data are taken into account by varying the coefficient of variation of the material V_ε as stated, $V_\varepsilon = 0.05$, 0.10 and 0.15. Again, $k_T = k_{sh} = 1.65$ for 95 % fractile values. Further, as an extension of the final determination of the partial coefficients, 55 % fractile values are assumed for the temperature and the shrinkage induced strains to coincide with the assumed fractile value of the ultimate strain (45 % fractile), see Section 3.2. For environmental class A2 and $V_\varepsilon = 0.05$, 0.10 and 0.15, the partial coefficient $\gamma_r\gamma_s$ is taken as the values of the lowest curve in Figure 2a) presented in Table 7.

Table 7. Partial coefficient $\gamma_r\gamma_s$ from calculation with the probabilistic method for environmental class A2 and V_ε = 0.05, 0.10 and 0.15.

Environm. class	k_T, k_{sh}	Complete material data V_ε=0.05	Material data given in the code 360≤C≤430kg/m^3 V_ε=0.10	430≤C≤460kg/m^3 V_ε=0.15
A2	0.13 (55% fractile)	1.36	1.52	1.75
	1.65 (95% fractile)	1.15	1.29	1.48

4.2 Effects of exceeding the limit state condition

The calculation of partial coefficients above is chosen to be valid for environmental class A2. The effects of exceeding the limit state condition (cracking) in a structural member are smaller in environmental class A2 than in classes A3 and A4. Therefor an extra partial coefficient γ_n is introduced. The values of the extra partial coefficient γ_n are chosen as the mean ratio between the values in the rows in Table 1, see Table 8.

Table 8. Partial coefficient γ_n depending on environmental classes.

	Environmental class A2	A3	A4
γ_n	1.00	1.07	1.14

Final values of the partial coefficient $\gamma_r\gamma_s$ are obtained from Table 7 with partial coefficient γ_n in Table 8, see Table 9.

Table 9. Final values of partial coefficient $\gamma_r\gamma_s$ as determined by probabilistic method.

Environm. class	k_T, k_{sh}	Complete material data	Material data given in the code $360 \leq C \leq 430$kg/m^3	$430 \leq C \leq 460$kg/m^3
A2	0.13 (55% fractile)	1.15	1.29	1.48
	1.65 (95% fractile)	1.36	1.52	1.75
A3	0.13 (55% fractile)	1.23	1.38	1.58
	1.65 (95% fractile)	1.45	1.62	1.87
A4	0.13 (55% fractile)	1.32	1.48	1.70
	1.65 (95% fractile)	1.56	1.74	2.00

A comparison with the values that is stated in [1] and the values of the partial coefficients obtained by the probabilistic method are depicted in Figure 7. As can be seen, the values for $k_T = k_{sh} = 1.65$ (95 % fractile values) are somewhat higher than the values given in [1]. The values show good agreement even though the uncertainties in the chosen values of the variables used in the probabilistic method and that the partial coefficients stated in [1] only are based on experiences. For $k_T = k_{sh} = 0.13$ (55 % fractile values), the partial coefficients are much higher than the values in [1]. The reason for this is that with only 55 % fractile values of the temperature and the shrinkage induced strains, the risk of exceeding these values is increased. This implies an increased risk of exceeding the limit state condition, whereupon higher partial coefficients are needed.

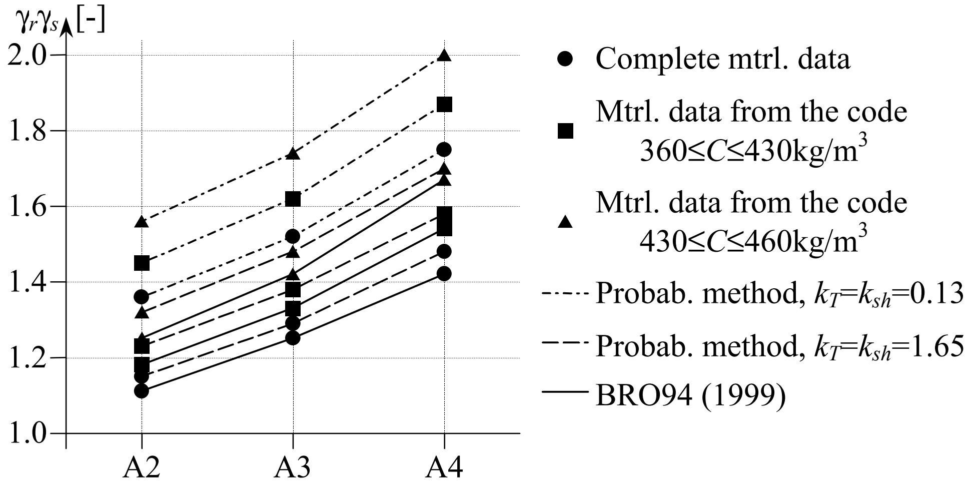

Figure 7. Comparison between partial coefficients stated in [1] and partial coefficients obtained by the probabilistic method.

5 DISCUSSION

It is possible to calculate partial coefficients for thermal cracking problems of young concrete. The values presented above coincide well with the crack safety values stated in the Swedish building code for bridges, [1]. However, the calculated values of the partial coefficient are based on many assumptions and simplifications and they shall not be seen as what is absolutely true right, further judgements are always necessary.

The used coefficients of variation of the thermal changes and of the shrinkage need further investigation. The values are roughly taken from [16] and are only assumed values that have not been well verified.

The crack safety values in [1] are all based on experience, so also these values are a bit vague. The calculated partial coefficients presented here can be seen as an attempt to verify the values in [1]. However, all estimations of the risks of thermal cracking of young concrete have to be based on more judgements and analyses of the problems as a whole rather than on the crack safety values given in [1].

The differences in the partial coefficient between the environmental classes need further investigations. The values that are stated in [1] are only based on logical arguments by the persons who have written the code, meaning that higher environmental class needs higher partial coefficients.

ACKNOWLEDGEMENT

The authors thank Professor Emeritus Lars Östlund for his way of describing the methodology behind the determination of the partial coefficients. Thanks are also sent to Professor Emeritus Krister Cedervall, Chalmers University of Technology, for his thorough and dedicated work as leader of the discussion at Martin Nilsson's licentiate seminar. Finally, Associate Professor Jan-Erik Jonasson is thanked for his contributions in the field of thermal cracking of young concrete and material properties of concrete.

REFERENCES

[1] BRO 94 (1999). *BRO94 Allmän teknisk beskrivning för broar, 9. Förteckning*. (General Technical Description for Bridges, 9. Catalogue). Borlänge, Sweden: Swedish National Road Administration. Publ 1999:20. pp. 139. ISSN 1401-9612. (In Swedish).

[2] Emborg, M, Bernander, S, Ekefors, K, Groth, P & Hedlund, H (1997). *Temperatursprickor i betongkonstruktioner - Beräkningsmetoder för hydratationsspänningar och diagram för några vanliga typfall* (Temperature Cracks in Concrete Structures - Calculation Methods for Hydration Stresses and Diagrams for some Common Typical Examples). Luleå, Sweden: Luleå University of Technology. Technical Report 1997:02. 100 pp. ISSN 1402-1536. (In Swedish).

[3] BBK94 (1994). *Boverkets handbok om betongkonstruktioner*. (The Swedish Building Administrations Handbook on Concrete Structures). Part 2 - Material, Performance and Control. Stockholm, Sweden: The Swedish Building Administration, Division of Buildings. pp. 116. ISBN 91-7332-687-9. (In Swedish).

[4] Schneider, J (1997). Introduction to Safety and Reliability of Structures. In: *Structural Engineering Documents, 5*. Zürich: IABSE, International Association for Bridges and Structural Engineering. 138 pp.

[5] AK79/81 (1982). *Allmänna regler för bärande konstruktioner. Principer, rekommendationer och kommentarer samt exempel på tillämpning*. (General Regulations for Structures. Principles, Recomendations, Comments and Examples of Application). Stockholm, Sweden: Statens Planverk, Rapport nr 50, Liber 1982, pp. 159. ISBN 91-38-07090-1. (In Swedish).

[6] NKB78 (1978). *Retningslinier for last- og sikkerhetsbestemmelser for baerende konstruktioner* (Guiding Rules for Loads and Safety Regulations for Structures). NKB-rapport nr. 35. 146 pp. ISBN 87-503-2951-0. (In Swedish).

[7] NKB87 (1987). *Retningslinier for last- og sikkerhetsbestemmelser for baerende konstruktioner* (Guiding Rules for Loads and Safety Regulations for Structures). NKB-rapport nr. 55. 107+55 pp. ISBN 87-503-6991-1, ISSN 0359-9981. (In Swedish).

[8] Nilsson, M (2001). *Thermal Cracking of Young Concrete - Partial Coefficients, Restraint Effects and Influence of Casting Joints*. Luleå, Sweden: Division of Structural Engineering, Luleå University of Technology. Licentiate Thesis 2000:27. pp. 267.

[9] Cornell, C A (1969). A probability-based structural code. In: *ACI Journal, Vol. 66*, pp. 974-985.

[10] BBK94 (1995). *Boverkets handbok om betongkonstruktioner*. (The Swedish Building Administrations Handbook on Concrete Structures). Part 1 - Design. Stockholm, Sweden: The Swedish Building Administration, Division of Buildings. pp. 185. ISBN 91-7147-235-5. (In Swedish).

[11] Östlund, L (1997). *Studium av erforderligt värde på partialkoefficienten för tåglast vid dimensionering av järnvägsbroar* (Study of Necessary Value of the Partial Coefficient for Load of Trains at Design of Railway Bridges). Borlänge, Sweden: Swedish Railroad Administration. Investigation on behalf of the Swedish Railroad Administration. pp. 19. (In Swedish).

[12] Nilsson, M, Ohlsson, U & Elfgren, L (2000). *Partialkoefficienter för betongbroar längs Malmbanan* (Partial Coefficients for Concrete Bridges along Malmbanan). Luleå, Sweden: Luleå University of Technology. Technical report 1999:03. 66 pp. ISSN 1402-1536. (In Swedish).

[13] Larson, M (2000). *Estimation of Crack Risk in Early Age Concrete*. Luleå, Sweden: Division of Structural Engineering, Luleå University of Technology. Licentiate Thesis 2000:10. pp. 170.

[14] Jonasson, J-E, Wallin, K, Emborg, M, Gram, A, Saleh, I, Nilsson, M, Larson, M and Hedlund, H (2001). *Tempertursprickor i betongkonstruktioner – Handbok med diagram för sprickriskbedömning inklusive åtgärder för några typfall; Del D och E* (Temperature cracks in concrete structures - Handbook with diagrams for crack risk estimation including measures for some typical cases). Luleå, Sweden: Division of Structural Engineering, Luleå University of Technology. Technical Report 2001:14. (In Swedish, in progress).

[15] ConTeSt Pro (1999). *Användarhandbok - ConTeSt Pro* (Users manual - Program for Temperature and Stress Calculations in Concrete). Developed by JEJMS Concrete AB in cooperation with Luleå University of Technology, Cementa AB and Peab Öst AB. Danderyd, Sweden: Cementa AB. pp. 207. (In Swedish).

[16] Jonasson, J-E, Emborg, M & Bernander, S (1994). Temperatur, mognadsutveckling och egenspänningar i ung betong (Temperature, Maturity Growth and Eigenstresses in Young Concrete). In: *Betonghandbok - Material*. (Concrete Handbook - Material). Edition 2. Stockholm, Sweden: AB Svensk Byggtjänst and Cementa AB. pp. 547-607. ISBN 91-7332-709-3. (In Swedish).

[17] Jonasson, J-E (1994). Krympning hos hårdnad betong (Shrinkage in Hardened Concrete). In: *Betonghandbok - Material*. (Concrete Handbook - Material). Edition 2. Stockholm, Sweden: AB Svensk Byggtjänst and Cementa AB. pp. 524-545. ISBN 91-7332-709-3. (In Swedish).

Water requirement of cement, W_{180} – A practical test method

Jouni Punkki,
Dr.Tech., Development Engineer
Parma Betonila Oy
P.O. Box 76, FIN-03101 Nummela, Finland
E-mail: jouni.punkki@parmabetonila.fi

Vesa Penttala,
Prof., Dr.Tech.
Helsinki University of Technology
FIN-02151 HUT, Finland
E-mail: vesa.penttala@hut.fi

ABSTRACT

Water requirement of cement is a very important factor affecting the quality of concrete. In spite of its importance the water requirement of cement is difficult to measure, only few test methods are available. In the present paper, a practical test method is presented. The water requirement can be measured simply and reliably. With the method also the effects of the admixtures and additives on the water requirement can be analysed.

Key words: water requirement, cement, consistency, workability, quality.

1. INTRODUCTION

In cement production, the quality of cement is mainly controlled with help of compressive strength development of cement. The quality variation of cement clinker is normally compensated by grinding the clinker in different fineness or using different amounts of mineral additives in cement. However, this easily leads to variation in water requirement of cement. And in concrete production, the water requirement of cement is a very important factor, often even more important than the compressive strength. Variation in the water requirement causes variation on the final quality of concrete in several ways; mechanical properties, durability properties and surface quality of concrete can be affected by the water requirement.

In spite of its importance for concrete production the water requirement of cement is not very well known. In cement factory, the water requirement is normally checked in the setting time test (Vicat), but the method (Standard consistency) /1/ is rather insensitive. The Standard consistency test is primarily made to adjust the consistency of cement paste suitable for the setting test, not to analyse the water requirement of cement. Also, the test is made using pure cement paste without admixtures. In concrete factory, the water requirement is very seldom determined, because suitable test methods are not commonly known. The test method for such purpose should be practical, reliable and fast to carry out. In addition, the test method should reflect the workability of concrete used in the particular production. In the present paper, a test method is presented.

2. PRINCIPLE OF THE METHOD

The principle of the test method is to determine the water-cement ratio of cement mortar, which gives a certain, easily measurable consistency. The principle is very similar as used in DIN 1060 /2/ for determination of water requirement of building limes.

In the present method cement mortar is used instead of cement paste or concrete. Cement mortar better simulates the real situation compared to cement paste. The composition of mortar can be varied according to the particular concrete product; the mortar can contain admixtures and/or additives. Thus, also the compatibility of cement and admixtures can be effectively analysed. Effects of aggregate on test results are minimised by using standardised sand. Cement mortar tests gives more accurate test results compared to tests made using concrete. The smaller amounts of the materials allow more precise control of the material quality. Also a larger number of tests can be performed with mortar tests.

The consistency of mortar is determined using the mortar flow table (Figure 1). The equipment is used for determination of the consistency of mortar in a German Standard /3/. In the present method, the tests are carried out using different water-cement ratios so that the water-cement ratio giving a flow of 180 mm can be interpolated. The interpolated water-cement ratio reflects the water requirement of mortar. When the method is used to analyse the water requirement of cement, the interpolated water-cement ratio can be called: *Water requirement of cement* (W_{180}). However, the value is dependent on the composition of mortar (sand, admixtures) and, therefore, the value can be used only for comparison purposes.

Figure 1 - Mortar flow table.

3. MATERIALS AND TEST PROCEDURE

Test mortar consists of cement, additives (optional), admixtures (optional), sand and water. The composition of mortar can be varied, but in the normal case a weight ratio of 1.5 between sand and cement (+ additives) is used. The ratio of 1.5 corresponds to a concrete mix having a relatively high cement content. In some cases (e.g. lean mixes), a higher ratio would better correspond to the real situation. For example for cement content of 300 kg/m^3 or below, a sand-cement ratio near 2 would be more correct. The ratio (= 3) used for the determination of strength of cement is normally too high for this purpose. A low ratio is preferred because with high ratios the quality of aggregate may have a significant effect on test results. Two different types of sand can be used:

a) Standard sand, EN 196-1 /4/
b) Laboratory sand;
dried, glacial / fluvial sand, combined of minimum three sieved fractions.

If the test results need to be fully comparable with other results, the standard sand has to be used. If the test method is used for indicating variation in water requirement or for compatibility between cement and superplasticizer, laboratory sand can be used. Then, the test results are dependent on the quality of sand and are not fully comparable with the results made by using different sands. The combined grading of the laboratory sand shall fulfil the requirements presented in Table 1.

Table 1 - Requirements for the grading of the laboratory sand.

Sieve size [mm]	Passing [%]
0.125	2 ± 2
0.5	35 ± 3
1	70 ± 3
2	98 ± 2

Principally, also the normal production sand (e.g. 0-2 mm or 0-4 mm) can be used. Then the test would perfectly reflect the real situation. However, the properties of sand vary and this causes additional variation to the test results. Especially, the quality variation of the finest particles (< 0.125 mm) may affect the results. Consequently, use of standard or laboratory sand is recommended.

In the case of standard sand, 900 g cement and 1350 g sand is used. A bag of standard sand contains 1350 g and a sand-cement ratio of 1.5 gives a suitable composition of mortar. If the sand-cement ratio differs from 1.5, the content of cement has to be corrected. In the case of laboratory sand, the amounts of cement and aggregate can be freely selected; e.g. 500 g cement and 750 g give an adequate amount of mortar.

The mortar flow table consists of conical mould and flow table. Two different types of mortar flow table are available:

a) ASTM flow table /5, 6/
b) DIN flow table /2/

In the case of the ASTM flow table, the mould has the following dimensions: $Ø_{bottom}$ = 101.6 mm, $Ø_{top}$ = 69.9 mm and h = 50.8 mm. The diameter of the table is: $Ø_{table}$ = 254 mm and the height of drop: h_{drop} = 12.7 mm. In the case of the DIN flow table, the respective dimensions are: $Ø_{bottom}$ = 100 mm, $Ø_{top}$ = 70 mm, h = 60 mm, $Ø_{table}$ = 300 mm and h_{drop} = 10 mm. In the present paper, the ASTM flow table is always used. The mixer is described in the standard /4/. The temperature of the materials, equipment and laboratory has to be 20 ± 2 °C and the relative humidity of air 60 - 80%.

Cement (+ additive) and sand is first dry-mixed for about 15 s. Water (+ admixture) is added and the mixture is mixed for 30 s using the first gear. The mixer is stopped and the bowl and blade are cleaned using a rubber spatula and the mixing is continued using the second gear. The total mixing time (after adding the water) is 3 min. Superplasticizer can be added delayed e.g. 1 min after the initial water. Then, the cleaning is carried out just before adding the superplasticizer.

Immediately after mixing the specimen is moulded on the flow table. The flow mould is filled and compacted in two levels. The compaction shall be just sufficient to ensure uniform filling of the mould. The mould is removed and the dropping of table is started at 45 s after the ending of mixing. The flow table is dropped 15 times during 15 s. The spread (total diameter) is measured in 3 or 4 directions (depending on the type of table) and the average value is calculated. The test is repeated until the water-cement ratio (or water-binder ratio when additives are used) giving a spread of 180 mm can be interpolated. The water-cement ratio is varied by altering the water content, the contents of other constituents are not changed. The two nearest water-cement ratios around the water requirement value (step: 0.01) shall be tested. The principle is illustrated in Figure 2. When admixture is used, it is recommended that the water content of admixture (normally app. 60%) is taken into account when calculating the water-cement ratio.

Figure 2 also shows the effect of water-cement ratio / superplasticizer dosage on the slope; without admixture the slope is typically about 5 mm / 0.01 in water-cement ratio. With superplasticizer the slope is clearly higher.

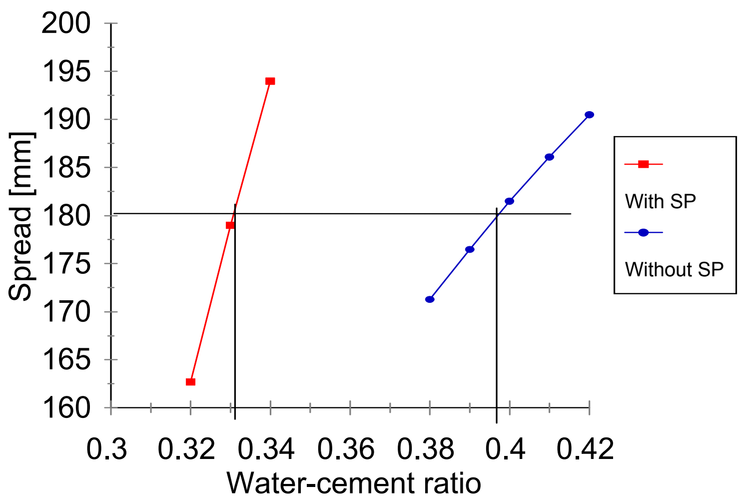

Figure 2 - Principle of water requirement test. Tests have been made with and without superplasticizer. The calculated water requirement values are: 0.331 and 0.397. Napthalene-type superplasticizer, 4% SP (25% solution) by weight of cement, very rapid hardening cement (CEM II A 52.5 R).

4. REPEATABILITY AND REPRODUCIBILITY OF THE METHOD

The errors of repeatability can be caused by the following factors:

1. Variation in the mixing procedure

2. Variation in the filling / removing the flow mould

Especially when a superplasticizer is used attention should be paid on the mixing procedure. As commonly known the addition time of superplasticizer significantly affects the rheological properties of cement paste. Therefore, a fixed addition time of superplasticizer has to be used.

If the consistency of mortar is low, a proper filling of the mould can be difficult. However, with a consistency giving a spread near 180 mm this is not normally a problem. In the case of high superplasticizer dosages, cement mortar may adhere on the walls of the mould and, thus, affect the test results.

Repeating the whole test six times tested the repeatability of the method. The test series were made both without and with superplasticizer. The results have been collected in Table 2. Generally, a very good repeatability was achieved. For example using two parallel tests, the confidence limits of the average would be ±0.0028 in both cases. Even with a single test the repeatability is good (error typically max. ±0.004 without SP and ±0.007 with SP). Based on the results, it is recommended that the results are given by using three significant numbers (three decimals) when at least two parallel tests have been carried out. In the case of single test, the accuracy of 0.005 is recommended.

Table 2 - Repeatability of water requirement test. Results of six parallel tests have been presented. Tests have been made without and with superplasticizer. Naphthalene-type superplasticizer, 4% SP (25% solution) by weight of cement, very rapid hardening cement (CEM II A 52.5 R).

	Water requirement of cement				
	Average	Standard deviation	Coefficient of variation	Minimum	Maximum
Without SP	0.429	0.0020	0.47%	0.427	0.431
With SP	0.332	0.0020	0.60%	0.330	0.337

In addition to the factors causing repeatability errors, the errors of reproducibility can be caused by the following factors:

1. Variation in the quality of sand
2. Variation in testing temperature
3. Variation caused by test equipment and operator

The water requirement of sand directly affects the measured water requirement value. Two very different types of sand (for example well-rounded glacial sand and crushed sand) may give over 0.05 difference in the measured water requirement value. However, between glacial / fluvial sands the difference is much smaller. The reference sand EN 196-1 is very well rounded, quartz rich fluvial sand and thus gives a low water requirement value. In Table 3, the standard sand and laboratory sand has been compared. The standard sand was produced by Normensand Gmbh, Germany and the laboratory sand by Optiroc Oy, Finland. The laboratory sand consists of three fractions (0.1-0.6, 0.5-1.2 and 1-2 mm). The sand is glacofluvial, granitic aggregate.

According to the tests, the laboratory sand gives rather similar water requirement values compared to the standard sand. When no superplasticizer was used, the laboratory sand gave slightly higher water requirement values. This is obviously due to the more rounded particle shape of the standard sand. Also the content and quality of the finest particles (< 125 µm) may be different between the aggregate types. When a superplasticizer was used, the difference was negligible. The role of the cement paste is probably so dominant that small differences in the quality of sand do not significantly affect the test results. If a higher sand-cement ratio is aimed at also the effect of the quality of sand might be larger.

Table 3 - Effect of the aggregate type on the results of water requirement tests. Tests have been made without and with superplasticizer. Naphthalene-type superplasticizer, 4% SP (25% solution) by weight of cement, very rapid hardening cement (CEM II A 52.5 R). Averages of two parallel tests have been presented.

Type of aggregate	Water requirement			
	Without SP		With SP	
	average	range	average	Range
Standard sand	0.417	0.005	0.338	0.001
Laboratory sand	0.426	0.001	0.337	0.001

Temperature has a significant effect on the early consistency of cement mortar. Compared to concrete, the effect of temperature is bigger because of the higher cement content. Therefore, the operating temperature has to be controlled (acceptable temperature range: 18 - 22 °C) .

The method is rather insensitive to variation in the test equipment or operators. However, different types of flow table give slightly different results. Therefore, the type of flow table has always to be mentioned. If the results of two laboratories need to be fully comparable, reproducibility tests have to be carried out.

5. LIMITATIONS OF THE METHOD

The consistency of mortar giving a spread of 180 mm can be considered as equivalent to the consistency of concrete typically used in the prefabricated production (slump approximately 150 mm). Therefore, the method is not necessarily very suitable if the water requirement of cement for no-slump or self compacting concrete is analysed. For example, the effect of superplasticizer may depend on the consistency of mortar / concrete.

In two-point system of cementitious material rheology, the consistency is divided into yield stress and plastic viscosity. The present test method can be considered as a one-point method because it mainly measures the yield stress (it is also slightly affected by the plastic viscosity). From the test methods for consistency of concrete, the German flow table measures the similar rheological properties as the present method. Compared to mortar / concrete viscometer the method gives rather incomplete information. In order to get more accurate information from rheological properties, mortar / concrete viscometer should be used. However, viscometer tests may be too difficult and time-consuming in factory environment.

6. EXAMPLES

In the following, the water requirements of different types of cement have been presented (Table 4). As can be seen from Figure 3 the fineness is a very important factor affecting the water requirement, but the fineness alone cannot explain the differences between the cement types. Also, the effect of superplasticizer dosage on the water requirement has been illustrated (Figure 4). In Figure 5, use of water requirement test in the quality control of cement has been demonstrated. Eight different lots of cement have been tested in a concrete factory.

Table 4 - Water requirement of different types of cement. Tests have been made without and with superplasticizer. Naphthalene-type-superplasticizer, 4% SP (25% solution) by weight of cement. Results of single test have been presented. The cements were produced by Finncement, Finland except the white cement, which was produced by Aalborg Portland, Denmark.

Cement type	Description	Composition [%] (C_3S, C_2S, C_3A, C_4AF)	Fineness Blaine [m^2/kg]	Water requirement	
				Without SP	With SP
CEM II A 42.5 R	Rapid hardening cement	62, 11, 8.5, 8.5 [1]	450	0.393	0.323
CEM II A 52.5 R	Very rapid hardening cement	62, 11, 8.5, 8.5 [1]	540	0.422	0.349
CEM I 42.5 SR	Sulphate-resistant portland cement	70, 10, 1.0, 13	340	0.350	0.290
CEM I 52.5 R	White portland cement	70, 19, 4.5, 1.0	385	0.345	0.305 [2]

[1] = composition of clinker, typical values given by the producer
[2] = melamine-type superplasticizer, 0.8% dry SP by weight of cement.

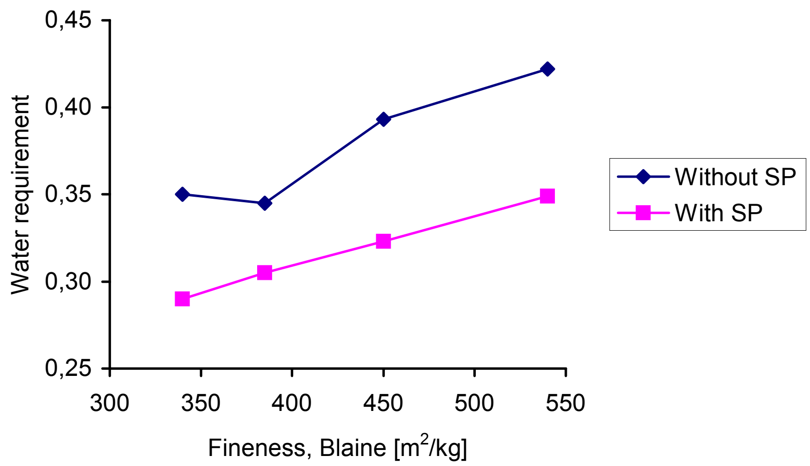

Figure 3 – Effect of fineness of cement on the water requirement. The cements are the same as presented in Table 4.

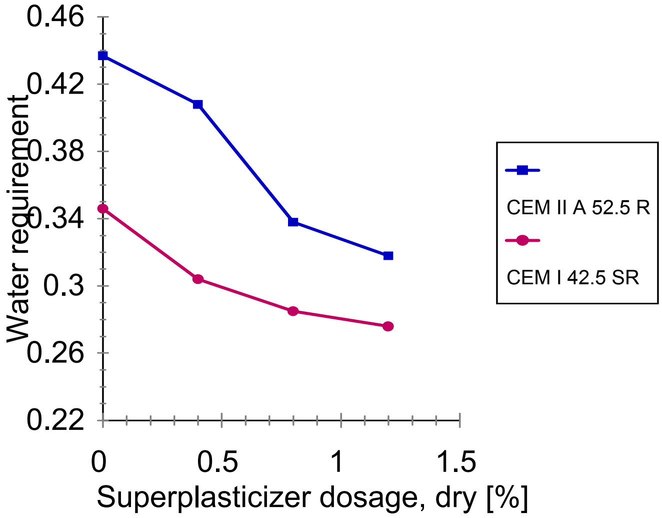

Figure 4 –
Effect of superplasticizer dosage on the water requirement. Naphthalene-type superplasticizer, very rapid hardening cement (CEM II A 52.5 R) and sulphate-resistant portland cement (CEM I 42.5 SR). Results of single test have been presented.

As demonstrated in Figure 5, the method effectively reveals the variation in the compatibility of cement and superplasticizing admixture. The methods made for pure cement paste without admixtures (e.g. standard consistency) may not reflect very well the real situation where also admixtures are used. In Figure 5, for example, the cement lot which had the lowest water requirement without superplasticizer gave the second highest water requirement with superplasticizer.

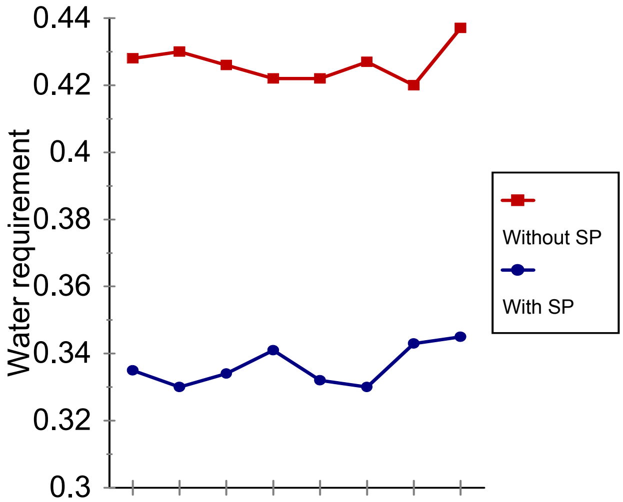

Figure 5 –

Use of water requirement test in the quality control of cement. Eight different lots of cement have been tested. Tests have been made without and with superplasticizer. Naphthalene-type superplasticizer, 4% SP (25% solution) by weight of cement, very rapid hardening cement (CEM II A 52.5 R). Results of single test have been presented.

7. CONCLUSIONS

The proposed test method for determination of water requirement of cement has proved to be applicable for testing of cement and plasticizing admixtures as well as quality control of cement. The test is relatively rapid to carry out (takes 0.5 - 1 h) and the test results are well reproducible. Based on the repeatability tests two parallel tests normally give an adequate accuracy.

REFERENCES

1. EN 196-3. Method of testing cement - Part 3: Determination of setting time and soundness.1994. European Committee of Standardization. 8 p.
2. DIN 1060 Teil 3. Baukalk; Physikalische Prüfverfahren. 1982. Deutches Institutt für Normung e.V. 9 p.
3. DIN 18555 Teil 2. Prüfung von Morteln mit Mineralischen Bindemitteln; Frishmörtel mit dichten Zuschlägen; Bestimmung der Konsistenz, der Rochdichte und des Luftgehalts. 1982. Deutches Institutt für Normung e.V. 4 p.
4. EN 196-1. Method of testing cement - Part 1: Determination of strength.1994. European Committee of Standardization. 17 p.
5. BS 4551. Methods of testing mortars, screeds and plasters. Part 1. Physical testing. 1998. British Standards Institution. 28 p.
6. ASTM C230-90. Standard Specification for Flow Table for Use in Tests of Hydraulic Cement. 1990. Annual Book of ASTM Standards, Vol. 04.01, pp. 182-186.

Study of the Energy Use Characteristics of Concrete Multi Family Dwelling Buildings and the Relevance for Economy and Environment

Mats Öberg
Ph.D. Student
Department of Building Materials
Lund University, Box 118, SE-221 00 Lund
E-mail: mats.oberg@cementa.se

ABSTRACT

Reduction of energy use in buildings is fundamental for sustainable development. A computer program for the prediction of energy use in buildings was assessed by comparisons with the energy performance of existing buildings. The program was then used to evaluate the energy saving characteristics of concrete such as air tightness and heat capacity.
The impacts on global environmental aspects and life cycle costs were examined. In a multi-family dwelling building a concrete building structure can contribute to a reduction of the annual requirement for space heating by up to 8%.

Key words: Energy use, Heat capacity, LCA, LCC, Thermal storage

1. INTRODUCTION

1.1 General

Representing 11% of the GNP and 40% of the total energy use within the EU [1], construction and operation of buildings has a large impact on economy and environment. The environmental council of the Swedish Building sector 'Byggsektorns Kretsloppsråd' [2] has established that energy required during the usage phase is the most critical environmental aspect for houses. The aspect of heating costs should also be considered. According to statistics for Swedish multi-dwelling buildings produced after 1986 this is in average 67 SEK/m^2 per year. [3] The significance of energy use implies that also relatively small differences regarding energy related characteristics within the built environment are important and that the prediction tools must be suited to appreciate this.

This is a study within the 'Optimal Concrete Building', a research project applying integrated life cycle design on multi-family dwelling buildings to explore the functional and economical advantages of concrete as building material.

1.2 Background

The potential energy demand for space heating and cooling of a building, at given outdoor climatic conditions and at a set interval of indoor temperature, depends on conductivity (transmission), convection (air movement through leaks) and radiation through the climate shell, ventilation rate and heat gains from people, equipment, lightning etc. The thermal inertia of a building can even out temperature fluctuations and thus reduce the required heating or cooling energy (thermal storage). The main thermal fluctuation cycle within a building is the twenty-four hour period. The energy saving potential of concrete buildings is related to their thermal mass, and in case concrete has the function of a vapour barrier in the climate shell also to air tightness. Concrete, however, has high thermal conductivity why careful design to avoid heat bridges is essential.

The impact of the thermal inertia depends on the effective heat capacity, that is the share of the total heat capacity that contributes to the heat exchange between component and indoor air during the fluctuation cycle. Furthermore, the indoor temperature must be allowed to fluctuate at least 2 to 3°C. Johannesson [4] modelled the heat balance of rooms including the effective heat capacity using the analogy with electrical resistances and capacitances, and finite difference equations for the calculations. The effective thickness of a 250 mm concrete wall or slab in contact with the room is 90 mm from the exposed surface, at a thermal transmittance of concrete of 1.2 $W/m^2 °K$. In a field study Akander [5] has compared measured effective heat capacity and analytical results based on the principles defined by Johannesson and found adequate agreement.

Convection is driven by differences in air pressure over the climate shell, caused by wind or thermology (stack effect) and depends on the air tightness. In buildings with mechanical exhaust ventilation tightness has little influence on the energy requirement, as air leaks only substitute the fresh air taken in through valves. In the case of balanced or natural ventilation air leaks can correspond to between 10 and 30% of the heating energy requirement. In either case, air leaks affect the thermal comfort and may lead to moisture related problems within the climate shell.

In a review by Bergsten [6] on commercially available energy balance programs in Sweden in 2001, a total of 12 programs were accounted for, ranging from simple shareware tools, providing for crude estimations for single-family house applications, to customized versions of sophisticated university programs. Energy balance calculation programs can be grouped into dynamic and steady state. Steady state programs work in principle like hand calculations and their main advantage is that the computation effort is very small as they exclude complicated algorithms and the time resolution is at least a whole 24-hour period. The accurateness of a steady state program depends on the similarity between the specific conditions and those for which the calculation has been adapted. Such programs are therefore suitable for simple and standardised buildings, such as prefabricated single-family homes, where calibrations could be made based on the actual performance. The combined effect of, for instance, surplus energy, air leakage and thermal storage can thus be approximated but not calculated with a steady state program. The program mostly used in Sweden today, ENORM [7], is a steady state program that was developed at a time when the capacity of common PC-computers restricted the possibility to use dynamic programs. According to an analysis with this particular program on four multi family dwelling buildings by Adalberth [8] the actual energy use was underestimated by in average 27% and in a validation on 16 multi family dwelling buildings by Sandberg in 1998 [9] by as much as 50%. Besides the limitations with regard to the calculation method in steady state programs the large discrepancy can also be attributed to incorrect input data with regard to user behaviour and technical performance. For instance, there are approximated values for gain of solar energy and internal surplus heat based on experiences from houses built during the 60s and 70s that are not valid for the buildings currently produced. For general applications, such as multi-family dwelling buildings, dynamic programs are advisable. Currently there are several user-friendly dynamic programs available according to [6]. The European and ISO standard 'Thermal Performance of Buildings – Calculation of Energy Use for Heating' [10] employs the steady-state approach but the effect of thermal storage is quantified with a so called utilisation factor which is function of the heat loss, heat gains and the time constant of the particular building. The time constant is defined as the total effective heat capacity divided by the total heat loss by transmission, convection and ventilation. Akander [5] calculates the difference with regard to potential energy requirement in multi-family dwelling buildings with different thermal inertia with a dynamic energy balance calculation program and also with the above mentioned standard and concludes that the supplied energy for heating of the heavy building is 86-94% of the light building depending on the specific conditions.

Environmental goals defined by the Swedish Ministry of Housing and Planning for new dwelling buildings state that the total annual energy use should be limited to 90 kWh/m^2 per year in 2010 and further to 60 kWh/m^2 per year in 2020 [11]. Average annual energy use in currently produced multi-family dwelling buildings is 35 kWh/m^2 electricity and 140 kWh/m^2 space heating. For the development of more energy efficient buildings accurate prediction tools are essential.

1.3 Aim of the study

The aims of this study are as follows.

- To improve predictability of energy use for the operation of multi family dwelling buildings and to verify links between the building as well as heating and ventilation systems and the energy performance. This is a key to the improvement and optimisation of the building with regard to energy performance
- To evaluate the potential effect on energy performance in concrete buildings of selected parameters such as heat capacity, air tightness of the climate shell, heat bridges, indoor temperature and the ventilation system. In particular the interaction between building materials and ventilation system will be examined
- To evaluate the energy performance related effects on costs and global environmental aspects over the life cycle of the building

The underlying hypotheses are, firstly that a suitable program with proper input data can predict the energy performance with an accurateness of ± 10%, which is deemed to be sufficient. Secondly, that the effects on energy use with regard to heat capacity and air tightness of a concrete building frame and shell can be evaluated and that these effects have significance with regard to life cycle cost and global environmental aspects for residential buildings.

2. METHOD

The energy performance of an existing multi family dwelling building, over a period of one year, was mapped. This data was compared to results of calculations on the particular building made with an energy balance program employing the particular climatic conditions in order to assess the predictability of the energy balance of buildings. The program was then used to explore the effects on the potential energy use by differences with regard to building structure and ventilation system.

2.1 Case study on energy use in multi family dwelling buildings

A modern building with uncomplicated geometrical layout and ventilation and heating system was selected in order to focus on the comparison between calculated and real energy performance. It was one of eight similar two-floor blocks with eight flats each comprising a 520 m^2 net floor area, located in Svedala in the south of Sweden and owned by the semi-public company Bostads AB Svedalahem. See Figure 1. The building was completed in 1998.

Figure 1. Case study. 'Erlandsdal 1b'. Svedala.

The building frame was cast *in situ* on precast concrete floor plates see Figure 2, below. The exterior walls were clad with brickwork in a curtain wall of wood scantlings and insulation on the long sides and on insulation and concrete wall on the gables. Hot water radiators furnished by a natural gas boiler provide the space heating and the flats are equipped with mechanical exhaust ventilation.

Energy characteristics for the building over a period of one year (2000) were determined comprising charged energy for space heating, electricity used in the households and for general purposes in the building, ventilation rates and tap-water consumption. Indoor temperatures, number of inhabitants and airing frequenses were examined by a questionnaire on indoor climate developed by Engvall [12], that was used to evaluate the indoor climate which will be reported in another paper. Heat from persons was calculated by assuming that the occupants are inside their flats half of the time. The release of energy from one people was set to 60 W [13]. All electric energy used by the occupants inside their flats is regarded as gained within the energy balance whereas common electricity for ventilation fans and exterior lighting was excluded as the corresponding heat is generated outside the flats. Heating of hot water was estimated by the energy needed to increase the temperature of half of the tap water consumed during 2000 by 50°C.

2.2 Energy balance calculations

The program VIP+ [14] was used for the energy balance calculations. VIP+ is a dynamic program providing that can assess the impact of thermal inertia and air leaks. The program manages energy supply from space heating, solar radiation, internal gains (people, appliances) heat recovery from ventilation and energy release by transmission, ventilation, air leaks, hot water production and cooling. There are two specially designed calculation modules, one for the calculation of airflows through ventilation and air leaks according to Nylund [15] and one for heat capacity according to Johannesson [4].

The energy balance program was evaluated by calculating the energy requirement for space heating given the measured input data and comparing the results with the charged energy use for the specific year and then used to simulate the potential effects on energy use of different types of building frames and ventilation systems.

2.3 Evaluation of environmental and economical impacts of energy use

Environmental aspects
Emission factors from the particular energy sources including extraction and use: natural gas and electricity, were collected from a database for the computer program 'Life Cycle Inventory Tool' [16], see Table 1. Only the emissions addressed by the socio economic evaluation, described in Table 2, were selected. These emissions are deemed to be representative with regard to the most severe global ecological damages such as global warming, eutrophication, acidification and ozone depletion. Other substances also contribute to these damages but in the case of energy production these other emissions occur with good correlation to the chosen substances. Socio economic costs generated by the emissions according to the Swedish National Road Administration [17] are presented in Table 2. The socio economic cost principle was chosen because it operates with a unit that is directly comparable to the real costs.

Table 1. Emissions from different energy sources

Emission factors for selected energy sources (g/MJ)	CO_2	NOx	SO_2	VOC
Electricity. Swedish mix	12	0.02	0.01	0.003
Natural Gas	62	0.06	-	0.002

Table 2. Socio economic costs for emissions to air according to the Swedish National Road Administration

Socio economic cost SEK/kg	CO_2	NOx	SO_2	VOC
	0.015	60	20	30

Economy
Life cycle costs were calculated using a spread-sheet program developed for a study on life cycle costs in multi-family dwelling buildings. [18] The present value of annually recurring future events was calculated with the standard formula

$$PV = P_n\, p/(1-(1+p)^{n}) \text{ where} \tag{1}$$

P_n = cost for event at price level when it occurs
n = number of years until event occurs. Here: 60 years
p = discount rate

where p = real interest rate – annual increase of price above inflation
Here real interest rate 3.5 % (Average Swedish real interest rate 1960-2000) and increase of energy cost 0%, 3% or 6% above inflation.

3. RESULTS

3.1 Case study: energy use in a Swedish concrete multi family dwelling building

The use of energy and tap water during 2000 was obtained from Bostads AB Svedalahem and Sydkraft AB. In order to refine the evaluation of the program, quantifications on actual gains from persons and use of electricity were applied instead of available default values within the computer program. The indoor temperature, 22ºC, and the number of inhabitants, 16, were determined by a questionnaire. Table 3 displays the calculated energy balance and the charged energy for heating and it can be noted that reasonable coherence between calculated and charged energy use for heating has been achieved. Charged energy use was 144.5 kWh/m^2 which should be compared with the calculated 130.9 kWh/m^2 and is close to the accurateness pursued (± 10%). Error sources are related to the tenants behaviour but also to technical aspects such as the efficiency of the gas boiler that supplies the space heating and hot tap water and according to the manufacturer, Viessmann, is close to 1 or the stability of the ventilation system. Furthermore average climatic data were used for the calculations instead of data for the specific year.

Table 3. Case study: calculated energy balance (kWh/m^2)

Energy demand				Energy supply			
Transmission	Air leaks	Ventilation	Hot water	Solar radiation	Gains from electricity	Gains from persons	Heating
72.5	0.8	65.3	53.8	33.8	27.7	8.1	130.9

3.2 Potential influence of building materials and ventilation system on energy use

To study the effects of changes in the building frame, climate shell and ventilation system the original building frame of the case study (a) was compared with two alternative types according to Figure 2 and Table 4.

Table 4. Parametric study

Ventilation system/Type of building frame	Original	Heavy	Light
Mechanical exhaust. AL*=3, 64% of window area facing north	a1N		
Mechanical exhaust. AL*=3 **	a1	b1	c1
Balanced ventilation. AL*=3 **	a2	b2	c2
Balanced ventilation. AL*=1.5 in heavy structures, **	a3	b3	

* Air leakage through component at 50 Pa pressure difference measured in m^3/m^2,h
** 64% of window area facing south compare Annex A.

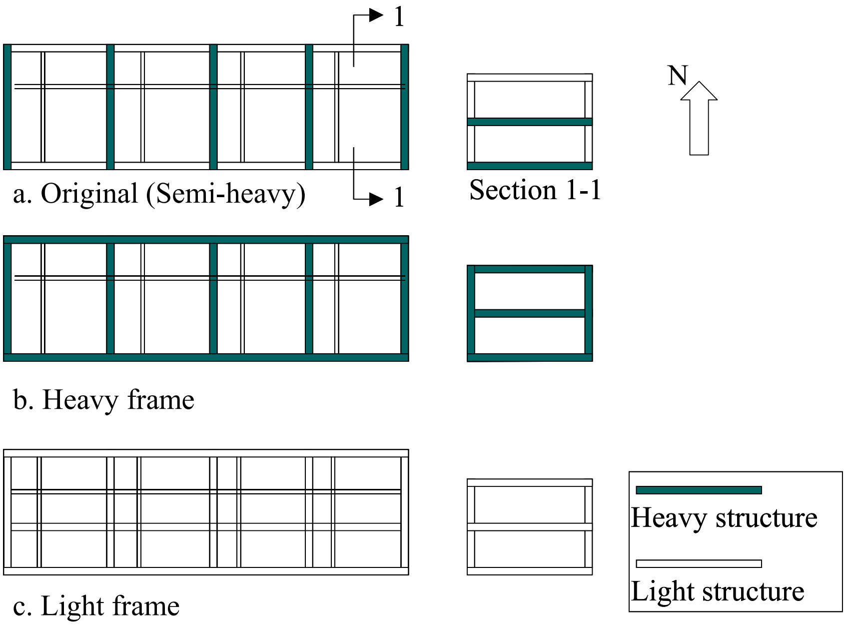

Figure 2. General layout of three different frames

For each case two different types of ventilation systems were studied: mechanical exhaust ventilation as in the original building and balanced ventilation with heat recovery. According to the orientation of the original building 64% of the window area faced directly to the north and 36 % to the south. An opposite distribution was used for the simulation of the impact of thermal inertia. Details on structures and energy related aspects are tabled in Annex A. Results of energy balance calculations are presented in Table 5, below and in detail in Annex B.

3.3 Impacts on energy use, economy and environment over the life cycle of the building

In table 5 the impact on annual costs, socio economic costs and present value of costs, at different increase of energy costs, for the alternatives examined within the parametric study are displayed. Note that performance of the cases of group 1 (mechanical exhaust ventilation) should not be directly compared with the results of group 2 (balanced ventilation with heat recovery).

Comparing the potential energy use the heavy building (b) requires about 95% of the bought energy for space heating of the light (c) structure due to thermal inertia. (Comparisons b1-c1 or b2-c2) This conforms with the results reported by Akander [5]. If differences in air tightness are taken into account the gap increases. The simulations indicate that from the annual cost perspective the impact of differences with regard to energy use between the alternative structures is small, 1 to 4 SEK/m^2 which should be viewed in relation to the average heating cost 67 SEK/m^2 in modern Swedish multi family dwelling buildings [3]. However with regard to life cycle costs, were the present value is a relevant indicator, the difference can be regarded as significant, ranging from 30 to 350 SEK/m^2 with regard only to thermal inertia and as much as 720 SEK/m^2 for the combined effect of thermal inertia and air tightness at an increase of energy cost of 3% above inflation. This can be compared with a typical production cost of a building frame of 3000-6000 SEK/m^2. The socio economic calculation show that there is an additional cost with regard to environmental aspects that is of the same magnitude as the straight cost.

Table 5. Energy use, Socio economic cost, annual cost and present value

Case*	Annual requirement of bought energy for space heating (kWh/m^2)	Annual Socio economic cost (SEK/m^2)	Annual Cost (SEK/m^2)	Present value. (SEK/m^2) Increase of energy cost more than inflation 0%	3%	6%
a1N	77.1	27	38	1066	2310	6697
a1	60.9	21	30	841	1824	5288
b1	59.6	21	30	825	1788	5184
c1	64.7	23	32	894	1938	5619
a2	40.2	14	20	556	1206	3496
b2	39.1	14	20	542	1176	3410
c2	43.5	15	22	603	1308	3792
a3	38.9	13	19	540	1170	3392
b3	33.8	12	17	468	1014	2940

* Cases according to table 4: a: original; b:heavy structure; c: light structure.

4. FURTHER WORK

The energy balance calculation program VIP+ will be further assessed by examining other existing multi family dwelling buildings. The air tightness of different types of exterior walls: light curtain walls, precast sandwich walls and cast in situ concrete walls, will be studied by field tests in existing buildings, to secure input data for calculations. The influence of concrete on the room temperature will be examined as that is an important indoor air quality aspect. Possibilities to reduce the required effect installed for space heating with regard to the thermal inertia will also be examined.

5. CONCLUSION

The two advantages of concrete with regard to energy savings; namely the heat capacity of the structures that are exposed to the indoor air and the possibility to obtain durable air tightness of the climate shell can contribute significantly to the life cycle performance of a building. This can be evaluated during the design phase by applying an adequate energy balance program and life cycle cost estimations. The effect with regard to global environmental aspects can be examined by a socio-economic calculation. The magnitude of the economical and ecological impacts motivates the application of this type of analysis to guide design decisions.

6. ACKNOWLEDGEMENTS

The author gratefully acknowledges the financial support of the Swedish Foundation for Strategic Research (SSF) and Cementa AB, as co-sponsor, for the project, "New research directions for the building sector", which forms part of the Swedish national graduate school and research program, *Competitive Building*.

The author gratefully acknowledges the assistance from Jörgen Grabo, Bostads AB Svedalahem, to aquire data for the case study.

REFERENCES

1. Sjöström, C., "Challenges of Sustainable Construction in the 21st Century," *Proceedings* RILEM/CIB/ISO Symposium on Integrated Life-Cycle Design, Helsinki 2000, Keynote lecture.
2. Byggsektorns Kretsloppsråd, "Byggsektorns betydande miljöaspekter," Miljöutredning för byggsektorn. Final Report. Stockholm, 2001, Sweden. (In Swedish)
3. Statistics Sweden, "Yearbook of Housing and Building Statistics 2000," Stockholm, Sweden, 2000.
4. Johannesson, G. "Active heat Capacity – Models and Parameters for Thermal performance of Buildings,". Report TVBH-1003. Lund University. Dep. of Building Physics, Sweden, 1981.
5. Akander, J. "Active heat Capacity – Models and Parameters for Thermal performance of Buildings,". Bulletin 180 Royal Institute of Technology. Dep. of Building Sciences, Stockholm, Sweden, 2000.
6. Bergsten, B. "Energiberäkningsprogram för byggnader" Report 2001:03. Effektiv CIT/SP/Chalmers. Gothenburg, Sweden, 2001 (In Swedish)
7. ENORM. Computer program for energy balance calculations. Energiforskning AB. Stockholm, Sweden
8. Adalbert, K., & Petersson, Ö., "Energy Use and Environmental Impact of new Residential Buildings" Report TVBH-1012. Lund University. Dep. of Building Physics, 2000, p 29.
9. Sandberg, E.,"Energimål – kort sikt, Hammarby Sjöstad". ATON Teknik Konsult AB, Stockholm, Sweden, 1998 (In Swedish)
10. EN ISO 13790. Thermal performance of buildings – Calculation of energy use for buildings. CEN. Brussel
11. Swedish Ministry of Housing and Planning, Boverket "God bebyggd miljö".Karskrona, Sweden, 1999 (In Swedish)
12. Engvall, K..Norrby, C, "Upplevt inomhusklimat i Stockholms bostadsbestånd," Report Nr 1992:4, Stockholms Stad. Utrednings och Statistikkontor, Stockholm., 1992, 40 (In Swedish)
13. Markus, T.A., Morris, E. N., "Buildings, Climate and Energy", Pitman Publishing Ltd., London, U.K.,1980, pp 42-43.
14. VIP+. Computer program for energy balance calculations. Skanska IT-Solutions. Stockholm, Sweden
15. Nylund,. P-O. Infiltration and Ventilation. Report D22:1980. Swedish Council for Building Research, Stockholm, Sweden, 1980. (In Swedish)
16. LCAiT. Computer program. Chalmers Industriteknik. Gothenburg, Sweden
17. Swedish National Road Administration, "Samhällsekonomiska Beräkningsförutsättningar," Vägverkets publikation 1999:170, Borlänge, Sweden, 1999, (In Swedish)
18. Johansson, C, Öberg, M, "Life Cycle Costs and Affordability Perspectives for Multi-Dwelling Buildings in Sweden," Proceedings 2nd Nordic Conference on Construction Economics and Organization, Gothenburg, Sweden, 2001, pp 287-297.

ANNEX A. Input data for energy calculations

Table A. Building structures. Areas and energy related data

Structure	Type	Area	U-value	Air leakage	Glass share/ Transmittance
a1N		m^2	$W/m^{2o}C$	$m^3/m^2,h$	%
Wall North	Light	125.5	0.194	3	
Wall South	Light	157.0	0.194	3	
Wall East.	Concrete	48.0	0.194	3	
Wall West	Concrete	48.0	0.194	3	
Window North		15.7	1.50	3	70/80
Window South		47.2	1.50	3	70/80
Glas door North		16.9	1.50	3	45/80
Door South		16.9	1.50	3	
Roof, Light		260.3	0.116	3	
Floor on ground	Concrete	224.3	0.234		
Floor on ground	Concrete	36.0	0.360		
Inner wall	Concrete	98.0			
Inner wall	Light	150.0			
Inner floor	Concrete	260.3			
a1, a2, a3		m^2	$W/m^{2o}C$	$m^3/m^2,h$	%
Wall South	Light	125.5	0.194	3	
Wall North	Light	157.0	0.194	3	
Wall East	Concrete	48.0	0.194	3. In a3: 1,5	
Wall West	Concrete	48.0	0.194	3. In a3: 1,5	
Window South		15.7	1.50	3	70/80
Window North		47.2	1.50	3	70/80
Glas door South		16.9	1.50	3	70/80
Door North		16.9	1.50	3	
The rest like a1N					
b1, b2, b3		m^2	$W/m^{2o}C$	$m^3/m^2,h$	%
Wall. North	Concrete	125.5	0.194	3. In b3: 1,5	
Wall South	Concrete	157.0	0.194	3. In b3: 1,5	
Wall.East	Concrete	48.0	0.194	3. In b3: 1,5	
Wall West	Concrete	48.0	0.194	3. In b3: 1,5	
Roof	Concrete	260.3	0.116	3. In b3: 1,5	
The rest like a1					
c1, c2		m^2	$W/m^{2o}C$	$m^3/m^2,h$	%
Wall.East	Light	48.0	0.194	3	
Wall West	Light	48.0	0.194	3	
Inner wall	Light	248.0	0.116	3	
Inner floor	Light	260.3			
The rest like a1					

ANNEX B. Energy calculations. Results

Table B. Calculated energy balance. (kWh/m^2)

	Trans-mission	Air leaks	Ventilation	Excess* ventilation	Heat recovery.	Solar gains	Internal gains	Heating **
a1N	72.5	0.8	65.3	7.0	-	33.8	34.8	77.1
a1	76.8	0.8	67.0	14.2	-	63.3	34.8	60.9
b1	76.8	0.8	67.0	12.7	-	63.3	34.8	59.6
c1	76.6	0.9	66.8	18.5	-	63.3	34.8	64.7
a2	79.8	17.1	60.6	16.9	36.9	63.3	34.8	40.2
b2	79.9	17.1	60.7	15.3	36.7	63.3	34.8	39.1
c2	79.2	17.2	60.3	21.2	37.0	63.3	34.8	43.5
a3	80.0	15.3	60.8	17.1	36.9	63.3	34.8	38.9
b3	80.7	9.4	61.2	16.5	36.9	63.3	34.8	33.8

* Ventilation due to exceeded maximum indoor temperature (28°C), **Hot tap water production excluded

NORDIC Ph.D. PROJECTS

In the Nordic countries extensive research is conducted within the fields of material technology, durability, execution and design.

Over the past few years, the number of Ph.D. students studying different items related to cement and concrete has increased significantly. This is caused partly by an increase in public funding of such studies and partly by an increase in financing from private companies.

In order to improve the opportunity for co-operation between Ph.D. students, and the institutions or companies, to which they are affiliated, the Research Committee of the Nordic Concrete Federation decided to make a survey of current Ph.D. projects. A total of 76 projects carried out at 16 different university departments are listed on the following pages, with information on institution, project, student, and supervisor and not least a contact e-mail address.

It is intended that the list may facilitate an increase in a sharing of experience and knowledge within fields of interest, which might lead to improvements of the individual projects. Furthermore, creation of personal networks between students and their supervisors may be valuable for future research and practical application.

Any comments or remarks to the list are of course very welcome. It is the intention to up-date this list at least once a year, and to publish it on our internet homepage.

It is the hope of the Research Committee that the list will be of interest for the students and their supervisors as well as for all readers of Nordic Concrete Research.

Dirch H. Bager
Chairman of the Research Committee.

DENMARK

Aalborg University – AAU
Department of Building Technology
Sohngaardsholmsvej 57
DK – 9000 Aalborg

Project:	**Frost induced transport of salts in concrete**
Project period	January 1999 – June 2002
Project type & financial support	Industrial Ph.D. Danish Academy of Technical Sciences & Danish Technological Institute
Ph. D. Student	M. Sc. Marianne Tange Jepsen
Supervisors	Prof. Per Freiesleben Hansen/AAU & Section Manager, Ph.D. Mette Glavind/Danish Technological Institute, Concrete Centre
Information	This project concerns the interaction of salt transport and ice formation in freezing concrete. One of the issues is the development of a method to map ice formation in hardened cement paste or concrete by continuous temperature scanning of the test specimen.
e-mail	marianne.t.jepsen@teknologisk.dk

Project:	**Physical and thermodynamic properties of green concrete**
Project period	January 1999 – December 2001
Project type & financial support	University Ph.D.
Ph. D. Student	M.Sc., Jacob Thrysøe
Supervisors	Prof. Per Freiesleben Hansen /AAU
Information	Investigation of decomposition reactions and heat of evaporation of water phases in well-cured cement paste subjected to high temperatures, using a newly developed Differential Pressure Analysis-apparatus. Determination of activation energy in cement paste systems using a newly developed isochor volumeter.
e-mail	i6jt@civil.auc.dk

Project:	**Activation energy of hardening portland cement systems**
Project period	Febuary 1999 – January 2002
Project type & financial support	University Ph.D.
Ph. D. Student	Peter Astrup Simmelsgaard
Supervisors	Prof. Per Freiesleben Hansen /AAU
Information	The project aims at theoretical and experimental investigation of activation energy of hardening high-performance concrete. Temperature dependence of the puzzolanic reaction is studied using a newly developed measuring technique.
e-mail	I6pas@civil.auc.dk

Project:	**Water-Entrained High-Performance Concrete**
Project period	October 2000 – October 2003
Project type & financial support	University Ph.D.
Ph. D. Student	Thomas Østergaard
Supervisors	Prof. Per Freiesleben Hansen /AAU
Information	The project aims at theoretical and experimental investigation of mechanical, hardening and shrinkage properties of water-entrained cement based materials.
e-mail	i6to@civil.auc.dk

Technical University of Denmark - DTU
Department of Civil Engineering
Building 118 – Brovej
DK – 2800 Lyngby

Project: **Durability of Concrete Produced from White Portland Cement subjected to Chemical Attack**

Project period	July 201 – June 2004
Project type & financial support	Ph.D. Aalborg Portland A/S
Ph. D. Student	Erik Pram Nielsen
Supervisors	Chiefgeologist Duncan Herfort / Aalborg Portland & Ass. Prof., Ph.D. Mette Geiker / BYG.DTU
Information	The aim of the project is to develop a model that predicts the combined transport of chloride and sulfate ions in concrete produced from Portland cement (with special emphasis on White Portland cement). The transport rate of ions in solution will be derived from the resulting microstructure of the mix based on its physical microstructure, e.g. porosity, pore size distribution, etc. The interaction of ions with the solid phases in the paste will be modelled from a physical and mineralogical point of view and therefore require a thorough investigation of the chloride binding capacity of the AFm phases and any adsorption on the surfaces of the gel pores.
e-mail	epn@aalborg-portland.dk

Project: **Rheology of Self Compacting Concrete**

Project period	2001 – 2004
Project type & financial support	Industrial Ph.D. Danish Academy of Technical Sciences & Danish Technological Institute
Ph. D. Student	Lars Nyholm Thrane
Supervisors	Head of Section, Ph.D. Mette Glavind / Danish Technological Institute, Concrete Centre & Ass. Prof. Ph.D. Mette R. Geiker / BYG.DTU Ass. Prof. Ph.D. Henrik Stang / BYG.DTU Ass. Prof. Ph.D. Peter Szabo / KT Concrete Technologist. Jørgen Feldborg Skaarup / 4K-Beton
Information	
e-mail	Lars.nyholm.thrane@teknologisk.dk & c961021@student.dtu.dk

Project: **Instability of masonry and concrete walls**

Project period	
Project type & financial support	Industrial Ph.D. Danish Academy of Technical Sciences & ???
Ph. D. Student	Lars Z. Hansen
Supervisors	Project manager, Ph.D. Bent Steen Andreasen & Professor Dr. Techn. Mogens Peter Nielsen
Information	The aim of the project is to develop a new theory to calculate the load carrying capacity of masonry and concrete walls, which fail due to instability. The main goal is to find an estimate of the deformation at the peak load, which is safe. When the deformation at the peak load is known an analysis using the theory of plasticity is possible. The theory will be compared with experiments.
e-mail	Lzh@byg.dtu.dk

Project:	**Crack Formation in Concrete Structures during the Hardening Phase**
Project period	Sept. 1999 – Sept. 2002
Project type & financial support	University Ph.D.
Ph. D. Student	Lennart Østergaard
Supervisors	Ass. Prof. Henrik Stang / BYG.DTU, Ass. Prof. Lars Damkilde / BYG.DTU & Ass. Prof. David Lange / UIUC
Information	Mechanisms governing the crack formation in an early stage are investigated, and experimental results together with mathematical modelling are used to predict the risk of cracking at early age.
e-mail	los@byg.dtu.dk

Project:	**2'd order theory of plastcity**
Project period	April 2001 – april 2004
Project type & financial support	University Ph.D.
Ph. D. Student	Tim Gudmand-Høyer
Supervisors	Project manager, Ph.D. Bent Steen Andreasen & Professor Dr. Techn. Mogens Peter Nielsen
Information	The aim of the project is to develop a new theory to calculate the load carrying capacity of concrete walls, including axial forces. The main goal is to find an estimate of the deformation at the peak load. When the deformation at the peak load is known an analysis using the theory of plasticity is possible. The theory will be compared with experiments.
e-mail	TimGH@get2net.dk

Technical University of Denmark - DTU
Department of Environment & Ressources
Building 115 – Bygningstorvet
DK – 2800 Lyngby

Project:	**Life cycle assessment of road construction and reuse of residues from solid waste incineration**
Project period	October 2001 – September 2004
Project type & financial support	University Ph.D. Financial support from Amagerforbrænding I/S; Vestforbrænding I/S; Vejteknisk Institut; Aalborg Portland A/S & DTU
Ph. D. Student	Harpa Birgisdottir
Supervisors	Prof. Thomas H. Christensen & Ass. Prof. Michael Hauschild
Information	The aim of the project is to develop a LCA model for road construction including the use of residues from solid waste incinerators as substitute for virgin material. This also includes the use of incineration residues in concrete used for road construction. The LCA deals with the use of resources, energy and emissions associated with the exploitation of natural resources, manufacturing of materials, construction of different kinds of roads, maintenance and demolition of roads. With respect to the waste incineration residues (bottom ash, stabilised fly ashes and air-pollution-control residues) the same issues are dealt with in relation to upgrading of materials and changes in construction and maintenance. Also the environmental savings in avoiding landfilling of the residues are considered.
e-mail	hab@er.dtu.dk

University of Copenhagen - KU
Geologisk Institut
Øster Voldgade 10
DK – 1350 Copenhagen K

Project: **Mineralogical and thermodynamic processes by sulphate and seawater attack on Danish concrete**

Project period	August 1999 – July 2002
Project type & financial support	Industrial Ph.D. Danish Academy of Technical Sciences & Aalborg Portland A/S
Ph. D. Student	Iver A. Juel
Supervisors	Chief geologist Duncan Herfort / Aalborg Portland & Ass. Prof. Jens Konnerup-Madsen / KU & Niels Thaulow / R.J. Lee, USA
Information	The project seeks to establish a better understanding of the long-term properties of concrete in sulphate and seawater environments. A model based on fundamental mineralogical and thermodynamic principles is developed. The model describes the durability of concrete in sulphate and chloride containing environments. The model is tested on concrete samples and laboratory made paste specimens.
e-mail	Iaj@aalborg-portland.dk

University of Aarhus - ÅU
Instrument Centre for Solid-State NMR Spectroscopy
Department of Chemistry
Langelandsgade 140
DK – 8000 Århus

Project: **Structural, quantitative and kinetic investigations of Portland cement components and hydration reactions using solid-state NMR spectroscopy**

Project period	September 2000 – August 2004
Project type & financial support	University Ph. D. The Danish Research Councils: Materials Research Programme
Ph. D. Student	Morten Daugaard Andersen
Supervisors	Dr. Jørgen Skibsted (ÅU) and Prof. Hans J. Jakobsen (ÅU)
Information	Solid-state NMR spectroscopy has become an important tool in characterization of the hydration reactions of cement-based materials. The aim of the project is to develop new methods in solid-state NMR to obtain improved structural and quantitative information about cementitious materials. These methods will be employed in studies of the aluminate (AFm) phases in Portland cements and in variable-temperature NMR investigations of the phase transitions that occur for some of these phases (e.g. Friedels salt). Furthermore, solid-state ^{29}Si and ^{27}Al NMR will be utilized in a number of structural and kinetic investigations of the hydration reactions for the calcium silicate and aluminate phases of Portland cements employing different admixtures.
e-mail	mad@chem.au.dk

Project: **Structural investigations of clay minerals and new concretes obtained by addition of layered silicates**

Project period	September 2000 – August 2004
Project type & financial support	University Ph. D. The Danish Research Councils: Materials Research Programme
Ph. D. Student	Hanne Krøyer
Supervisors	Dr. Jørgen Skibsted, (ÅU) Prof. Hans J. Jakobsen (ÅU), and Dr. Holger Lindgreen (GEUS, Copenhagen).
Information	The principal aim of the project is to characterize the hydrational effects by addition of clay minerals to Portland cement. This includes solid-state NMR studies of the hydration kinetics for the calcium silicate and aluminate phases of Portland cements in the absence/presence of clay materials. This information will be combined with the results from powder X-ray diffraction (XRD) and microscopy methods as well as the results from a number of physical measurements on similar concretes. The project will also include fundamental structural investigations of some layered materials, employing a combination of NMR and XRD, and studies of the basic relationships between NMR parameters and structural data.
e-mail	kroyer@chem.au.dk

FINLAND

Tampere University of Technology – TUT
P.O. Box 600
FIN – 33101 Tampere

Project:	**Service life of cement-based patch repairs in concrete facades and balconies**
Project period	1998 - 2001
Project type & financial support	Industrial project, funding by Tekes (Government), Akademy of Finland as well as several private companies.
Ph. D. Student	Mr. Jussi Mattila, lic.tech.
Supervisors	Prof. Ralf Lindberg
Information	The durability of cement-based patch repairs is studied experimentally from the viewpoint of carbonation induced corrosion. The project is a part of COST 521
e-mail	Jussi.mattila@tut.fi

Helsinki University of Technology - HUT
Department of Civil and Environmental Engineering
P.O. Box 2100
FIN – 02015 HUT

Project:	**Coatings for rapid construction work and their emissions**
Project period	01.01.2002 – 31.12.2003
Project type & financial support	The financial support is not yet approved.
Ph. D. Student	M. Sc. Leif Wirtanen
Supervisors	Prof. Vesa Penttala / HUT
Information	The aim of the research project is to clarify the chemical emissions from building materials in rapid construction work i.e. rapid curing materials. The moisture and emission characteristics of rapid curing coatings (plasters, levelling agents, adhesives, and paints) are the target of this study. The interactions between coatings and substrates, the influence of moisture on these interactions, and the emitted compounds subjected to different moisture loads will thus be clarified. Determining the correlation between pore structure, relative humidity, pH and emitting compounds of the different materials and material combinations during a moisture load will carry this out. The moisture induced physical and chemical changes in the materials will also be clarified.
e-mail	leif.wirtanen@hut.fi

Project:	**Effects of ageing processes and frost attack on the microstructure and durability of High Performance Silica Fume Concrete**
Project period	2001 - 2004
Project type & financial support	Part of the EU-CONLIFE research project “Life-time prediction of High - Performance Concrete with respect to durability”
Ph. D. Student	M. Sc. Andrzej Cwirzen
Supervisors	Prof. Vesa Penttala / HUT
Information	The aim of the research project is to define the influence of the ageing processes and freezing - thawing cycles on the microstructure and durability of High Performance Silica Fume Concrete. The mixes differ in the w/c ratio, silica fume and air content. Ageing is realised by storing the samples for the period of 12 months in laboratory and field conditions. The frost attack is simulated by repeated freezing - thawing cycles following CIF/CDF and “Slab test” procedures as well as exposure of the specimens to the natural arctic conditions of Northern Finland. Freezing - thawing tests will be done with both non-aged and aged concrete.
e-mail	Cwirzen@rakserver.hut.fi

Åbo Akademi University - ÅAU
Domkyrktorget 3
FIN – 20500 Åbo

Project:	**Behaviour of granular materials under shear and pressure**
Project period	1998-2000
Project type & financial support	Government (TEKES) and private companies
Ph. D. Student	Erik Nordenswan
Supervisors	Prof. Jarl B. Rosenholm / ÅAU
Information	Research applies to compaction of no-slump concrete. The studies are not completed.
e-mail	Erik.nordenswan@addtek.com

Project:	**Alternative fuels / The impact of alternative fuels on the clinker production**
Project period	1998 - 2002
Project type & financial support	Scancem Doctor of Engineering Programme
Ph. D. Student	Ursula Kääntee
Supervisors	Prof. Mikko Hupa / ÅAU & Bo-Erik Eriksson / Cement Nordic AB Karl-Erik Nyman / Finnsementti Oy
Information	The clinker manufacturing process is modelled with kiln and pre-heater systems. The model is used to predict possible impacts and changes that different alternative fuels might have on the combustion and clinker formation processes.
e-mail	Ursula.Kaantee@Finnsementti.fi

SWEDEN

Royal Institute of Technology (KTH)
Department of Structural Engineering
Structural Design and Bridges
SE-100 44 Stockholm

Project: **The Design and Structural Behaviour of Concrete Block Pavements**

Project period	1997 – 2003
Project type & financial support	Ph.D. Project. Swedish Agency for Innovation Systems, Cementa, Swedish Concrete Block Paving Association (Cementa, Skanska Prefab, Starka, Swerock), and KTH.
Ph. D. Student	Mr. Mattias Wäppling, M.Sc., Lic. Tech.
Supervisors	Prof. Johan Silfwerbrand
Information	Licentiate Thesis: February 2001. The aim is to develop new knowledge on the structural behaviour of concrete block pavements and to develop improved functional properties and refined design methods. Measurements on concrete block pavements in Göteborg and Malmö as well as a test pavement in Uppsala are used as imput to the project.
e-mail	Mattias.waeppling@struct.kth.se

Project: **Functional Properties of Concrete Roads**

Project period	1997 - 2003
Project type & financial support	Ph.D. Project. Swedish Agency for Innovation Systems, Cementa, and KTH.
Ph. D. Student	Ms. Malin Löfsjögård, M.Sc., Lic. Tech.
Supervisors	Prof. Johan Silfwerbrand (assisting: Mr. Örjan Petersson, M.Sc., Lic. Tech., CBI)
Information	Licentiate Thesis: May 2000. The aim is to investigate, analyse, and quantify relationships between the properties of the concrete pavement and social factors such as environment, economy, traffic safety, road user comfort, and economy. The goal is to establish a model that can be used to optimise the designing and composition of the concrete pavement in order to obtain maximum possible benefit for society.
e-mail	Malin.lofsjogard@cbi.se

Project: **Integrated Design and Construction of Industrial Floors**

Project period	2001 - 2004
Project type & financial support	Ph.D. Project. The Development Fund of the Swedish Construction Industry through the contractor NCC.
Ph. D. Student	Mr. Jerry Hedebratt, M.Sc.
Supervisors	Prof. Johan Silfwerbrand
Information	The aim of the project is to develop the construction process of industrial floors further. The goal is to establish integration from design to construction. Within the project, methods for improved co-operation between selection of structural type, design, detailing, construction, quality control, and feedback will be developed. The project covers both plain and reinforced concrete floors.
e-mail	Jerry.hedebratt@struct.kth.se

Project:	**Lifetime Issues Concerning Prestressing Steel in Concrete Structures**
Project period	2001 - 2004
Project type & financial support	Ph.D. Project. The Swedish Nuclear Watchdog.
Ph. D. Student	Mr. Thomas Roth, M.Sc.
Supervisors	Prof. Johan Silfwerbrand (assisting: Prof. Håkan Sundquist, KTH)
Information	The aim of the project is to develop new knowledge of these problems both generally and specifically concerning Swedish nuclear power stations. The project covers both bonded and unbonded prestressing steel.
e-mail	Thomas.roth@struct.kth.se

Project:	**Design and Construction of Concrete Bridges without Ordinary Reinforcement**
Project period	1997 - 2003
Project type & financial support	Ph.D. Project. Swedish Agency for Innovation Systems, Skanska, and KTH.
Ph. D. Student	Mr. Lütfi Ay, M.Sc., Lic. Tech.
Supervisors	Prof. Håkan Sundquist (assisting: Prof. Johan Silfwerbrand)
Information	Licentiate Thesis: 2000. The aim is to develop concrete bridges in which steel fibres and prestressing completely replace conventional reinforcement. A major part of the work deals with high performance steel fibre reinforced concrete.
e-mail	Lutfi.ay@struct.kth.se

Project:	**Remaining Structural Life of Railway Bridges**
Project period	1997 - 2003
Project type & financial support	Ph.D. Project. The Swedish National Rail Administration and KTH.
Ph. D. Student	Ms. Ulrika Johansson, M.Sc.
Supervisors	Prof. Håkan Sundquist (Assisting: Prof. Johan Silfwerbrand)
Information	The aim is to study the remaining load carrying capacity of concrete bridges primarily subjected to fatigue.
e-mail	Ulrika.johansson@struct.kth.se

Project:	**Punching Shear Capacity of Column Supported Flat Slabs**
Project period	2001 - 2004
Project type & financial support	Ph.D. Project. The Development Fund of the Swedish Construction Industry and KTH.
Ph. D. Student	Mr. Ghassem Hassanzadeh, M.Sc., Lic. Tech.
Supervisors	Prof. Håkan Sundquist
Information	Licentiate Thesis: 1998. The aim is to study the punching shear capacity of column supported flat reinforced concrete slabs. Some interesting topics are investigated, e.g., strengthening of existing slab-column connections, effects of varying the location of prestressing cables, and use of steel fibres.
e-mail	Ghassem.hassanzadeh@struct.kth.se

Royal Institute of Technology (KTH)
Department of Structural Engineering
Concrete Structures
SE-100 44 Stockholm

Project:	**Load carrying capacity of steel fibre reinforced shotcrete**
Project period	1998 - 2002
Project type & financial support	Swedish Rock Engineering Research, Swedish National Rail Administration, Swedish National Road Administration, The Development Fund of the Swedish Construction Industry through the contractor Besab
Ph.D. student	Mr Ulf Nilsson, MSc, LicTech
Supervisor	Prof. Jonas Holmgren
Information	www.struct.kth.se/research/concrete/ulfn_design.htm
e-mail	ulf.nilsson@struct.kth.se

Project:	**Repair and strengthening of concrete structures with advanced, cement based fibre composites**
Project period	1998 - 2002
Project type & financial support	Swedish National Rail Administration, Swedish National Road Administration, Cementa, Tyréns
Ph.D. student	Mr Anders Wiberg, MSc, LicTech
Supervisor	Prof. Jonas Holmgren (assisting: Prof. Åke Skarendahl)
Information	www.struct.kth.se/research/concrete/anwi_upgrading%20.htm
e-mail	anders.wiberg@struct.kth.se

Project:	**Design of structural elements of reinforced foam concrete**
Project period	1998 - 2003
Project type & financial support	KTH
Ph.D. student	Mr Daniel Masanja, MSc
Supervisor	Prof. Jonas Holmgren
Information	www.struct.kth.se/research/concrete/damas_design.htm
e-mail	daniel.masanja@struct.kth.se

Project:	**Self compacting concrete**
Project period	2002 - 2003
Project type & financial support	Cement and Concrete Institute
Ph.D. student	Mr Peter Billberg, MSc, LicTech
Supervisor	Prof. Jonas Holmgren (assisting: Prof. Åke Skarendahl)
Information	Studies of the tixotropy of self compacting concrete
e-mail	peter.billberg@cbi.se

Project:	**Interaction between existing concrete structures and repair materials.**
Project period	2002 - 2004
Project type & financial support	Cement and Concrete Institute
Ph.D. student	Mr Pål Skoglund, MSc
Supervisor	Prof. Jonas Holmgren (assisting: Prof. Åke Skarendahl)
Information	Studies of transport mechanisms at the interface of existing concrete and repair materials
e-mail	pal.skoglund@cbi.se

Project:	**Protection structures in high strength concrete and rock subjected to weapon effects**
Project period	2001 - 2005
Project type & financial support	The Swedish Defence, The Swedish Defence Research Agency (FOI)
Ph.D. student	Mr Johan Magnusson, MSc
Supervisor	Prof. Jonas Holmgren
Information	Studies of the design of protection structures with special reference to the development of weapons and materials
e-mail	jomag@foi.se

Project:	**Protection structures in concrete subjected to weapon effects**
Project period	2001 - 2005
Project type & financial support	The Swedish Defence, Sycon
Ph.D. student	Ms Sofia Belin, MSc
Supervisor	Prof. Jonas Holmgren
Information	Studies of the design of protection structures with special reference to the development of weapons and materials
e-mail	sofia.belin@sycon.se

Chalmers University of Technology - CTH
Division of Building Materials
SE – 412 96 Gothenburg

Project: **Mechanical properties of concrete sleepers**

Project period	2000 – 2002
Project type & financial support	Scancem Doctor of Engineering Programme CHARMEC (Chalmers Railway Mechanics)
Ph. D. Student	Tekn lic Rikard Gustavson
Supervisors	Prof. Kent Gylltoft
Information	In railway traffic, new demands for increased speed and comfort as well as axle load are constantly put forward. This in turn increases the demands on the track structure concerning load carrying capacity, stability etc. New concrete products for railway tracks for ordinary- and especially high speed traffic are requested. The development requires methods and models for detailed and accurate analyses. The mechanical properties of a prestressed concrete sleeper is to a large extent dependent on the bond between the prestressed strands and the concrete. A numerical model of the strand-concrete interface is developed and calibrated by use of results from experimental tests.
e-mail	Ricard.gustavson@ste.chalmers.se

Project: **Composite structures – Confined Concrete**

Project period	1998 – 2002
Project type & financial support	Doctorand FORMAS (The Swedish Research Council for Environment, agricultural sciences and Spatial Planning), SBUF (the Development Fund of the Swedish Construction Industry)
Ph. D. Student	Tekn lic. Mathias Johansson
Supervisors	Prof. Kent Gylltoft
Information	The aim of this study is to increase the knowledge of the structural behaviour of composite columns consisting of circular hollow steel sections filled with concrete. The main topics of interest are to study how the structural behaviour of the column is influenced by: the bond strength between the steel tube and the concrete core; the increased concrete compressive strength due to confinement; and various means of load application to the column..
e-mail	Mathias.johansson@ste.chalmers.se

Project:	**Industrial bridge construction**
Project period	1999 – 2003
Project type & financial support	Infrastrukturprogrammet Väg Bro Tunnel NUTEK (the Swedish National Board for Industrial and Technical Development)
Ph. D. Student	Civ ing Peter Harryson
Supervisors	Prof. Kent Gylltoft
Information	Development of new techniques and methods in bridge construction has not been very progressive in Sweden over the last decades; present building codes for bridges do not encourage such a development. Bridges in Sweden are often cast in-situ, involving a massive use of manpower and many techniques that can be described as more or less crafts manlike; for example pre-cast concrete elements are not used very often. The aim is, proceeding from today's conventional bridge construction, to provide techniques, design methods and construction methods in order to develop a more industrial building process for bridge construction.
e-mail	Peter.harryson@ste.chalmers.se

Project:	**Structural Concrete Systems – New concepts for in-situ concrete construction**
Project period	1999 – 2003
Project type & financial support	Doctorand Thomas Concrete Group AB
Ph. D. Student	Civ ing Ingemar Löfgren
Supervisors	Prof. Kent Gylltoft
Information	The aim is to develop innovative structural building systems for buildings, allowing for a more industrialised and cost-effective production process. The project will be focused on in-situ cast concrete apartment- and office buildings. The intention is to consider structural aspects of concrete structures, such as load-carrying capacity, stability, flexibility, fire protection etc, and to some extent handle human oriented aspects such as architecture, comfort, climate conditions, acoustics etc.
e-mail	Ingemar.lofgren@ste.chalmers.se

Project:	**Dynamic behaviour of concrete structures subjected to blast and fragments**
Project period	2000 – 2004
Project type & financial support	Doctorand Statens Räddingsverk (the Swedish Rescue Service)
Ph. D. Student	Civ ing Joosef Leppänen
Supervisors	Prof. Kent Gylltoft
Information	A new reinforcement detailing, using spliced reinforcement loops within the frame corners have been introduced in civil defence shelters. Static tests and analyses have shown that the construction will have a ductile behaviour and good load bearing capacity. The aim for the project is that the effects of the splinter and heat can be taken into account in the analysis of the civil defence shelter subjected to an explosion.
e-mail	Joosef.leppanen@ste.chalmers.se

Project:	**Fracture mechanics for concrete structures – compression modelling**
Project period	2000 – 2004
Project type & financial support	Doctorand FORMAS (the Swedish Research Council for Environment, Agricultural Sciences and Spatial Planning), Stiftelsen Svensk Betongforskning (the Foundation of Swedish Concrete Research)
Ph. D. Student	Civ ing Peter Grassl
Supervisors	Prof. Kent Gylltoft & Tekn. Dr. Karin Lundgren
Information	In earlier projects at the Division of Concrete Structures two failure modes of concrete structures were treated, i.e. tensile and bond failure. In this project the third basic failure mode will be studied: compressive failure in concrete. The aim of the project is to develop a model that takes into account the localisation of the compressive failure and describes the influence of a tri-axial stress state in a reasonable way.
e-mail	Peter.grassl@ste.chalmers.se

Project:	**Dynamically loaded concrete structures – measurement and analysis of response**
Project period	2001 – 2005
Project type & financial support	Infrastrukturprogrammet Väg Bro Tunnel NUTEK (the Swedish National Board for Industrial and Technical Development), Skanska
Ph. D. Student	Civ ing Per-Ola Svahn
Supervisors	Prof. Kent Gylltoft & Prof. Kennet Axelsson
Information	The load capacity of driven concrete piles have been utilized more and more efficient for static loads during the last decades. Hence the phase of installation has been even more critical. The reinforced concrete element is subjected with transient loads at a high stress level. Splitting failure will sometimes cause big damage and interaction with surrounding water will under certain circumstances decrease the capacity significant.
e-mail	Per-ola.svahn@ing.hj.se

Project:	**Environmental assessment of cement and concrete**
Project period	1998 – 2004
Project type & financial support	Industrial Ph.D. project. Scancem Doctor of Engineering Programme
Ph. D. Student	Karin Gäbel
Supervisors	Prof. Anne-Marie Tillmann / Chalmers
Information	The project aims at building up a computer-based simulation LCI model of Cementa’s plants, including local environment impact. The model is to be limited to the ”craddle to gate” part of the process, i.e. the raw materials used in production will be traced upstream to the point at which they are removed as a natural resource, but the products will not be traced downstream, to the building processes, use and demolition.
e-mail	Karin.gabel@cementa.se

Project:	**Mechanism and chemistry of modern rendering systems based on mineral binders modified by different admixtures as organic resins and fibres**
Project period	2001 - 2006
Project type & financial support	Ph.D project Scancem Doctor of Engineering Programme
Ph. D. Student	Carl-Magnus Capener
Supervisors	Prof. Lars-Olof Nilsson & Dr. Jadwiga Palicka / Optiroc Group AB
Information	The aim of the project is to clarify the relationships between the composition and substrate on one hand and the hardening process, structure, properties and their influence on frost resistance on the other hand. The study will be concentrated on the interaction between the chemistry of the hardening process, the received macro and microstructure and various water and moisture transfer properties. Among the decisive properties of the hardened renders the focus will be kept on moisture permeability.
e-mail	capener@bm.chalmers.se

Project:	**Probabilistic Service Life Design of Concrete Structures**. **Environmental Actions and Response**
Project period	1998 - 2004
Project type & financial support	PhD-project Funding from the Swedish Research Council for Environment, Agricultural Sciences and Spatial Planning
Ph. D. Student	Lic. Techn. Anders Lindvall
Supervisors	Prof. Lars-Olof Nilsson
Information	Tools for probabilistic service life design are lacking precise input data for material properties and environmental actions. The project aims at quantifying and model the interaction between the regional, local and surface climate around a concrete structure and the environmental response by concrete surfaces. The focus is reinforcement corrosion and environmental actions on marine structures and structures exposed to de-icing salts.
e-mail	Lindvall@bm.chalmers.se

Project:	**Rheology of Fresh Concrete with Mineral Additions**
Project period	March 2001-February 2006
Project type & financial support	PhD project Thomas Concrete Group AB
Ph. D. Student	MSc Eng. Oskar Esping
Supervisors	Prof. Lars-Olof Nilsson & Ass. Prof Per-Erik Petersson, SP
Information	The aim of this project is to increase the knowledge of how properties and composition of the admixtures are connected to the rheology of fresh concrete. The focus is on fresh self-compacting concrete for buildings. Combines of, in Sweden normally used, cement, filler and aggregates together with a plasticizer are to be used. The effect of mineral fillers, both as naturals and industrial by-products, on the workability is of special interest.
e-mail	Espring@bm.chalmers.se

Lund technical University - LTH
Division of Building Materials
P.O. Box 118
S – 221 00 Lund

Project:	**Influence of ageing on the frost resistance of concrete**
Project period	1996-2002
Project type & financial support	Ph.D-projekt
Ph. D. Student	Civ. Eng. Peter Utgenannt
Supervisors	Prof. Göran Fagerlund, adj. Prof. Per-Erik Petersson
Information	The aim of the project is to study the influence ofe ageing effects on the durability of concrete. Carbonation is of special interest. An important part of the project deals with field exposure in marine environment and environments exposed to de-icing salt.
e-mail	Peter.utgenannt@sp.se

Project:	**Industrial waste materials and filler in concrete: Early strength development, especially for winter conditions**
Project period	2000-2003
Project type & financial support	Ph.D-projekt
Ph. D. Student	Civ. Eng., Monica Lundgren
Supervisors	Prof. Göran Fagerlund, adj Prof Per-Erik Petersson
Information	The aim is to study how the use of industril waste materials (blast furnace slag, fly ash, silica fume) and filler influences the earky strengt development under winter conditions. The project is mainly based on laboratory studies.
e-mail	Monica.lundgren@sp.se

Project:	**Industrial waste materials and filler in concrete: Influence on long term properties/durability**
Project period	2000-2005
Project type & financial support	Ph.D-projekt
Ph. D. Student	Civ. Eng., Dimitios Boubitsas
Supervisors	Prof. Göran Fagerlund, adj Prof Per-Erik Petersson
Information	The aim of the project is to study how the use of industrial waste materials (blast furnace slag, fly ash, silica fume) and filler influences the long term properties and durability of reinforced concrete. The project will mainly be based on laboratory studies but field exposure will be an important part of the project as well.
e-mail	Dimitrios.boubitsas@byggtek.lth.se

Project:	**Internal frost damage of concrete**
Project period	1997 - 2002
Project type & financial support	Ph.D. Financed 50% by industry (Cementa AB) and 50% by government (Vinnova)
Ph. D. Student	Katja Fridh
Supervisors	Prof. Göran Fagerlund
Information	The aim of this PhD-project is to explain the mechanism of internal frost damage in concrete. The methods used are length-change measurements and ice-formation measurements both separately and combined. The climate is varied both externally (freezing rate, duration and lowest temperature) and internally (degree of saturation) during studies of the response in length-change and ice formation.
e-mail	katja.fridh@byggtek.lth.se

Project:	**The Optimal Concrete Building**
Project period	2000 – 2004 (with licentiate thesis in 2002)
Project type & financial support	Industry doctoral project associated to the national Swedish reseach programme’Competitive Building’. Financial support from the Swedish Foundation for Strategic Research (SSF) and Cementa AB.
Ph. D. Student	Mats Öberg
Supervisors	Prof. Göran Fagerlund, dep. of Building Materials, Lund University
Information	The aim of the project is to practise integrated life cycle design (’ILCD’) on a concrete multi-family dwelling building under Swedish conditions to examine how the long term performance (economy, function, ecology…) can be predicted and optimised from priorities given in the specific project. By doing this it is expected that the overall functional quality of the building over the entire life cycle can be enhanced and that the inherent qualities of concrete as a building material can be exposed and exploited.
e-mail	mats.oberg@cementa.se

Project:	**Non-shrinking inorganic binder systems**
Project period	1997 - 2002
Project type & financial support	Scancem Doctor of Engineering Programme
Ph. D. Student	Cecilie Evju
Supervisors	Prof. Jan-Olov Bovin + doc. Staffan Hansen / Materials Chemistry, LTH & Rainer Ålgars / Optiroc Group AB
Information	Characterisation of early hydration of special binder systems forming ettringite. Emphasis on phase formation and volume stability during hardening. Techniques: synchrotron radiation and isothermal calorimetry. Study the influence of sulfate source on the ettringite formation and the influence of accelerators and retarders.
e-mail	Cecilie.Evju@materialkemi.lth.se

Project:	**Chemical emissions from concrete**
Project period	1998 – 2003
Project type & financial support	Fil. Dr.
Ph. D. Student	Tina Hjellström
Supervisors	Lars Wadsö / LTH
Information	In this project the aim is to collect knowledge about emissions from building materials, both what comes out and potential emissions. The focus is on transport in and emissions of volatile organic compounds from concrete. The first part in the project is to try different methods and proceedings for conditioning, sampling and detection of volatile organic compounds, formaldehyde and ammonia. The second part deals with the study of emissions from concrete. In this part the factors are additives, aggregates, fillers, form-oil, water to cement ratio, temperature and humidity. Also potential contributors like grinding aids and fillers in cement will be studied.
e-mail	Tina.hjellstrom@research.scancem.com

Luleå University of Technology - LTU
Division of Structural Engineering
S – 971 87 Luleå

Project:	**Hardening Technology: Self-compacting concrete**
Project period	1999 - 2004
Project type & financial support	Ph.D.
Ph. D. Student	Sofia Utsi
Supervisors	Jan-Erik Jonasson, Mats Emborg, Lennart Elfgren, LTU
Information	Hardening technology and rheology of self-compacting concrete is studied. The effect of different types of aggregate, cement content, admixtures and filler contents is tested with a viscometer. The results are intended to give a useful and reliable test method that is adjustable for testing in the field. The influences of restraint stresses as a result of temperature and creep are important parts of the project.
e-mail	Sofia.Utsi@ce.luth.se

Project::	**Strengthening of Concrete Structures with Prestressed Reinforcement**
Project period	1998 - 2003
Project type & financial support	Ph.D.
Ph. D. Student	Håkan Nordin
Supervisors	Björn Täljsten, Skanska/LTU; Thomas Olofsson, L Elfgren, LTU
Information	Carbon Fibre Reinforced Polymers, CFRP, are used to strengthen concrete structures. The possibility to use prestressed CFRP are studied.
e-mail	Hakan.Nordin@ce.luth.se

Project:	**Monitoring of Structures**
Project period	2001 - 2005
Project type & financial support	Ph.D.
Ph. D. Student	Arvid Hejll
Supervisors	Thomas Olofsson, LTU; Björn Täljsten, Skanska/LTU; Lennart Elfgren, LTU
Information	Methods to monitor deformations in structures will be investigated in order to form a basis for assessment and maintenance programs.
e-mail	Arvid.Hejll@ce.luth.se

Project:	**Hardening Technology. Structural Modelling. User-friendly methods.**
Project period	1998 - 2003
Project type & financial support	Ph.D.
Ph. D. Student	Mårten Larsson
Supervisors	Jan-Erik Jonasson, Mats Emborg, Lennart Elfgren, LTU
Information	An understanding of how different types of cracks arise will give a direct base to propose possible measures to be taken and it will also give a rational background to the estimation of the risk of early cracking. The following areas are treated: I. Modelling of crucial material properties for a thermal stress analysis. II. Improvement of simplified methods for thermal crack estimation. III. Formulation of a simplified method for practical use. IV. Comparison of results from a simplified method formulated for practical use with results from full-scale field observations. In 2000 Mårten Larsson presented a Techn. licentiate thesis summarising the results up to now: Estimation of Crack Risk in Early Age Concrete. Simplified Methods for Practical Use, Division of Structural Engineering, Luleå University of Technology, April 2000, 170 pp
e-mail	Marten.Larsson@ncc.se

Project:	**Steel Fibre Reinforced Self Compacting Concrete as a base for a more industrialised construction**
Project period	1998 - 2003
Project type & financial support	Ph.D.
Ph. D. Student	Jonas Carlswärd
Supervisors	Mats Emborg, Jan-Erik Jonasson, Lennart Elfgren, LTU
Information	The project comprises studies on steel fibre reinforced and self-compacting concrete both from a design as well as a production point of view. Basically, this means that part of the work aims at establishing test and design methods for typical applications of the new material while another part deals with rheological aspects, i.e. studies on the fresh concrete properties. Also, as the material is presently used at a regular basis the project also involves full-scale studies and follow-ups.
e-mail	Jonas.Carlswärd@ce.luth.se

Project:	**Steel Fibre Reinforced Sprayed Concrete. Corrosion and Durability**
Project period	1998 - 2003
Project type & financial support	Ph.D.
Ph. D. Student	Erik Nordström
Supervisors	Lennart Elfgren, LTU; Jan Alemo, Vattenfall
Information	An extensive series of field tests are carried out on steel fibre reinforced sprayed concrete, SFRSC, in three environments: in a river; close to a high way; in an urban tunnel. Crack widths and corrosion rates are studied and modelled. In 2000 Erik Nordström presented a Techn. licentiate thesis summarising the results up to now: *Steel Fibre Corrosion in Cracks. Durability of Sprayed Concrete. Licentiate Thesis 2000:49, Division of Structural Engineering, Luleå University of Technology, December 2000, 103 pp.*
e-mail	Erik.Nordstrom@vuab.se

Project:	**Strengthening of Concrete Structures**
Project period	1998 - 2003
Project type & financial support	Ph.D.
Ph. D. Student	Anders Carolin
Supervisors	Björn Täljsten, Skanska/LTU, Lennart Elfgren, LTU
Information	Design and analysis of strengthening methods are studied. In 2001 Anders Carolin presented a Techn. licentiate thesis summarising the results up to now: *Strengthening of Concrete Structures with CFRP. Field tests and Shear Strengthening. Licentiate Thesis 2001:01, Division of Structural Engineering, Luleå University of Technology, June 200.*
e-mail	Anders.Carolin@ce.luth.se

Project:	**Hardening Technology. Influence of Restraint**
Project period	1998 - 2003
Project type & financial support	Ph.D.
Ph. D. Student	Martin Nilsson
Supervisors	Jan-Erik Jonasson, Mats Emborg, Lennart Elfgren
Information	The influence is studied of what kind of restraint a slab gives to a wall which is casted on top of the slab. Cracking, shrinkage and creep are studierd and modelled for young concrete. Probabilistic methods are applied. In 2000 Martin Nilsson presented a Techn. licentiate thesis summarising the results up till now: *Thermal cracking of young concrete. Partial coefficients, restraint effects and influences of casting joints. Licentiate Thesis 2000:27, Division of Structural Engineering, Luleå University of Technology, October 2000, 267 pp.*
e-mail	Martin.Nilsson@ce.luth.se

Project:	**Evaluation of Concrete Structures: Strength Development and Fatigue Capacity**
Project period	1998 - 2003
Project type & financial support	Ph.D.
Ph. D. Student	Håkan Thun
Supervisors	Ulf Ohlsson, Lennart Elfgren
Information	The project can be divided into two parts: (1) Create realistic refined methods to calculate the concrete fatigue capacity. Present codes are conservative. Recent work shows a great potential. At present a hypothesis regarding strain and energy is studied as an alternative to the classic Wöhler method with stress variations. (2) Develop better criteria and basis for evaluation of actual concrete strength in existing structures.
e-mail	Hakan.Thun@ce.luth.se

NORWAY

Norwegian University of Science and Technology - NTNU
Department of Building Materials
N – 7491 Trondheim

Project: **Condition Assessment and Service Life Management of Concrete Harbor Structures**

Project period	January 1996 – December 2001
Project type & financial support	Ph.D.
Ph. D. Student	Arne Gussiås
Supervisors	Prof. Odd E. Gjørv
Information	To develop strategies, systems and procedures that will facilitate the maintenance of concrete harbor structures both on a project level and network level.
e-mail	Argu@interconsult.no

Project: **Instrumentation and Monitoring of Steel Corrosion in Concrete Structures**

Project period	August 1998 – June 2002
Project type & financial support	Ph. D.
Ph. D. Student	Franz Pruckner
Supervisors	Prof. Odd E. Gjørv
Information	To provide more basic information about performance and reliability of various sensor systems for automatic monitoring of steel corrosion in concrete structures
e-mail	Franz.pruckner@protector-group.no

Project: **Performance of Concrete Structures Mechanically Repaired due to Steel Corrosion**

Project period	August 2002 – June 2002
Project type & financial support	Ph.D.
Ph. D. Student	Bård Arntsen
Supervisors	Prof. Odd E. Gjørv & Prof. Geir Horrigmoe
Information	To study and analyse the effiency and long-term performance of mechanical repairs due to chloride induced steel corrosion in concrete structures
e-mail	Baard.arntzen@tek.norut.no

Project: **Surface Protection of Concrete Structures**

Project period	August 2000 – June 2004
Project type & financial support	Ph.D.
Ph. D. Student	Guofei Liu
Supervisors	Prof. Odd E. Gjørv
Information	To provide more basic information on the use of surface protection of concrete structures in chloride containing environment
e-mail	Guofei.liu@bygg.ntnu.no

Project:	**Service Life of Concrete Structures and Performance-Based Quality Control**
Project period	January 2001 – December 2004
Project type & financial support	Ph.D.
Ph. D. Student	Vemund Årskog
Supervisors	Prof. Odd E. Gjørv & Prof. Bernt J. Leira
Information	To contribute to a more controlled service life of concrete structures by developing a better basis for performance-based quality control during construction
e-mail	Vemund.aarskog@hials.no

Project:	**Service Life Design of Concrete Structures in Marine Environment**
Project period	August 2001 – August 2003
Project type & financial support	Ph.D.
Ph. D. Student	Rui Miguel Ferreria
Supervisors	Prof. Said Jalali & Prof. Odd E. Gjørv
Information	To provide a better basis for implementation of probalistic-based durability design of concrete structures in marine environment
e-mail	Rmf@civil.uminho.pt

Project:	**Utilization of Ethiopian Natural Pozzolanic Materials in Concrete**
Project period	August 1998 – August 2002
Project type & financial support	Ph.D.
Ph. D. Student	Surafel Ketema Desta
Supervisors	Prof. Odd E. Gjørv & Prof. Harald Justness
Information	To investigate Ethiopian natural pozzolanic materials and to provide a better basis for the Ethiopian construction industry to utilize such materials in concrete
e-mail	Surafel.ketema@bygg.ntnu.no

Project:	**Rheological description on fresh concrete as a function of time, the multi-phase model.**
Project period	1998 – 2001
Project type & financial support	Financial support: Borregaard Ligno Tech Inc & The Norwegian Research Council
Ph. D. Student	M.Sc. Jon Elvar Wallevik
Supervisors	Prof. Erik J. Sellevold / NTNU; Prof. Fridtjov Irgens / NTNU & Sverre Smeplass /Selmer Skanska
Information	A specific material model and a mathematical approach is used in the attempt to increase the understanding of the workability and workability loos of fresh concrete. The main objective is to give rheological description of fresh concrete as a function of time (i.e. the workability and workability loss), including the role of plasticizers in this process. Major emphasis will be put on the effect of various types of lignosulfonates, as a part of developing process in the aim of increasing the workability retention with potential new products from Borregaard Ligno Tech in the near future.
e-mail	Jon.wallevik@bygg.ntnu.no

Project:	Temperature effects on corrosion processes related to concrete reinforcement
Project period	2001 – 2005
Project type & financial support	Financial support: Norwegian Public Roads Administration & Norwegian Research Council
Ph. D. Student	Jan-Magnus Østvik Jr.
Supervisors	Prof. Øystein Vennesland / NTNU & Dr. Ing. Claus Kenneth Larsen
Information	Corrosion of reinforcing steel is a world wide problem. Still the knowledge of corrosion is limited. The objective of this project is to detect the electrode (anode/cathode) processes variation with temperature. Also to investigate the concrete conductivity's variation with temperature. In short terms this project is related to corrosion versus temperature both in field and in laboratory.
e-mail	Jan.ostvik@bygg.ntnu.no

Project:	Slipforming of Vertical Concrete Structures. Friction between concrete and slipform panel
Project period	1997 – 2001
Project type & financial support	Financial support: Aker Engineering AS; Selmer Skanska AS; Veidekke ASA; NCC Anlegg AS; Norcem AS; Gleitbau Ges.m.b.H & Research Council of Norway
Ph. D. Student	Kjell Tore Fosså
Supervisors	Prof. Magne Maage, former assistent professor Sverre Smeplass & Prof. Malvin Sandvik
Information	The prime objective of the research program is to improve the understanding of the slipform technique as a construction method in order to ensure high quality concrete structures. The objective is to identify the parameters affecting the friction that occur during lifting of the slipform panel. It is assumed that decreased friction will reduce the risk for any surface damages during slipforming.
e-mail	Kjell.fossa@bygg.ntnu.no

Project:	Creep deformations due to self-stresses in hardening high performance concrete, effect of temperature
Project period	2000 – 2002
Project type & financial support	Financial support: Norwegian Research Council & Norwegian Concrete Industry
Ph. D. Student	Dawood Atrushi
Supervisors	Terje Kanstad & Erik J. Sellevold
Information	The main topic is assessment of the risk of early age cracking in concrete due to restrained volume changes. The project particularly focuses on experimental determination and modelling of creep in young concrete. Creep in compression and tension as well as the influence of temperature on creep is studied experimentally
e-mail	Dawood.atrushi@bygg.ntnu.no

Project:	**Deformations and crack sensitivity at early ages. Materials technology and calculation methods**
Project period	2002 – 2004
Project type & financial support	Financial support: Norwegian Research Council & Norwegian Concrete Industry
Ph. D. Student	Ji Guomin
Supervisors	Erik J. Sellevold, Øyvind Bjøntegaard & Terje Kanstad
Information	Modelling of the experimental behaviour of concrete at early ages exposed to realistic temperature histories and variability degree of restraint. Further development of the materials models and calculation tools developed within IPACS and the parallel Norwegian research projects.
e-mail	

Project:	**Deformations in concrete cantilever bridges, observation and theoretical modelling**
Project period	1998 – 2001
Project type & financial support	Financial support: Norwegian Research Council through SINTEF's research program "Computional mechanics in civil engineering"
Ph. D. Student	Peter F. Takacs
Supervisors	Terje Kanstad
Information	Deformation in segmental cast cantilever bridges are studied. Deformations are monitored in three bridges in Norway. Numerical models are investigated as robust analysis tools for deformation prediction. The main emphasise is laid on creep and shrinkage modelling. Probabilistic methods are used to take into account the significant uncertainty in the prediction of these phenomena.
e-mail	Peter.takacs@bygg.ntnu.no

Project:	**Structural behaviour of post tensioned concrete structures. Flat slab. Slabs on ground**
Project period	1996 – 2001
Project type & financial support	Financial support: Norwegian Concrete Industry
Ph. D. Student	Steinar Trygstad
Supervisors	Terje Kanstad
Information	Experimental and theoretical studies of prestressed concrete. Full scale failure test of one slab (16x19m) and three slabs on ground (4x4m). Nonlinear and time dependent FE analysis (Diane, TNO, NL) and simplified calculation methods have been used
e-mail	Steinar@spennconsult.no

Norwegian University of Science and Technology - NTNU
Department of Structural Engineering
N – 7491 Trondheim

Project: **Properties of environment friendly cements in self-compacting concrete**

Project period	1997 – 2002
Project type & financial support	Financial support: Norcem Scancem Doctor of Engineering Programme
Ph. D. Student	Tom. I Fredrik
Supervisors	Prof. Erik J. Sellevold
Information	The trend is towards more environment friendly solutions and greater use of fillers in the production of cement and concrete. The project is focusing on replacing parts of the clinker with alternative raw materials (e.g. fly ash, limestone and slag) to produce blended cements. The properties of the environment-friendly cements will be characterised in self-compacting concrete.
e-mail	Tom.fredvik@norcem.no

Project: **Utilization of alkali reactive crushed rock fines in concrete production**

Project period	1999 – 2003
Project type & financial support	Financial Support: NorBetong AS Scancem Doctor of Engineering Programme
Ph. D. Student	Bård Pedersen
Supervisors	Prof. Magne Maage / NTNU
Information	The main purpose of this project is to clarify which reactions are taking place when using alkali reactive aggregates crushed down to filler, and the consequences in terms of durability of concrete structures. Studies on effect on fresh concrete including self-compacting concrete are included in this project. A main issue is to develop knowledge to maintain full ressource utilisation at the production plants by being able to use what was earlier supposed to be waste.
e-mail	Bard.pedersen@bygg.ntnu.no

Telemark University - HiT
Department of Technology
Kjølnes Ring 56
N – 3918 Porsgrunn

Project: **The impact of the process factors on the LWA process with priority on the kiln process**

Project period	1998 – 2002
Project type & financial support	Scancem Doctor of Engineering Programme
Ph. D. Student	Martin Siljan
Supervisors	Prof. Morten C. Melaaen / HiT & Bernt M. Tvete / Optiroc Group
Information	In this project the focus will be on understanding and improving the production process for of LWA, especially the drying of the clay. The two main tools are computer-simulations, both CFD in FLUENT and modelling of the drying process in a locally developed code, and a pilot plant where several tests will be performed over the next two years. The goal for the work is: • To help in development of the production line • To reduce energy consumption through increased production • To form a basis for development of new production line concepts
e-mail	Martin.siljan@optiroc.com